GEOLOGICAL ASSOCIATION OF CANADA
ASSOCIATION GÉOLOGIQUE DU CANADA

Mineralogical Association of Canada
Association minéralogique du Canada

Volcanogenic massive sulphide and orogenic gold deposits in northern Southeast Alaska

Field trip leaders:
Patrick J. Sack, Susan M. Karl, Nathan Steeves and J. Bruce Gemmell

June 4-8, 2016

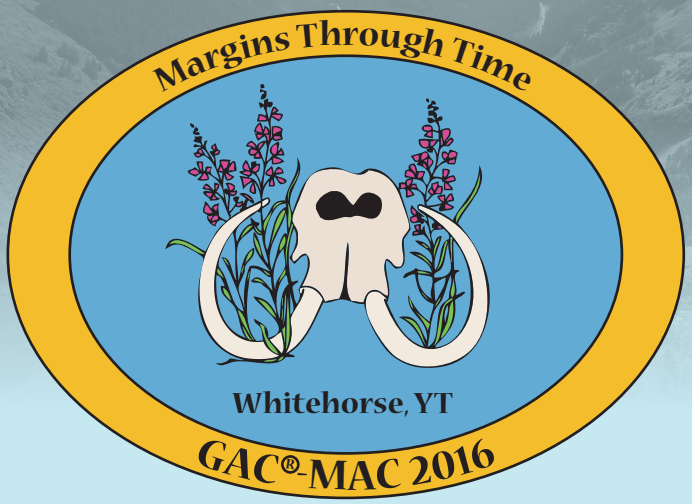

Contents

INTRODUCTION

Structure of this guidebook

This five-day field trip visits the most significant mineral deposits in northern southeast Alaska. The trip begins and ends with regional transects in the interior Intermontane terranes around Whitehorse, Yukon, and the Insular terranes along the northern Chatham Strait region of southeast Alaska (Fig. A-1 and Fig. A-2; Plate-1). To put the deposits in a regional tectonic framework, the guidebook begins with an introduction to northern Cordilleran geology, tectonics and metallogeny. The foci of the deposit portion of the field trip are Late Triassic volcanogenic massive sulphide (VMS) deposits of the Alexander Triassic metallogenic belt and Paleogene orogenic gold deposits of the Juneau gold belt. Details of the local geology are further elaborated in each segment of the guide book (Days 1-5). The data that provide the basis for the VMS deposit interpretations come from a series of PhD and MSc studies by the Centre of Excellence in Ore Deposit Research (CODES) at the University of Tasmania and the University of Ottawa. These deposit-scale studies are complimented by a long history of regional mapping and research by the U.S. Geological Survey (USGS).

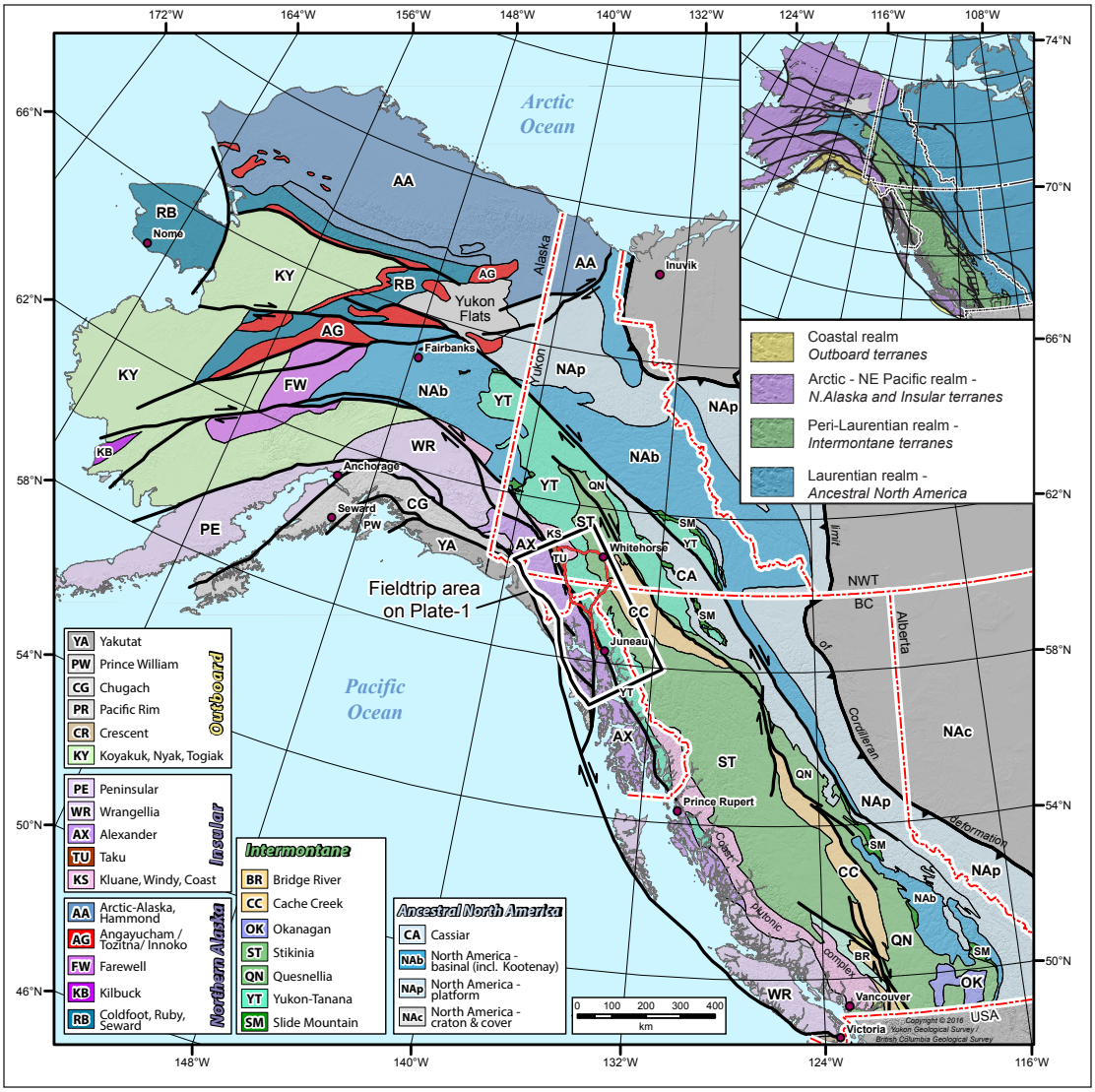

Figure A-1. *Terranes of the northern Cordillera (Colpron and Nelson, 2011). Terranes are grouped in the legend according to paleogeographic affinities shown in inset from Nelson et al. (2013). Field trip route shown in red.*

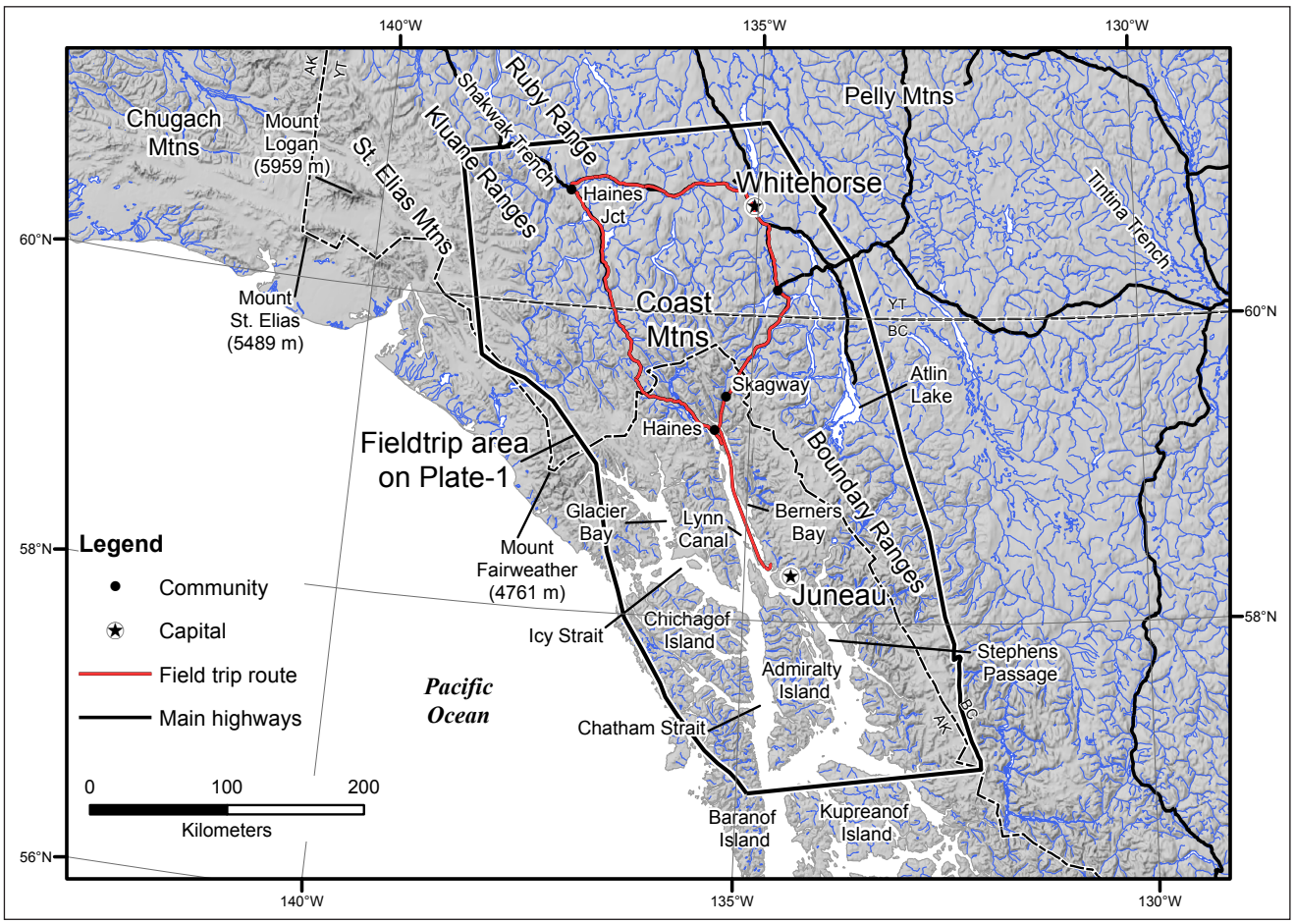

Figure A-2. *Physiographic map of northern B.C., southern Yukon and southeastern Alaska. Mtns = Mountains.*

Northern Cordilleran tectonic overview

Within the northern Cordillera, Proterozoic to Triassic continental margin strata of western Laurentia extend from eastern British Columbia, through Yukon and into east-central Alaska. Farther west, most of British Columbia, Yukon and Alaska are made up of Paleozoic to Mesozoic volcanic, plutonic, sedimentary and metamorphic assemblages that represent magmatic arcs, continental fragments and trapped ocean basins accreted to western Laurentia in Mesozoic and younger time. These accreted rocks, and those of ancestral North America, are overlain by syn- and post-accretionary clastic deposits, while the western and inner parts of the northern Cordillera are pierced by post-accretionary plutons and in places overlain by thick accumulations of relatively young volcanic strata.

The majority of the northern Cordillera is composed of three first-order tectonic entities defined by their interpreted paleogeographic position in the Paleozoic, plus fringing Mesozoic and younger accretionary complex terranes (Fig. A-1 inset; Nelson *et al.*, 2013):

1) Ancestral North America - the craton and associated continental margin rocks;

2) Intermontane terranes – periccratonic fragments with ties to ancestral North America;

3) Insular and Northern Alaska terranes – rocks that evolved independent of the ancestral North American craton in the Proterozoic to Mesozoic, in Panthalassa and possibly the Uralian Sea; and

4) Outboard terranes – Mesozoic and younger accretionary complexes that formed on the oceanward margins of the Intermontane and Insular terranes in the Coastal realm.

Ancestral North America (Laurentia) includes the western craton margin, and associated platformal and basinal terranes (Cassiar, North America – craton, platform, basinal; Fig. A-1). The western, oceanward boundary of ancestral North America is marked by discontinuous slivers of the Slide Mountain oceanic terrane that are remnants of a Late Devonian to Permian rift basin developed between the continent and a belt of pericratonic fragments collectively termed the Intermontane terranes. Closure of the Slide Mountain ocean and initial re-accretion of the inner margin of Yukon-Tanana and Quesnellia terranes occurred in the Triassic (Nelson *et al.*, 2013).

The Intermontane terranes (Yukon-Tanana terrane, Quesnellia and Stikinia; Fig A-1) have early Paleozoic linkages to ancestral North America (Nelson et al., 2013). Yukon-Tanana consists of mid to late Paleozoic continental margin, arc and marginal basin assemblages that have been complexly deformed and metamorphosed (Colpron *et* al., 2006). Yukon-Tanana is the basement upon which the Triassic to Jurassic Stikinia and Quesnellia arcs were formed (Colpron *et al.*, 2006; Nelson *et al.*, 2013; Nelson *et al.*, 2006). The belt of pericratonic terranes was in turn bounded on its oceanward margin by a companion Devonian to Jurassic accretionary complex, the Cache Creek terrane. The present position of the Tethyan-derived Cache Creek terrane, enclosed within the pericratonic belt, is a constructional anomaly that has been explained by oroclinal enclosure that developed as the Intermontane pericratonic terranes amalgamated and accreted to the continent in the Jurassic (Mihalynuk *et al.*, 1994). On the field trip we will make a few roadside stops in the Intermontane terrane, but will remain west of the cratonic rocks of ancestral North America.

The Insular terranes (Alexander, Wrangellia, and Peninsular; Fig. A-1) are exotic to North America. Their early faunal and isotopic affinities are consistently Siberian and Baltican (Bazard *et al.*, 1995; Beranek *et al.*, 2012; Beranek *et al.*, 2014; Bradley *et al.*, 2003; Soja and Antoshkina, 1997; White *et al.*, 2016). The Insular terranes consist of Neoproterozoic to Mesozoic arcs and basins which developed mainly within the paleo-Arctic realm, and were at tropical latitudes at the time of deposition. The largest

of the Insular terranes are the Alexander terrane and Wrangellia, traditionally thought to have been amalgamated into the Wrangellia composite terrane by the middle Pennsylvanian (Gardner *et al.*, 1988). Recent studies suggest tectonic and stratigraphic ties between the terranes as early as Devonian in the north (Israel *et al.*, 2014), and after the Pennsylvanian in the southern parts of the composite terrane (Dostal *et al.*, 2013; Karl *et al.*, 2010a). Late Triassic rifting of the Alexander terrane portion of the composite Alexander-Wrangellia-Peninsular terrane resulted in the formation of the Alexander Triassic metallogenic belt (ATMB) which is the focus of the volcanogenic massive sulphide (VMS) portion of this field trip.

As the Insular terranes approached the accreted Intermontane terranes during the mid-Jurassic (Aberhan, 1999; Smith *et al.*, 2001), several margin-parallel basins, including the Gravina-Nutzotin belt, developed along the Insular-Intermontane boundary. Sedimentation in these overlap basins continued through the Cretaceous as east-dipping subduction continued beneath the oceanward side of the Insular terranes. Subduction related magmatism resulted in the intrusion of Cretaceous magma into the Insular terranes and the overlap basins. Late Cretaceous to Paleogene contraction along the Insular-Intermontane boundary resulted in crustal thickening and emplacement of large volumes of felsic magma, the Coast plutonic complex (CPC), into the orogenic belt at the terrane boundary (Godwin, 1975; Hutchison, 1982). Changing plate trajectories in the early Tertiary (Engebretsen *et al.*, 1985; Lonsdale, 1988) resulted in Paleogene trans-tensional structures in the orogenic belt which served as conduits for gold-bearing vein systems of the Juneau gold belt (Goldfarb *et al.*, 2005) including the operating Kensington mine, and the historic Alaska-Juneau and Treadwell mines that we will be visiting.

The outboard terranes, the outermost belt of terranes in the northern Cordillera, contain accretionary assemblages derived from Mesozoic and younger oblique subduction of oceanic crust along the oceanward margin of the Insular composite terrane, including the Chugach, Prince William, Yakutat, Pacific Rim, and Crescent terranes (Fig. A-1). We will not travel far enough west to see these accretionary assemblages on this field trip.

Transcurrent faults of the northern Cordillera

The Canadian Cordillera is dissected by a series of late Early Cretaceous to Cenozoic, orogen parallel, strike-slip faults (Fig. A-3; Gabrielse *et al.*, 2006). The younger faults (mainly Eocene in age) are the most obvious as they correspond to well-defined morphogeological trenches. A prominent example is the Northern Rocky Mountain Trench, which is underlain by the Tintina fault. Similarly, the Shakwak Trench in southwest Yukon is underlain by the Denali fault, and the Coast Range megalineament in southeast Alaska (Brew and Ford, 1978; Twenhofel and Sainsbury, 1958) which may correspond to a portion of the Denali fault that is no longer active (Lanphere, 1978). The Tintina fault is constrained by tiepoints to post-Late Cretaceous dextral displacement of 400-430 km (Gabrielse *et al.*, 2006). The Denali fault is thought to have a similar magnitude of dextral offset with 370 km of post-Early Cretaceous displacement (Lowey, 1998), including 40 km of post-Eocene displacement (Lanphere, 1978), and 30 km of

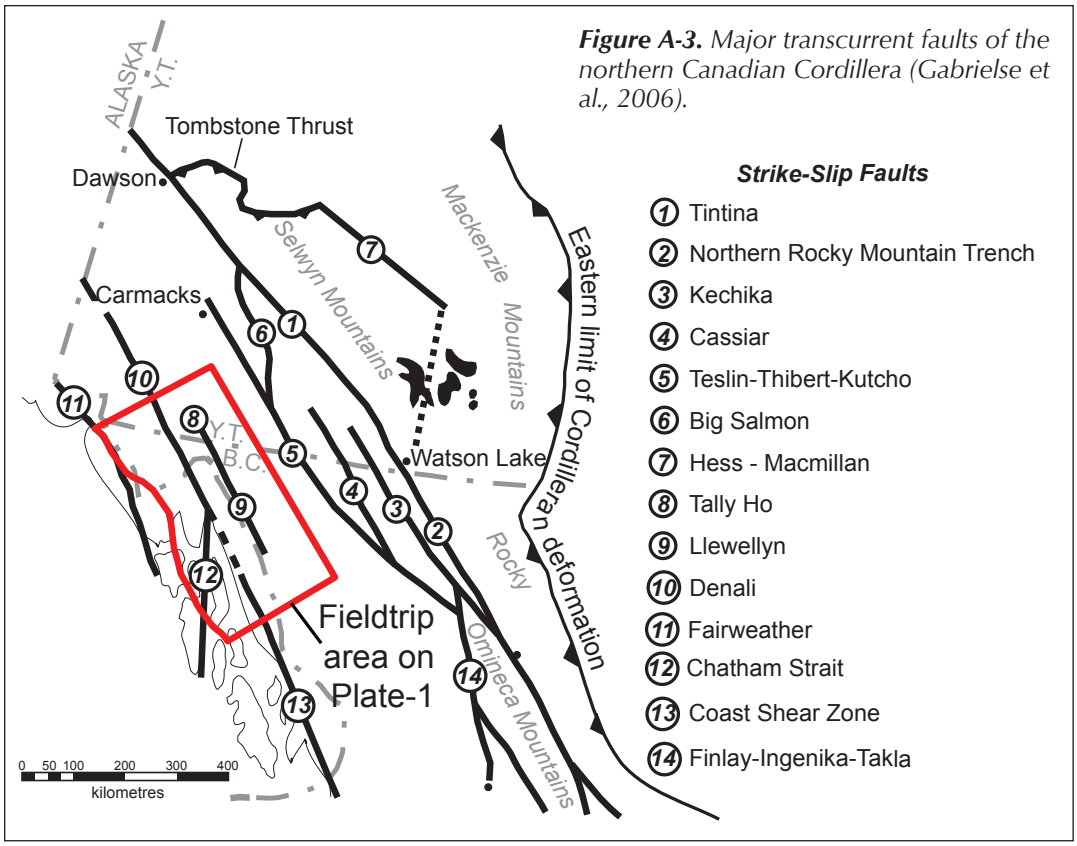

Figure A-3. *Major transcurrent faults of the northern Canadian Cordillera (Gabrielse et al., 2006).*

post-early Oligocene displacement (Trop *et al.*, 2004). Holocene activity on the eastern Denali fault system is estimated at 1.5±0.5 mm/yr of dextral slip and 1.5±0.6 mm/yr of contraction based on GPS measurements (Elliott *et al.*, 2010). A band of modern earthquakes follows the trace of the Duke River fault, suggesting it is involved in relative plate motions at the Pacific-North American plate boundary; there is modern seismicity on the Denali fault between the Duke River and Chatham Straight faults, but none on the Chatham Strait fault (Elliott *et al.*, 2010; Mazzotti *et al.*, 2008).

Mineral deposits in the western Intermontane terranes

The Intermontane terranes at which we will briefly stop on this trip are Stikinia and Yukon-Tanana terrane (Fig. A-1). The oldest and most notable syngenetic mineral deposits in western Yukon-Tanana terrane are Devonian VMS deposits such as Tulsequah Chief (Sherlock *et al.*, 1994). Stikinia hosts many early Mesozoic porphyry deposits along its length in British Columbia (Logan and Mihalynuk, 2014). Late Triassic to Early Jurassic Cu-Au±Mo deposits such as Highland Valley, Mt. Polley, Kemess, and Red Chris in British Columbia and Minto in Yukon are notable examples of this prolific mineralizing period (Nelson *et al.*, 2013). The next major period of mineralization locally includes skarn deposits associated with Cretaceous plutons of the Whitehorse suite where they intrude Late Triassic limestone of the Lewes River Group (Tenney, 1981).

More than 30 Cu±Au skarn occurrences form the Whitehorse copper belt, discovered in 1897 and mined periodically until 1982 (Héon, 2004). The final economically significant period of mineralization is represented by Au-Ag veins related to Late Cretaceous to Eocene magmatism. They are concentrated in two past producing districts: Montana Mountain, south of Carcross (*e.g.*, Stop 1-3), and the Wheaton District, northwest of Carcross (west of Grey Ridge and not visible from the highway).

Mineral deposits in Wrangellia

Mineral deposits in Wrangellia are found in Devonian and Jurassic rocks on Vancouver Island, and in Triassic rocks in Yukon and eastern Alaska. In southern Wrangellia on Vancouver Island, volcanic sequences of the Sicker Group host significant VMS mineralization in the Myra Falls district, the Mount Sicker mine, and the Lara deposit (Dawson *et al.*, 1992). Mineralization in northern Wrangellia is associated with voluminous Middle to Late Triassic flood basalts that reach thousands of meters in thickness. Magmatic Cr-Ni-Co-platinum group elements (PGE) deposits are associated with feeder dikes to these basalts, such as at the past-producing Wellgreen mine and Quill Creek (Hulbert, 1997). Copper and silver, derived from metamorphic and diagenetic fluids, is found in veins and stratabound deposits in Triassic carbonate rocks that overlie the flood basalts. The best known example is the Kennecott mine in the Wrangell Mountains of eastern Alaska (MacKevett *et al.*, 1997; Schmidt and Rogers, 2007). Skarn and porphyry copper mineralization is associated with the Early Jurassic Island Intrusive Suite and includes several significant deposits such as Argonaut and the Island Copper mine on Vancouver Island in southern Wrangellia (Dawson *et al.*, 1992).

Mineral deposits in the Alexander terrane

Mineral deposits in the Alexander terrane range in age from Neoproterozoic to Cenozoic. The oldest deposits are Zn-Pb-Cu VMS deposits that include Niblack, Nutkwa, Corbin, Copper City, and Big Harbor in southeast Alaska (Fig. A-4; Ayuso *et al.*, 2007; Oliver *et al.*, 2011; Slack *et al.*, 2007). These deposits formed in an oceanic arc environment in the late Neoproterozoic, at approximately 600 Ma (Gehrels and others, 1996; Oliver and others, 2011). The oceanic arc setting persisted through the early Paleozoic and continued to be conducive to the formation of mineral deposits. For example, Ordovician and Silurian mineral deposits include PGE, Ni-Cr, Cu, and Fe deposits such as the Salt Chuck, It, and Mount Andrew-Mamie mines (Himmelberg *et al.*, 1991; Warner and Goddard, 1961) and Zn-Pb, Ag, Cu VMS deposits such as Barrier and Datzkoo (Fig. A-4; Gehrels *et al.*, 1983; Slack *et al.*, 2007). The next major period of metallogenesis is Late Triassic VMS mineralization associated with intra-arc rifting that includes the Windy Craggy, Greens Creek, and Palmer deposits (Fig. A-4; Green *et al.*, 2003; Peter and Scott, 1999; Taylor *et al.*, 2008). Early Jurassic peralkaline intrusive rocks attributed to sinistral oblique transpression contain U-Th-rare earth element (REE) mineralization (Dostal *et al.*, 2013). In the Late Jurassic, a new arc formed on the oceanward margin of the Alexander terrane, and Cr-Co-Ni-PGE-Fe deposits such as

Klukwan, Port Snettisham, Union Bay, and Duke Island are associated with Alaska-Ural-type ultramafic-mafic complexes that formed beneath the arc in the Early Cretaceous (Himmelberg and Loney, 1995; Taylor, 1967). Collision of the Insular terranes with the Intermontane terranes previously accreted to the margin of North America produced an orogenic belt that contains middle Cretaceous Au mineralization along the east margin of the Alexander terrane (Karl *et al.*, 2010b; Newberry *et al.*, 1995). Late orogenic fluids mobilized and deposited Au in quartz veins along the boundary between the Insular and Intermontane terranes, such as at Treadwell, Kensington, Alaska-Juneau (more commonly referred to as the "AJ"), and Sumdum Chief in the Paleogene (Goldfarb *et al.*, 1991; Miller *et al.*, 1994; Miller *et al.*, 1995; Newberry *et al.*, 1995). This orogenic belt also contains gold-quartz veins, such as at Gold Nest and Mt. Sumdum (Berg, 1984), farther to the east in Yukon-Tanana terrane, on the western margin of the Intermontane terranes.

Along the western, oceanward margin of the Insular terranes, Eocene subduction of a spreading center induced melting of sediments in the accretionary wedge. This led to the formation of anatectic granites and Au-quartz veins such as at the Hirst-Chichagof mine and the Lucky Chance mine, dated at 49 Ma (Karl *et al.*, 2015; Zumsteg *et al.*, 2003; Haeussler *et al.*, 1995).

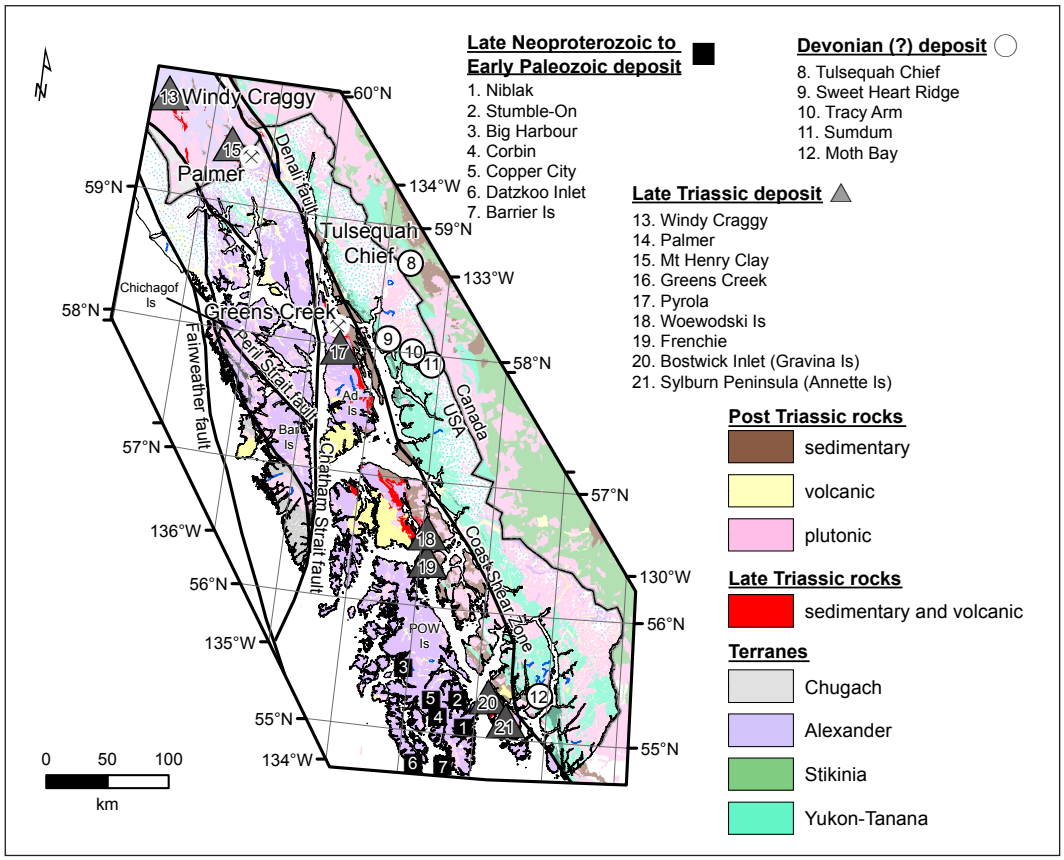

Figure A-4. *Terranes, faults and major volcanogenic massive sulphide deposits of southeast Alaska and northern British Columbia (modified from Newberry et al., 1997). The Late Triassic rocks (red) of the Alexander Triassic metallogenic belt host numerous volcanogenic massive sulphide deposits, including the Palmer, Greens Creek, and Windy Craggy deposits (modified from Taylor et al., 2010b). Ad = Admiralty, Bar = Baranof, POW = Prince of Wales, Is = Island.*

Triassic VMS deposits in southeast Alaska

The most economically important VMS episode in southeast Alaska, and the focus of the VMS portion of this field trip, occurred in the Late Triassic during the development of the Alexander Triassic metallogenic belt (ATMB, Fig. A-4; Taylor *et al.*, 2008). Geologic evidence such as basal breccias, restricted basin deposits, and the geochemistry of volcanic rocks support oblique rifting of an oceanic volcanic arc during the early Mesozoic (Gehrels and Berg, 1994; Taylor *et al.*, 2008). This rifting event resulted in significant massive sulphide mineralization throughout the Alexander terrane, from the Windy Craggy deposit in the north to the Sylburn Peninsula of Annette Island in the south, a distance of 750 km (Fig. A-4; Taylor *et al.*, 2008). The belt shows a transition from low energy, deep marine environments with carbonaceous shales in the north, to shallow-water, high energy depositional environments in the south, including thick packages of limestone and conglomerate (Fig. A-5; Taylor *et al.*, 2008). There is also a distinct change in magmatism from MORB-like and tholeiitic basaltic volcanism in the north to alkaline, basin-margin-type rhyolites in the central portion and finally to more calc-alkaline, proximal rhyolite-dominated arc volcanism in the south (Taylor *et al.*, 2008). These changes are reflected in the geochemical signature of mineral occurrences along the belt. A thick sequence of mafic, pillowed, amygdaloidal, and relatively undeformed volcanic rocks overlies the entire ATMB. The Greens Creek, Windy Craggy, and Palmer deposits are located in the central to northern portion of this belt. Windy Craggy, a 300 Mt Cu-Co-Au VMS deposit (Peter, 1989), is the largest deposit in the terrane; the 24 Mt Greens Creek is second largest; and the 8 Mt Palmer deposit is the third largest (Steeves *et al.*, 2016). Greens Creek is the only operating mine in the ATMB, and has been operating since 1989 with a 3-year hiatus in the mid-1990s (West, 2010). Between 2010 and 2014, Greens Creek produced 35 Moz (992 t) Ag, 300,000 oz (8.5 t) Au, 98,000 t Pb and 292,000 t Zn (www.hecla-mining.com/greens-creek, accessed April 4, 2016).

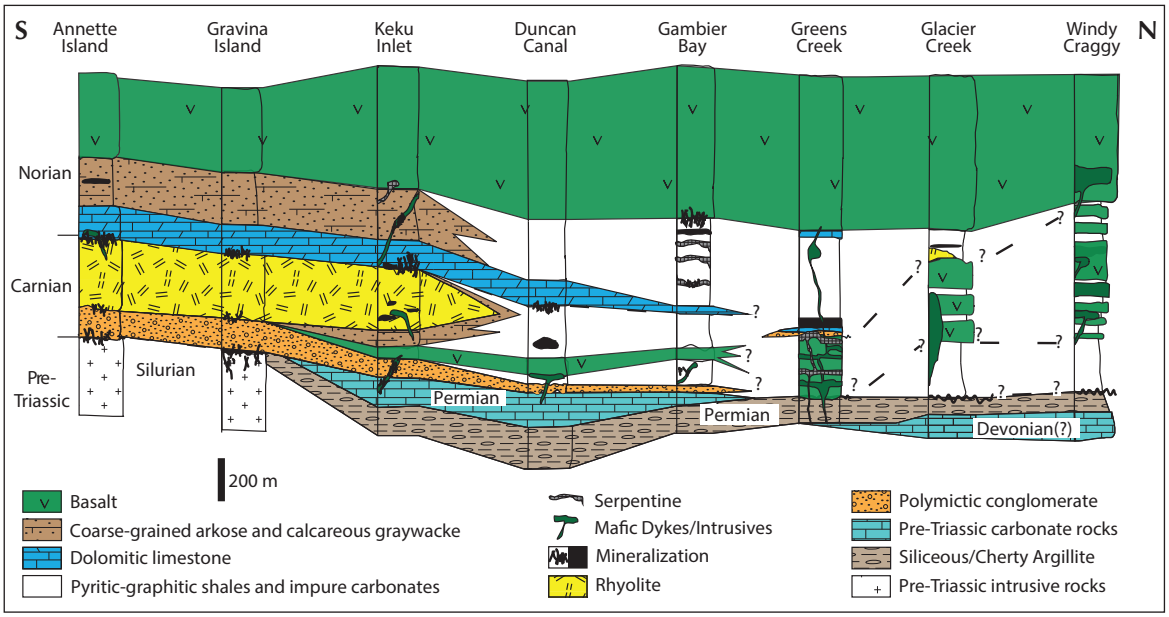

Figure A-5. *Schematic stratigraphic section, from south to north, of Late Triassic rocks across the Alexander Triassic metallogenic belt showing a general increase in the abundance of shales and mafic volcanic rocks, and a loss of felsic sedimentary and volcanic rocks toward the north. See Fig. A-4 for locations. Scale is approximate. From Steeves et al. (2016) after Taylor et al. (2008).*

Orogenic and intrusion-related gold deposits in southeast Alaska

In southeastern Alaska, the Juneau gold belt extends over 300 km in strike length (Fig. A-6), and is dominantly an orogenic gold belt, but includes a poorly understood early mineralizing event. This earlier event is Cretaceous, possibly intrusion-related gold mineralization such as at Jualin and Treadwell, where gold-bearing intrusive host rocks yielded U-Pb zircon ages of 105 ± 1 Ma and 91 ± 2 Ma, respectively (Gehrels, 2000; Newberry *et al.*, 1995). Fuchsite separates from vein material at the historic Maid of Mexico mine, which produced at least 100 oz of gold, yield a well-defined $^{40/39}$Ar plateau age of 92.0 ± 0.2 Ma (Taylor, 2003), providing evidence for orogenic gold mineralization as well in the Cretaceous. Gold-quartz veins mined in the Ketchikan mining district are hosted in metamorphic rocks of middle Cretaceous age, and are also part of this mineralizing event (Goldfarb *et al.*, 1988). These early gold mineralization events were followed by orogenic gold mineralization in the Paleogene which is the main, most economically important, mineralizing event in the Juneau gold belt, and is recognized in deposits such as at Sumdum Chief, AJ, Treadwell, and Kensington (Figs. A-6 and A-7) (Karl *et al.*, 2010b; Miller *et al.*, 1995). White mica $^{40/39}$Ar ages throughout the Juneau gold belt provide the best age control for the main mineralizing event and range from 52.8 to 56.5 Ma (Goldfarb *et al.*, 1991; Miller *et al.*, 1994).

The Juneau gold belt historically produced over 6.7 Moz (190 t) of gold prior to 1945 (Goldfarb *et al.*, 1991). The current resource at the Kensington mine is 1.58 Moz (44.8 t; at year-end 2014) making the endowment of the belt at least 8.3 Moz (235 t). Past production includes 24,000 oz (0.7 t) from the Sumdum Chief mine between 1895 and 1903, 3.1 Moz (87.9 t) Au and 151,000 oz (4.3 t) Ag from the Treadwell mine between 1885 and 1923, and 3.5 Moz Au (99 t) plus 1.9 Moz (54 t) Ag and 1140 t Pb from the AJ deposit between 1883 and 1944 (Redman, 1986). Current gold production within the Juneau gold belt is restricted to the Kensington mine, which since 2010 has produced approximately 572,598 oz Au (January 11, 2016 Coeur Alaska news release).

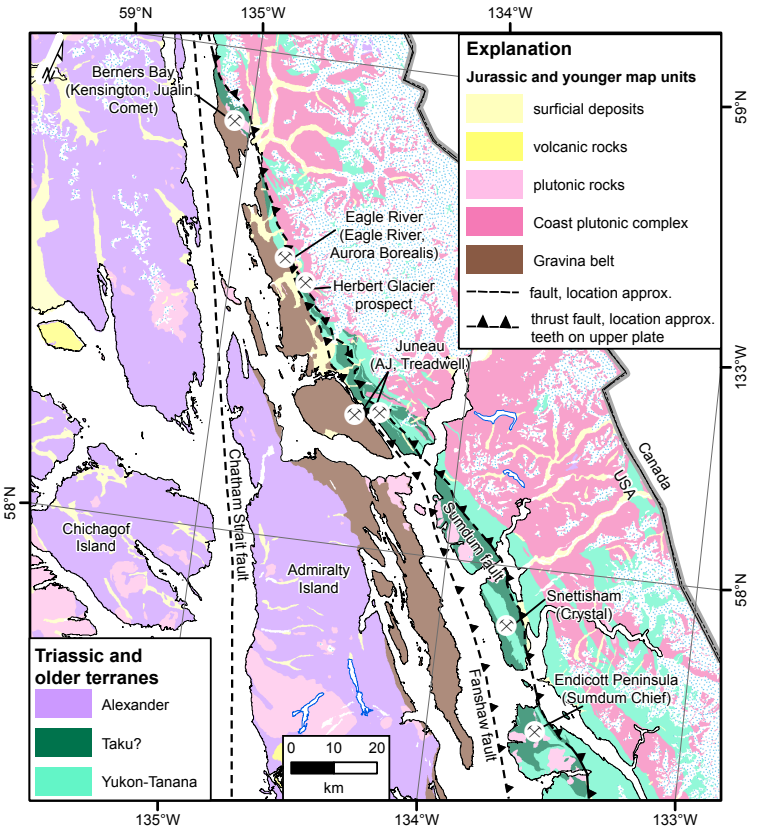

Figure A-6. *Location of gold districts of Juneau gold belt in southeast Alaska. Major deposits in each district are listed in parentheses (after Goldfarb et al., 1988). General geology and first-order structures from Miller et al. (1994).*

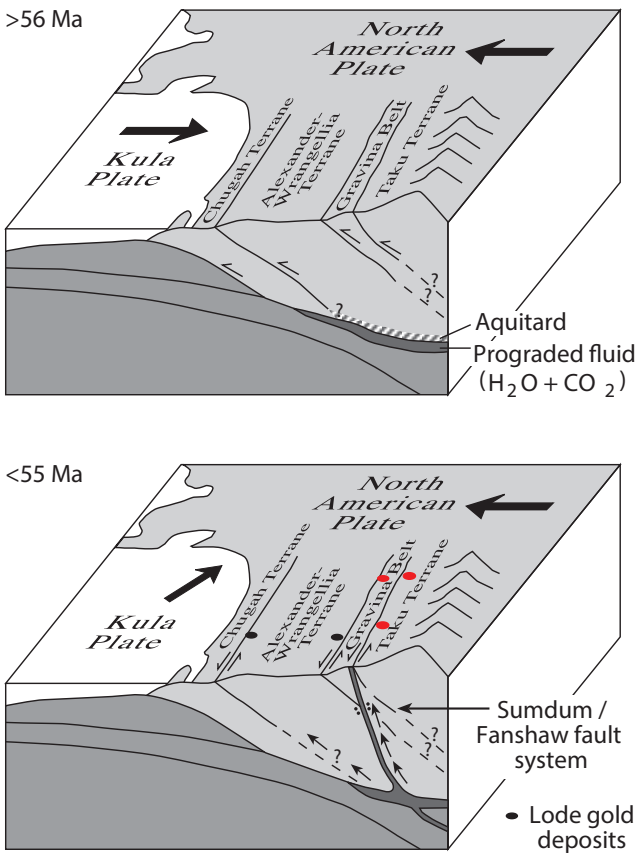

Figure A-7. *Change in plate motions in the northern Pacific basin at ca. 56 to 55 Ma. This change from orthogonal (thrusting) to oblique (strike-slip motion) far-field stress was critical for seismicity, fluid migration, and gold deposition along the Sumdum-Fanshaw deep-crustal fault system of the Juneau gold belt. Modified from Goldfarb et al. (2005), red circles represent deposits visited in the Juneau gold belt.*

Field trip transects and deposit tours

The field trip begins in Whitehorse, Yukon and travels south along the South Klondike Highway to Skagway, Alaska, essentially tracing, in reverse, the path of the miners heading to the Klondike goldfields in 1898. In Skagway, we will board an Alaskan state ferry and sail to Juneau, Alaska. This transect on the first day will provide regional geologic context for the deposits on the field trip and will take us from the Intermontane terranes, across the Cenozoic Coast plutonic complex and into the Insular terranes (Fig. A-8). The second day we will tour the active Kensington mine site with an optional evening tour of the historic AJ host rocks and a view of the AJ glory hole. The orogenic gold deposits on this day represent the different styles and host rocks within the Juneau gold belt, the largest lode gold producing district in Alaska (Freeman *et al.*, 2015). On day three, we will visit the Greens Creek mine, an enigmatic VMS deposit that is consistently one of the top silver-producing mines in the world. This evening will have an optional hike to the historic Treadwell mine, another of the past-producing lode gold deposits of the Juneau gold belt. The fourth day will take us back onto the state ferry system from Juneau to Haines, Alaska, where we will have a short drive to the Palmer VMS deposit, the most recent discovery in ATMB. The final day heads north from the Mosquito Lake Road junction with the Haines Road, through northern BC to the Alaska Highway at Haines Junction, Yukon, where we head east and finish in Whitehorse. This day will include a stop along the Denali fault, the boundary between the Insular and Intermontane terranes, and several stops in Jura-Cretaceous sedimentary rocks along this boundary before the final drive east back into the Intermontane terranes.

As the two highway legs (days 1 and 5) of this field trip involve long distance travel (Table 1), and because the highways themselves offer limited access to the geology, our choice of stops is small. The selected outcrops and the northern Cordilleran landscape will provide a context for discussions of the regional geology and metallogeny of the deposits we will see on this trip. The days that we visit company sites (days 2 through 4) will be long as they are dictated by mine schedules; activities in the evenings are

geological in nature but optional. The regional geologic map (Plate 1) that spans Yukon, British Columbia and southeast Alaska is based on the most recent digital maps available for each jurisdiction. These detailed maps, reports and related databases are available from the Yukon Geological Survey (www.geology.gov.yk.ca), the British Columbia Geological Survey (http://www.em.gov.B.C..ca/Mining/Geolsurv/de fault.htm), and the USGS (http://dx.doi.org/10.3133/sim3340) websites. The trip log is keyed to the green kilometre posts that are placed every 2 km along the north (or east) side of the major highways; road stops in Alaska include mile post distances in brackets. Coordinates in Universal Transverse Mercator (UTM) NAD83 projection are provided for the highway stops (Table 2). Unless otherwise noted, all units are metric.

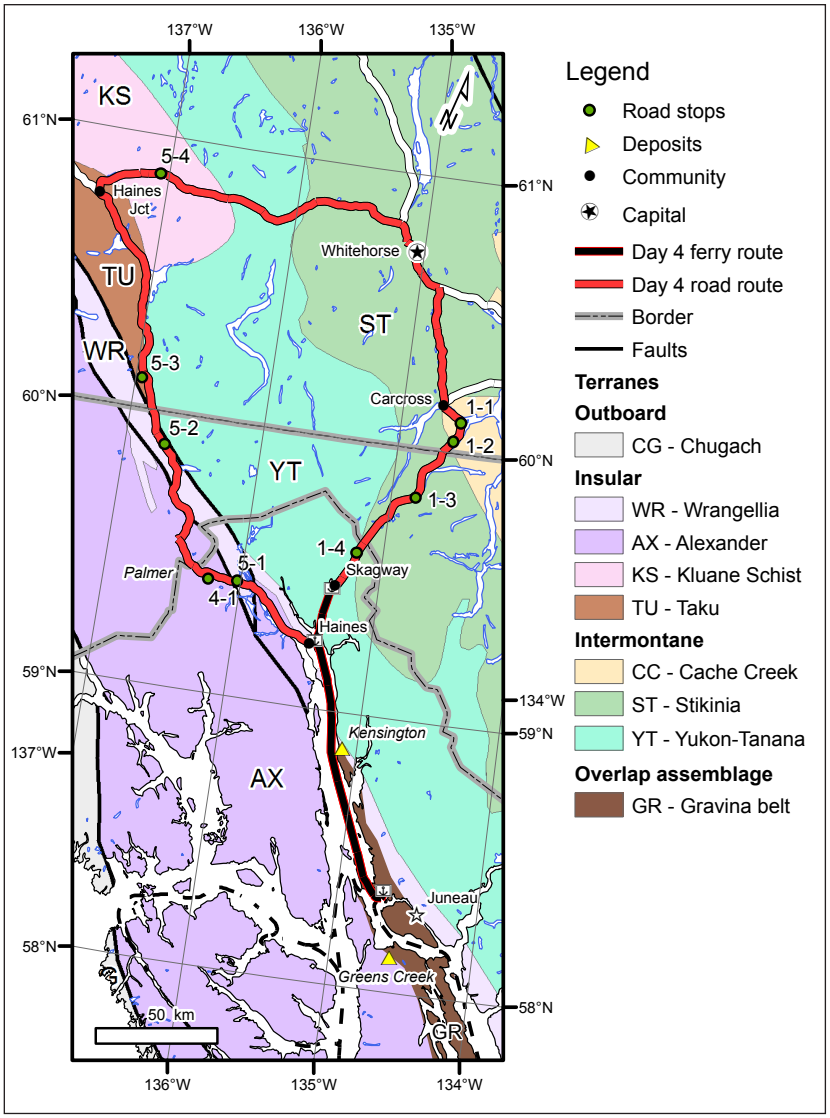

Figure A-8. *Simplified terrane map with field trip stops.*

Climate and other considerations

The highway portions of this trip (South Klondike, Haines and Alaska highways) can be done from May to early October most years, although variable snow cover on high peaks in spring and fall may limit the geological experience at some stops. Although the highways are drivable year-round, visiting these field trip stops between late October and May is not recommended as cold temperature, snow and/or mud are likely to limit access to some outcrops. The best viewing season for highway stops is between late June and September. During summer months, traffic along the highways can be frequent and fast. Care should be taken to park vehicles well off the road and in a visible location. Watch for traffic before crossing the highway.

Wildlife is commonly sighted along the field trip route. Moose, elk, and caribou are common along much of the route. Dall sheep can be encountered between Carcross and Skagway. Bison may be seen along the Alaska Highway between Whitehorse and Haines Junction. Grizzly and black bears are present throughout the area.

***Table 1**. Summary of distance traveled.*

Day	Location	Distance	Length of day	
Day 1	Whitehorse to Skagway road transect	180 km	4 hrs	7.5 hrs
	Skagway to Juneau ferry transect	165 km	3.5 hrs	
Day 2	Kensington mine tour	50 km	14 hrs	plus optional AJ Tour
Day 3	Greens Creek mine tour	30 km	14 hrs	plus optional Treadwell Tour
Day 4	Juneau to Haines ferry transect; Palmer deposit tour	150 km	12 hrs	
Day 5	Haines to Whitehorse road transect	375 km	8 hrs	
	Total	950 km	58 hrs	

***Table 2.** Highway field stop locations.*

Stop	UTM E	UTM N	Zone	Latitude	Longitude	Kilometre marker	Road	Description
1-1	524600	6664122	8	60.1134	-134.5574	94.8	South Klondike	Bove Island lookout
1-2	522606	6656248	8	60.0428	-134.5942	86.4	South Klondike	Venus mill
1-3	510516	6631195	8	59.8183	-134.8125	56.3	South Klondike	Plutonic-metamorphic complex contact
1-4	488801	6603230	8	59.5882	-135.1912	18.4 (11.5)	South Klondike	Migmatite pullout
4-1	429989	6586879	8	59.4147	-136.2335	NA	Porcupine Trail	Devonian limestone
5-1	441947	6587746	8	59.4243	-136.0231	43.5 (27.2)	Haines Road	Four Winds Complex
5-2	404580	6639025	8	59.8778	-136.7046	129.2	Haines Road	Denali-Duke River fault view point
5-3	391795	6664974	8	60.1075	-136.9464	159.1	Haines Road	Million Dollar Falls campground
5-4	387811	6748796	8	60.8585	-137.0653	1547.5	Alaska Highway	Canyon City pullout

Acknowledgements

We thank Steve Israel, Lara Lewis and Scott Casselman from Yukon Geological Survey (YGS), Liz Cornejo of Constantine Metal Resources Ltd. and Heather Burrell of Archer, Cathro and Associates (1981) Ltd., who participated in a trial run of this field trip in early September, 2015, and offered suggestions for improvement. Steve Israel also provided the stop descriptions for the Canadian highway stops on the final day. The coordinated digital geologic map was compiled with the assistance of Ric Wilson and Keith Labay of the US Geological Survey. The guidebook layout, most of the introduction figures, and previous unpublished guidebooks covering the transect from Whitehorse to Skagway (Johnston et al., 1993; Energy, Mines Ministers, 2006) were provided by Maurice Colpron of YGS. We are grateful for the hosting of deposit tours by Hecla Mining, Coeur Mining and Constantine Metal Resources. In addition, the efforts of the staff at each deposit have been amazing; Michelle Deal and Will Robinson at the Kensington mine, Rob Davidson at the Greens Creek mine and Liz Cornejo and Darwin Green at the Palmer deposit are gratefully acknowledged. Student sponsorship by GAC®-Mineral Deposits Division and Equity Exploration is also gratefully acknowledged. Any use of trade, firm, or product names is for descriptive purposes only and does not imply endorsement by the US Government.

DAY 1 – WHITEHORSE TO JUNEAU

Daily summary

We will meet at the Elijah Smith Building, 3rd Ave. and Main St., at 9:30 am and leave Whitehorse by 10:00 am. We will take approximately 4 hours to drive from Whitehorse to Skagway (2 hours of driving and 2 hours of geologic stops). From Skagway it will be a 2.5 hour ferry ride to Juneau; there will be two 30 minute lectures on the ferry beginning 30 minutes after the ferry departs. This night we will be staying at the Travelodge near the airport in Juneau.

Daily schedule

9:30 am – meet at the H.S. Bostock Core Library

10:00-1:00* pm – drive Whitehorse to Skagway (*Note – actual driving time is 4 hours with stops, southeast Alaska is 1 hour behind Yukon; all times in local time)

Stop 1-1 – km 94.8, Bove Island Lookout – Cache Creek terrane

Stop 1-2 – km 86.4, Venus Mill – historic gold mine

Stop 1-3 – km 56.3, Coast plutonic complex – Boundary Ranges metamorphic complex contact

Stop 1-4 – km 18.4 (mile 11.5), Highway pullout north of Moore Creek bridge – migmatites

1:00-2:30 pm – lunch in Skagway

2:30-4:30 pm – wait for ferry

4:30-7:00 pm – ferry from Skagway to Juneau

5:00 – Sue Karl regional geology talk

5:30 – Patrick Sack/Bruce Gemmell Greens Creek geology talk

7:00-7:30 pm – Juneau ferry to Travelodge hotel

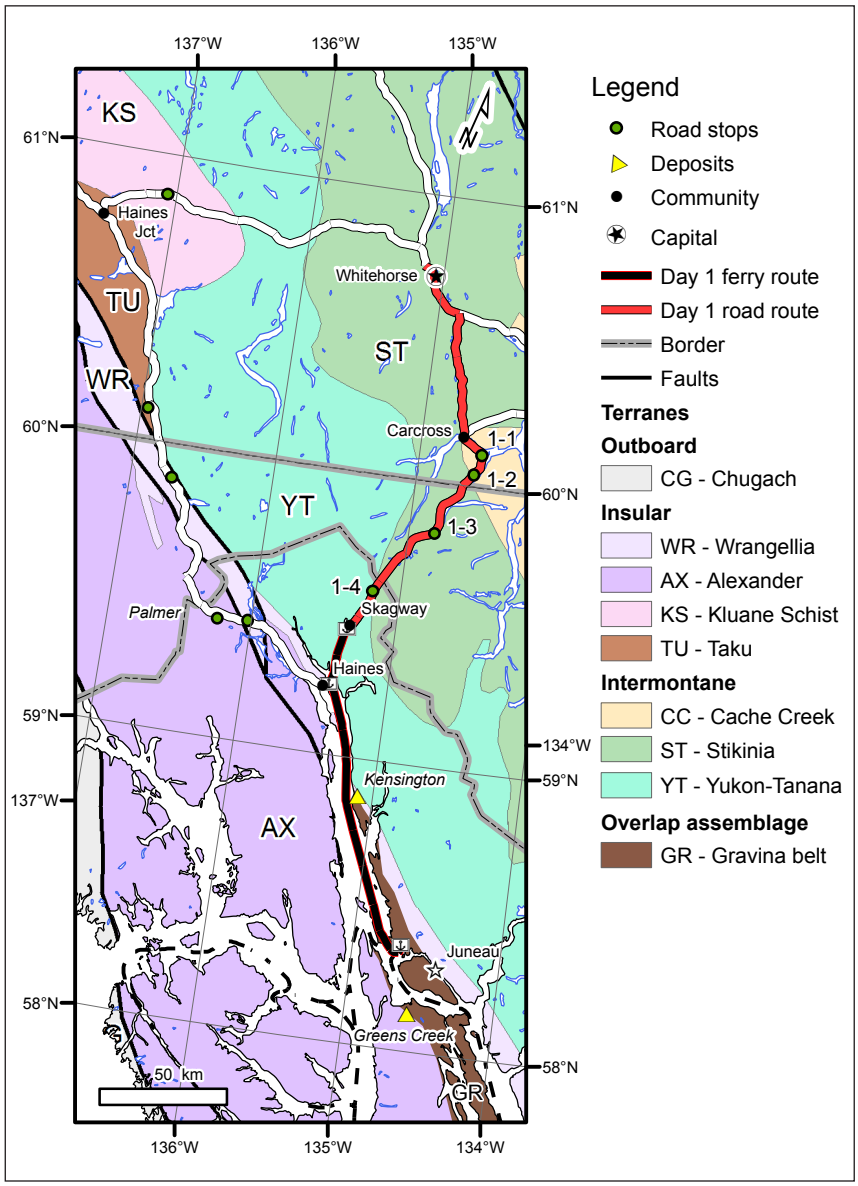

Figure 1-1. *Simplified terrane map with Day 1 route and field trip stops.*

Regional geology

Today's trip along the South Klondike highway from Whitehorse, Yukon, to Skagway, Alaska (via northwestern B.C.), traces back (in reverse) some of the terrain travelled by those seeking their fortune in the Klondike Gold Rush of 1898 (Fig. 1-1). The description of the stops on Day 1 are modified from Johnston *et al.* (1993). Day 1 takes us from the Interior Plateau of southern Yukon, a semi-arid region underlain primarily by late Paleozoic to Mesozoic accreted arc and oceanic terranes, to the heart of the Coast Mountains and its rainforest, where granitoid batholiths and metamorphic rocks predominate (Plate-1).

The Whitehorse area is underlain primarily by Upper Triassic sedimentary and volcanic rocks of the Lewes River Group, the northern extension of the Stikine terrane, and overlying sandstone, conglomerate, argillite and tuff of the Lower to Middle Jurassic Laberge Group (Whitehorse Trough). The limestone underlying Grey Mountain in Whitehorse is part of the Lewes River Group. The highway between Whitehorse and Carcross parallels the axis of the Whitehorse Trough adjacent to its western margin. For most of the drive, rocks of the Lewes River Group outcrop on the west side of the highway and those of the Laberge Group on the east side of the road.

At Carcross, the sedimentary rocks of the Whitehorse Trough are juxtaposed along the Crag Lake fault with late Paleozoic – early Mesozoic oceanic chert, basalt, limestone and ultramafic rocks of the Cache Creek terrane. The highway traverses the Cache Creek terrane until near the Yukon-B.C. border. In northern B.C., the Cache Creek

terrane is thrust over Whitehorse Trough strata along the Nahlin fault. Rocks of Whitehorse Trough are intruded by Cretaceous - Tertiary granitic rocks of the Coast Mountains south of Tutshi Lake. From this point on, the highway traverses mainly the Coast Mountains batholith to Skagway, with local enclaves of metasedimentary rocks of Nisling terrane – a mid- to late Paleozoic continent margin and arc terrane possibly correlative with Yukon-Tanana terrane exposed northeast of Whitehorse Trough in Yukon.

The crustal structure of the region is interpreted on the Lithoprobe SNORCLE Line 3 as a west-vergent thrust imbricate of the major terranes above an east-verging decollement above rocks of the North American craton (Fig. 1-2). The field trip follows SNORCLE Line 3 from Carcross to the Alaska border.

The area between Whitehorse and Skagway has a rich history of exploration and mining, with many of the discoveries dating back to the Gold Rush days. Near Whitehorse, mid-Cretaceous granitic intrusions of the Whitehorse plutonic suite produced Cu skarn mineralization along contacts with Lewes River limestone. This string of occurrences, the Whitehorse copper belt, was mined during two main episodes: between 1909 and 1920, and more recently from the early 1960s to 1982. Further south, Au-Ag veins related to Late Cretaceous to Eocene magmatism predominate. They are concentrated in two districts: Montana Mountain, south of Carcross (Stop 1-3) and the Wheaton District, northwest of Carcross (west of Grey Ridge and not visible from the highway).

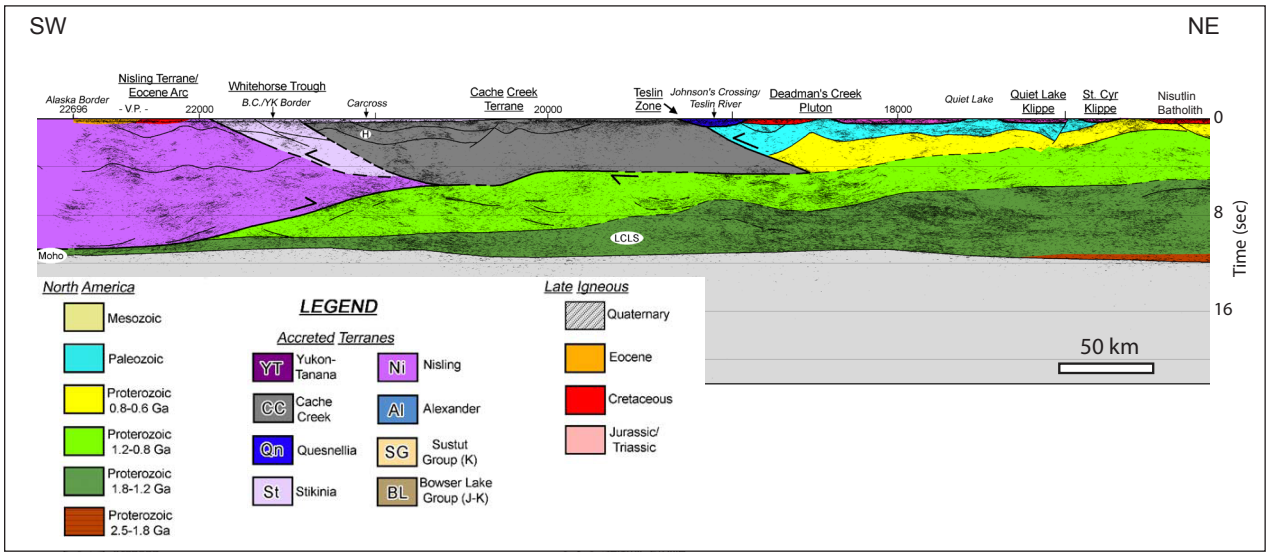

Figure 1-2. *SNORCLE Line 3 West was shot along the South Klondike Highway, the same route the field trip takes, between Carcross and the B.C.-Alaska border. Modified from Cook et al. (2004).*

The Klondike Highway – Whitehorse to Skagway

Stop 1-1 – km 94.8, Bove Island lookout – Cache Creek terrane

(description modified from Johnston et al., 1993)

To the southwest, across the Windy Arm of Tagish Lake, are spectacularly displayed, nearly vertical, southwesterly-directed, imbricate thrust faulted panels of upper Paleozoic Cache Creek (Horsefeed Formation) limestone, dolostone, marble and altered mafic volcanic rocks (Fig. 1-3). Abundant fusilinid collections suggest that they are dominantly middle Pennsylvanian to Early Permian and "younging" to the northeast. This structural style is typical of the Cache Creek, although younger normal and strike-slip faulting typically disrupt and further complicate the geology.

Bove Island is composed of middle Pennsylvanian carbonates with numerous thick sills/flows of altered mafic volcanic rocks. The carbonates contain a Tethyan ammonite which is also found in west Texas and the Canadian high arctic.

The road cut at this stop is composed of a white, slightly silicified marble which is cut by networks of black fractures and several near-vertical faults. It is locally intensely brecciated, contains evidence of ductile deformation, and may be representative of the rocks across the lake.

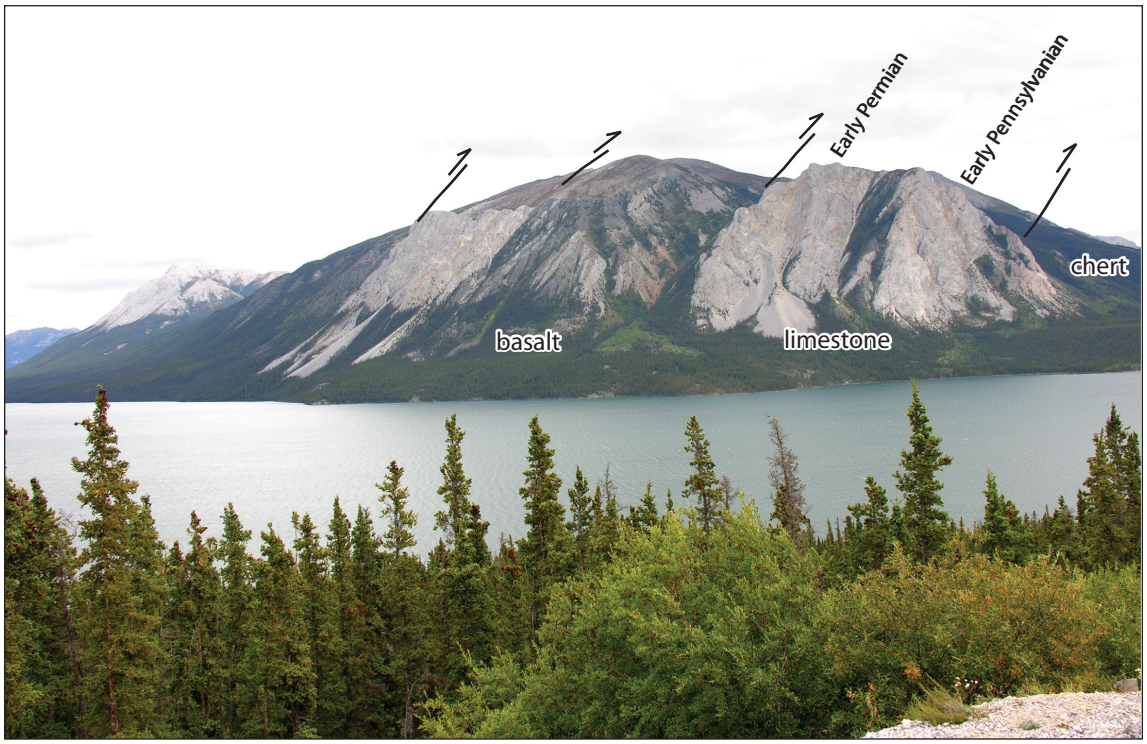

Figure 1-3. *From Bove Island lookout, a southwest-verging thrust imbricate of Cache Creek limestone, chert and basalt (from Energy, Mines Ministers Conference, 2006).*

Stop 1-2 – km 86.4, Venus Mill – historic gold mine

(description modified from Johnston et al., 1993)

The rocks in this region belong to the Montana Mountain volcanic complex. They are composed of dominantly andesitic volcanic rocks; the youngest rocks are rhyolite flows. The volcanic rocks were deposited unconformably on top of folded Whitehorse Trough strata. They are faulted against Whitehorse Trough strata to the south at Wynton Creek, and to the north against Cache Creek terrane along the reactivated trace of the Nahlin fault. Much of the complex is altered due to the extensive hydrothermal activity in the region and the intrusion of a granitic pluton (ca. 70 Ma).

Andesite and rhyolite from this volcanic complex yield U-Pb zircon dates of 95 and 84 Ma, respectively. The older age suggests these volcanic rocks belong to the Mount Nansen Group while the younger age is closer to that expected from the Carmacks Group. Plutons in the area have ages of 107 and 70 Ma.

History

Mineralized float was first discovered on the slopes of Montana Mountain by would-be miners on their way to the Klondike goldfields in the late 1890s. The polymetallic Venus vein was discovered by two young prospectors, Jack Stewart and Jack Pooly in 1900. This discovery caused a staking rush in the region which led to the discovery of several more similar veins. In 1904, Stewart and Pooly sold the Venus property to Colonel J.H. Conrad for $120,000! The colonel acquired, and did preliminary work on, most of the surrounding properties using the stock market to generate cash. By 1906, development work concentrated on three properties, including the Venus, and resulted in the building of the Conrad town site, aerial tramways up to 6.4 km long, and major underground development. Only the Venus mine produced ore. In 1917, D.D. Cairnes estimated that 6,000 tons of ore were mined between 1905 and 1912. In 1912, Colonel Conrad was forced into bankruptcy after spending $750,000 developing the properties.

The Venus vein has seen several phases of exploration and production. Prior to the 1980 production efforts, the Venus orebody hosted approximately 200,000 tons of 0.4 oz/t (11.4 g/t) Au, 7.5 oz/t (212.6 g/t) Ag and 3% combined Pb-Zn. Workings associated with this deposit can be seen on the hillside above the highway. The mill and the wooden buildings at the base of the mill were built on the shore ca. 1905 (Fig. 1-4). The ore was transferred between the different milling stages by gravity and the tailings were dumped into Windy Arm. Today the foundations of these buildings are partly submerged. This may be the result of 90 years of subsidence in the region behind the Coast Mountains which are currently being uplifted 2-3 cm/yr.

Figure 1-4. *Wooden structure at the site of the original Venus mill on the shore of the Windy Arm of Tagish Lake (from Energy, Mines Ministers, 2006).*

The Montana Mountain volcanic complex and associated rocks host greater than 20 gold-silver-lead-zinc-arsenic-bearing quartz veins. The largest of these, the Venus vein, has a strike length greater than 2 km with a northerly and northeasterly strike and a 45° northwesterly dip. Vein width is as much as 4 m but averages 1 m. The vein ends abruptly against the Nahlin fault which brings Cache Creek Group rocks into contact with the Montana Mountain and Stikinia rocks.

Looking across Windy Arm towards Escarpment Mountain, the rusty rhyolitic rocks at the south end are part of the Montana Mountain volcanic complex (Fig. 1-5). The north portion of the mountain is composed of Cache Creek greenstone with lesser chert. The fault zone which juxtaposes these two packages is the reactivated portion of the Nahlin fault, which is recognized as a terrane bounding fault between Cache Creek terrane and Stikinia. Montana Mountain volcanic rocks are also cut by this fault, hence it has been reactivated since the age of the youngest volcanic rocks (84 Ma).

To the south are the craggy peaks of Dall Peak. Its elevation is 1890 m.

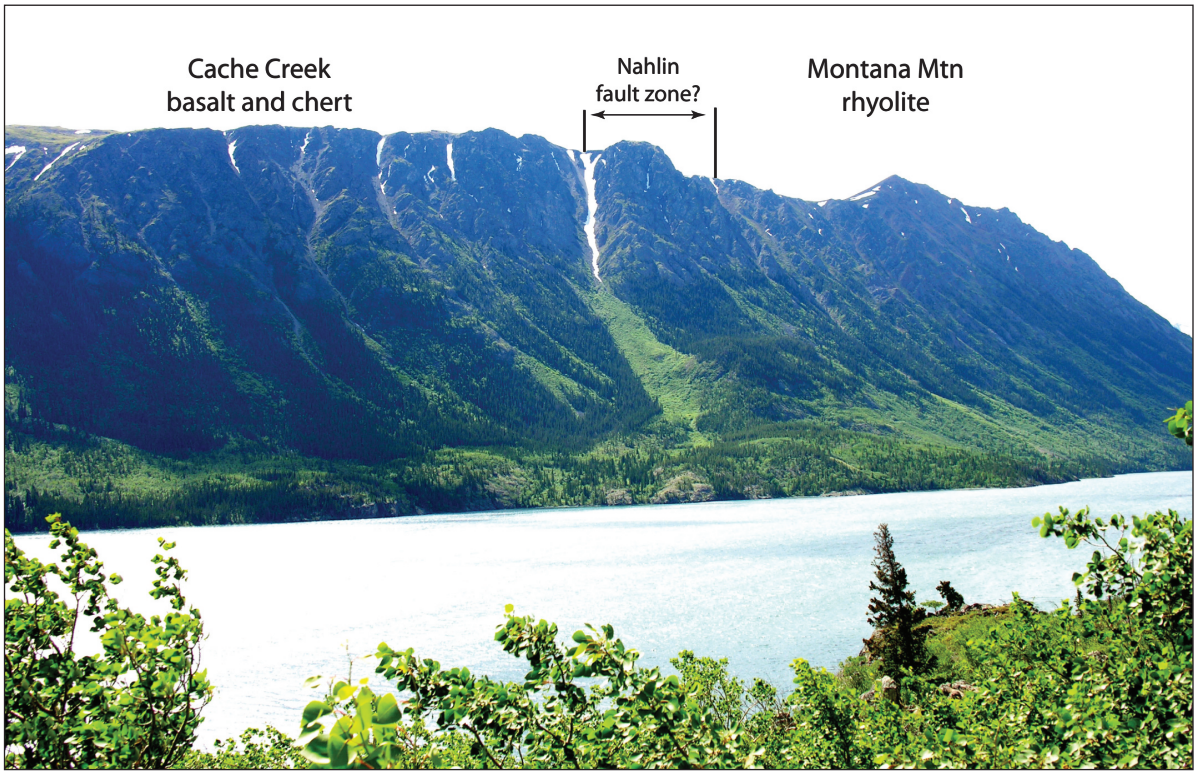

Figure 1-5. *View southeast towards Escarpment Mountain, where a reactivated segment of the Nahlin fault juxtaposes chert and basalt of the Cache Creek terrane with Late Cretaceous rhyolite of the Montana Mountain complex (from Energy, Mines Ministers, 2006).*

Stop 1-3 – km 56.3, Coast plutonic complex – Boundary Ranges metamorphic complex contact

(description modified from Johnston et al., 1993)

Overlooking Bernard Lake the vista to the east reveals an upland plateau flanked by mountains to the east and southwest. Easternmost limits of the plateau coincide with the eastern limit of granitic rocks of the Coast Mountains, known as the Coast plutonic complex (CPC). Mountains rising from the plateau to the east are underlain primarily by Mississippian and older Boundary Ranges metamorphic suite of the Yukon-Tanana terrane (Fig. A-1). The highest of these mountains in the near distance is Teepee Peak. It is capped by Eocene volcanic rocks which are in turn intruded by a coeval (comagmatic) stock dated by K-Ar at 55.3 ± 1.8 Ma. A very homogeneous pluton underlying the peaks in the southeast yielded a similar age.

At the pullout near the south end of Tutshi Lake, we drive across a fault contact between sedimentary and volcanic rocks of the uppermost Paleozoic to Mesozoic Stikine volcanic arc terrane and shallow marine sedimentary and volcanic rocks of the upper Paleozoic Yukon-Tanana continental margin arc terrane. Locally, these rocks are overlain by the Jurassic Laberge Group. Immediately south of the lake, we cross into granite of the Log Cabin pluton which intrudes the Stikine-Yukon-Tanana terrane contact. The Log Cabin pluton has a U-Pb zircon age of 72 Ma (Barker *et al.*, 1986) making it younger than the Laberge Group, which is in agreement with hornfels in the Laberge Group proximal to the Log Cabin pluton. This pluton is only a few kilometers from the eastern margin of the CPC, and is of similar age and composition, but whole-rock geochemistry suggests it is unrelated to the CPC (Barker *et al.*, 1986).

The Log Cabin granite is porphyritic, with phenocrysts of K-feldspar up to 5 cm in length, and a homogenous, coarse-grained pinkish-gray groundmass that contains 2-15% biotite and a trace of hornblende. Various element ratios indicate a calc-alkaline composition. Locally the granite is foliated and contains inclusions of biotite schleiren and fine-grained granite. Granite samples with ≥67% SiO_2 have higher K_2O, Rb and rare earth element (REE), and lower Sr_i contents than granitic rocks with the same silica content in the adjacent CPC to the west. The Log Cabin granite has a shallower chondrite normalized REE slope, and a lower $^{87/86}$ Sr_i ratio than do the granites to the west in the CPC. This led Barker *et al.* (1986) to infer that the Log Cabin granite has a different source than the other CPC granites. The $^{87/86}$ Sr_i ratio, at 0.7052, suggests minor assimilation of a 'short-lived' (late Paleozoic or Mesozoic) protolith (Barker *et al.*, 1986). These data support previous interpretations of two contemporaneous arcs in the Mesozoic (Godwin, 1975; Monger *et al.*, 1982). The Log Cabin granite may belong to the Late Cretaceous Casino suite, a volcanic-epizonal plutonic suite emplaced in the eastern arc, whereas Late Cretaceous rocks of different chemistry, and isotopic signatures on the west margin of the CPC may belong to the western arc.

History

Log Cabin, located at the north end of the Chilkoot trail, was a bustling community, with saloons and a hospital at the height of the gold rush. It was also an outpost of the Northwest Mounted Police for collecting duties on goods and monitoring treatment of pack animals. When the railroad was completed, the community no longer had a purpose and was soon abandoned.

The Log Cabin pluton is intruded to the south by the Summit Lake pluton, which is a pink to buff, medium-grained massive, homogenous leucocratic granite with sparse veinlets and pods of aplite and pegmatite. The granite has less than 5% biotite mafic minerals, 74-77% SiO_2, high K_2O and Rb, low Sr, and chondrite-normalized REE are light REE (LREE)-enriched with gentle slopes and a strong negative Eu anomaly (Barker *et al.*, 1986). On a plot of normative quartz-albite-orthoclase, the Summit Lake granite plots near the low-pressure, H_2O-saturated granite minimum, which combined with highly variable $^{87/86}Sr_i$ ratios ranging from 0.7048 to 0.7060, may be indicative of a partial melting origin (Barker *et al.*, 1986). A near-concordant U-Pb zircon age of 53 Ma is similar to a biotite K-Ar age of 52 Ma, suggesting rapid cooling and shallow emplacement (Barker *et al.*, 1986).

A large body of tonalite-granodiorite north of Summit Lake that yielded a U-Pb zircon age of 54 Ma is similar in composition to the tonalite-granodiorite suite of Skagway, and is intruded by the Summit Lake granite (Barker *et al.*, 1986). A tonalite-granodiorite body at White Pass is also intruded by the Summit Lake granite, and to the south of the Canada-U.S. border, the tonalite-granodiorite intrudes biotite-hornblende tonalitic orthogneiss. The orthogneiss yielded a zircon U-Pb apparent age of 61.7 Ma, a hornblende K-Ar age of 54.7 Ma, and a biotite K-Ar age of 49.4 Ma, which suggests resetting by the Skagway suite and the granites of Summit Lake and Clifton (Barker *et al.*, 1986). The orthogneiss has 57 to 69% SiO_2, high Al_2O3, Na_2O, Ba, and Sr, low to medium K_2O, low Rb, and chondrite-normalized REE with steep slopes that lack Eu anomalies (Barker *et al.*, 1986). The orthogneiss compositionally aligns with a diorite-tonalite-granite series, is geochemically compatible with fractionation from a high-Al basalt, and has $^{87/86}Sr_i$ ratios closely grouping at 0.7054 to 0.7058, indicating minor assimilation of crustal rocks (Barker *et al.*, 1986).

The tonalitic orthogneiss grades southward to migmatitic orthogneiss.

Stop 1-4 – km 18.4 (mile 11.5), Highway pullout north of Moore Creek bridge – migmatites

(description modified from Johnston et al., 1993)

Stop at the wide pullout on east side of highway just north of Moore Creek suspension bridge. Four phases of migmatite are present, from oldest to youngest they are: 1) foliated hornblende tonalite, 2) biotite hornblende granodiorite, 3) dikes of Clifton granite, and 4) dikes of plagioclase porphyritic andesite and amygdaloidal basalt. Textures in the migmatitic orthogneiss (Fig. 1-6) include wavy foliation, deformation and disruption of compositional banding, ovoid masses and irregularly shaped pods of agmatitic dark, hornblende-rich rock, deformed and disrupted xenoliths of metamorphic host rock, and pods and wavy dykes of aplitic, pegmatitic, and fine-grained trondhjemitic neosomes. The hornblende-rich ovoids may be “pillows” of basaltic magma that were injected into a tonalitic mush, and contain fractures filled with leucocratic melt (Barker *et al.*, 1986).

Figure 1-6. *Migmatite raft structures of the Coast plutonic complex from Tracy Arm.*

The migmatitic orthogneiss has identical composition and geochemistry to the nonmigmatitic tonalitic orthogneiss, and forms km-scale masses that are gradational to tonalite and tonalitic orthogneiss. Studies of migmatite in the CPC in the Juneau, Tracy Arm, and Petersburg areas identified compositionally and chronologically discrete phases of migmatite in the CPC, starting with 1) Late Cretaceous and Paleocene tonalite and tonalitic migmatite at ~70-60 Ma on the western margin of the CPC, intruded by 2) Paleocene K-feldspar porphyritic granodiorite and granodioritic migmatite that intrudes the tonalitic phases at ~56 Ma, all intruded by 3) Eocene granite with attendant leucocratic granite migmatite, and subsequently deformed, accompanied by the development of 4) leucocratic gneiss with aplitic-matrix migmatite at ~50 Ma (Karl and Brew, 1984; Karl *et al.*, 1996). The ages of the Skagway tonalite, tonalitic orthogneiss, the tonalite north of Summit Lake, and the Summit Lake granite are similar to those obtained for rocks of similar composition for more than 1000 km in the Coast Mountains of southeast Alaska and coastal British Columbia in the CPC (Fig. 1-7A, B).

Continue south on the highway

South of the Moore Creek bridge at mile 11 is a 50 m dike of fine-grained tonalite cutting the migmatitic orthogneiss, and just south of the runaway truck ramp is spectacular migmatite, but no safe place to park. The migmatite here includes four phases, from oldest to youngest: 1) agmatitic amphibolite and agmatitic amphibolite gneiss, 2) foliated hornblende tonalite of Skagway, 3) warped biotite-hornblende granodiorite dikes of variable thickness, and 4) vertical dikes of the Clifton granite, identical in age and composition to the granite of Summit Lake. These phases correspond to the first three migmatite phases in figure 1-7B; the youngest aplite-matrix leucogneiss phase is not recognized at this location. The Clifton granite has concordant U-Pb zircon ages of 48 Ma and miarolitic cavities indicating shallow emplacement of the granite body (Barker *et al.*, 1986). Calculations of aluminum content of hornblende in igneous rocks of the CPC indicate geobarometric pressures of 5 to 7 kb, which corresponds to depths of 20-25 km, for rocks with U-Pb zircon magmatic ages of 61.5 Ma and 60.4 Ma (Gehrels *et al.*, 1991b), and $^{40/39}$Ar plateau cooling ages of 57 Ma for hornblende (Karl *et al.*, 1996). Garnet-biotite-sillimanite geothermobarometric analyses of metamorphic rocks in the CPC also indicate pressures of 5-7 kb, at temperatures of 620-765°C (Karl *et al.*, 1996). These pressures and temperatures are consistent over a 35 km transect across the CPC in Tracy Arm; Al-in- hornblende calculations for 50 Ma plutons indicate emplacement at pressures of 2 to 3 kb,

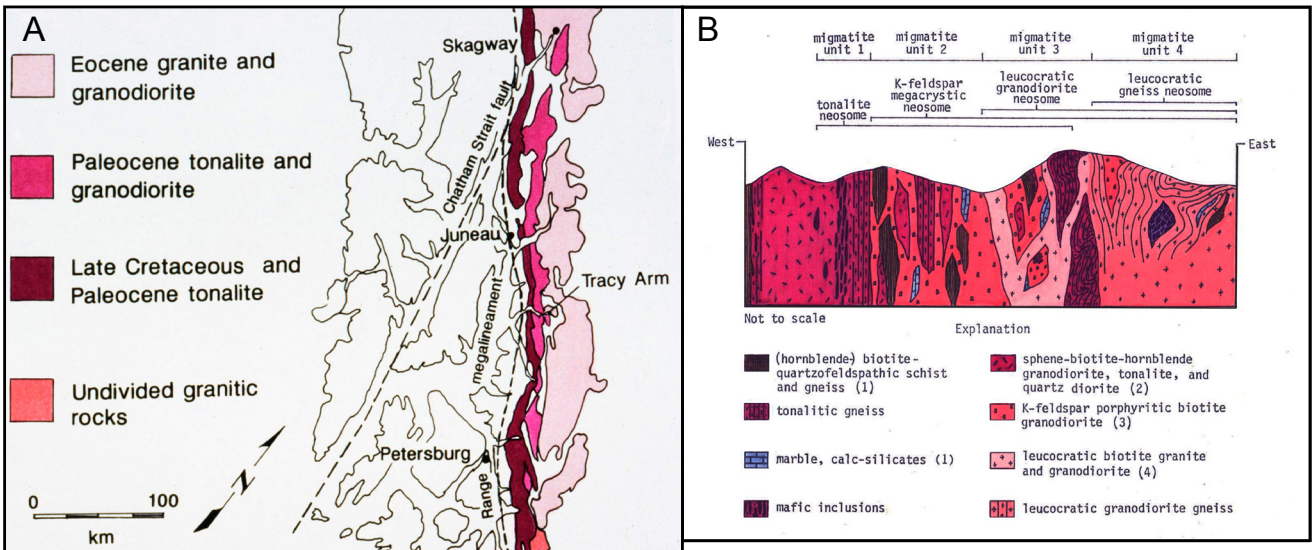

Figure 1-7. *A) Simplified geology of the Coast plutonic complex of southeast Alaska (Karl et al., 1996). B) Idealized cross-section through Coast plutonic complex of southeast Alaska (Karl et al., 1996).*

corresponding to depths of ~10 km (Karl *et al.*, 1996), suggesting rapid uplift without tilting of the CPC, and corroborating uplift rates of 2 mm/a in the same time interval for rocks in the CPC near Prince Rupert (Hollister, 1982).

At mile 9.5 the Clifton granite intrudes the migmatite with a swirly contact, and contains rafts of migmatite near the contact.

At mile 7.5 is K-feldspar porphyritic biotite granite of the Clifton granite, and this is the approximate location that yielded a U-Pb zircon age of 48.8 ± 1.0 Ma for the granite (Gehrels *et al.*, 1991b).

Mile 6.7, U.S. Customs Station

At mile 6.2 is the south contact of the Clifton granite with the Porcupine Creek body of the Skagway suite. To the south there are inclusions of schist, gneiss, and granofels in tonalite and granodiorite of the Porcupine Creek body. The tonalite and granodiorite are locally foliated, medium to coarse–grained, and contain common titanite as well as 15-20% hornblende and biotite of relatively equal proportions. Locally there are cross-cutting dykes of plagioclase porphyritic microdiorite. The tonalite and granodiorite typically have stubby hornblende prisms up to 15 mm long, and books of biotite up to 8 mm in diameter. The Skagway suite has 59-71% SiO_2, high Al_2O_3, moderate K_2O, high Sr, low Rb, chondrite-normalized REE that are LREE enriched with a moderate slope and small negative Eu anomalies, and a $^{87/86}Sr_i$ ratio of 0.7056 (Barker *et al.*, 1986). The Skagway suite also includes quartz diorite and granodiorite phases, part of the calc-alkaline diorite-tonalite-granite suite of the CPC, which is interpreted to consist of fractionates of a high-Al basalt with minor assimilation of crustal rocks (Barker *et al.*, 1986).

Just north of Skagway, granodiorite of the Burro Creek body of the Skagway suite yielded a U-Pb zircon lower intercept (crystallization age) of 57 ± 1 Ma (Gehrels, 2000). The reported upper intercept age of 1060 ± 150 Ma is an average inheritance age; all the samples Gehrels dated from the CPC have early Paleozoic to Proterozoic upper intercept (inheritance) ages (Gehrels, 2000).

Locally the migmatites and the intrusive rocks of the Skagway suite have a protoclastic overprint. Late protoclastic and cataclastic textures become more pervasive westward in the CPC.

Alaska Marine Highway – Skagway to Juneau

South of Skagway, granodiorite of the Skagway suite on the east side of Taiya Inlet yielded U-Pb zircon ages of 71 ± 2 Ma, and 63 ± 2 Ma (Gehrels, 2000). South and west of the Burro Creek and Taiya Inlet plutons are elongate foliated tonalite bodies commonly referred to as the tonalite sill suite (Brew and Ford, 1981), which forms the west margin of the CPC from at least the Ferebee pluton in Lutak Inlet to the Quattoon pluton in coastal British Columbia. The westernmost body of the Coast batholith at Skagway is the Ferebee pluton between the southern Taiya Inlet and Lutak Inlet. The Ferebee pluton consists of strongly foliated hornblende-biotite tonalite, hornblende diorite, and biotite quartz monzonite, with 15-20% mafic minerals, generally biotite dominant, and accessory titanite and garnet. The tonalite bodies are parallel to the fabric of marble, quartzite, and pelitic schist and gneiss that they intrude. Trains of elongate dioritic inclusions are common and aligned parallel to the foliation defined by mafic minerals, interpreted to indicate syndeformational emplacement of the tonalite (Ingram and Hutton, 1994). Tonalite from Lutak Inlet yielded a zircon U-Pb lower intercept crystallization age of 82.6 ± 2.4 Ma and an upper intercept average inheritance age of ~1130 Ma, and titanite yielded a concordant U-Pb age of 80.8 ± 1.0 Ma (Gehrels *et al.*, 1991b). Another tonalite on the shore of Lutak Inlet yielded a zircon U-Pb apparent age

of 68 Ma, and a quartz diorite yielded a hornblende K-Ar age of 60 Ma, and a biotite K-Ar age of 43 Ma (Barker *et al.*, 1986). East of Chilkoot Inlet, zircon from two localities yielded lower intercept crystallization U-Pb ages of 71 ± 2 and 70 ± 2 Ma, concordant U-Pb titanite ages of 70 ± 2 Ma and 65 ± 2 Ma, and upper intercept, average inheritance ages of ~1600 Ma and ~2000 Ma, respectively (Gehrels, 2000). Gehrels *et al.* (1991a) suggest the discrepancy in zircon crystallization ages may indicate composite intrusions. Ages of detrital zircons from the metamorphic host rocks of the CPC have age peaks very similar to those of Yukon-Tanana terrane and Laurentia (Gehrels, 2000; Gehrels and Kapp, 1998; Gehrels *et al.*, 1991a), and to ages of inherited zircons in igneous rocks of the CPC (Gehrels, 2000; Gehrels *et al.*, 1991b). Barker *et al.* (1986) suggest the K-Ar biotite age may record Eocene uplift of the CPC, as interpreted from a study of cooling ages of metamorphic minerals in southern British Columbia by Hollister (1982).

Mainland on east side of Chilkoot Inlet, Katzehin River

The steep walls that flank the Katzehin River on the mainland east of Chilkoot Inlet are composed of foliated tonalite. About 1 km south of the Katzehin River there is a km-scale lens of marble within the tonalite that is aligned parallel to the foliation of the tonalite. South of the marble the tonalite becomes increasingly migmatitic, and km-scale bands of foliated tonalite alternate with km-scale lenses of marble, calc-silicate gneiss, and garnet-quartz-biotite gneiss. The marble and gneiss lenses are screens of the host rocks to the tonalite, and are assigned to Yukon-Tanana terrane (Gehrels *et al.*, 1992). A tonalite sample east of the southern tip of the Chilkat Peninsula yielded a lower intercept U-Pb zircon crystallization age of 70 ± 2 Ma, an average upper intercept inherited zircon age of ~2000 Ma, and a concordant titanite age of 65 ± 2 Ma (Gehrels, 2000).

West side of Chilkoot Inlet, Chilkat Peninsula and Chilkat Islands

The Chilkat Peninsula is composed mainly of mafic volcanic flows, pillow basalt, volcanic breccia, and agglomerate, with subordinate tuff, volcaniclastic rocks, carbonaceous dark gray phyllite, and thin, meter-scale interpillow layers and lenses of gray and green chert and gray limestone. Trace element geochemistry of the basalts indicates they are LREE-enriched, high Nb-Ta basalts that plot in E-MORB and within-plate fields on various trace element diagrams (Davis and Plafker, 1985; Ford and Brew, 1993; Gehrels and Barker, 1993). A limestone lens less than a meter thick in pillow basalt contains *Halobia* and ammonites of Carnian age, and overlying calcareous wacke contains conodonts of latest Carnian to earliest Norian age (Plafker *et al.*, 1989). Thin-bedded limestone with volcaniclastic layers that overlies the basalt indicates a sub-wavebase, quiet marine, basin or slope depositional environment. Disconformably overlying the calcareous wacke is a 15 m section of gray to black chert with lenses of carbonate that contains late Norian to possibly Early Jurassic radiolarians (Plafker *et al.*, 1989). Columnar jointed basalt, pillow basalt, and subordinate bedded limestone and clastic rocks of probable similar Triassic age underlie the Chilkat Islands and Eldred Rock to the south of the Chilkat Peninsula. Based on age, composition, and trace element geochemistry, these rocks have been assigned to the Wrangellia terrane (Davis and Plafker, 1985; Ford and Brew, 1993; Gehrels and Barker, 1993; Plafker *et al.*, 1989). Restoration of as much as 18 km of dextral offset on inferred splays of the Chatham Strait fault in Chilkoot Inlet place these basalts along strike with the basalts of Lion's Head, which have identical

trace element chemistry to the Chilkat basalts, and which are also assigned to Wrangellia (Ford and Brew, 1993).

East of Eldred Rock

On the mainland east of Eldred rock, the western contact between the tonalite, banded marble, and quartz-biotite gneiss of the CPC and Yukon-Tanana terrane host rocks and the massive metabasite of the Wrangellia terrane is a steep cataclastic shear zone, which is at least 10 m wide at this location. Tonalite near this contact yielded a lower intercept U-Pb zircon age of 71 ± 2 Ma, an average upper intercept age of ~1600 Ma, and a concordant U-Pb titanite age of 70 ± 2 Ma (Gehrels, 2000). This tonalite may not be the oldest or lowest component of the CPC at this location because the amount of relative offset on this shear zone is unknown.

The west margin of the foliated tonalites of the CPC is invariably a broad m- to km-scale shear zone. An inverted metamorphic gradient (Himmelberg *et al.*, 1991; Ingram and Hutton, 1994) supports early west and southwest-directed thrusting along the west margin of the batholith until ~59 Ma, followed by dextral transpression and exhumation (Andronicos *et al.*, 2003; Andronicos *et al.*, 1999). This change in tectonic setting is attributed to a change in relative plate motion between the Kula and North American plates between 57 and 54 Ma (Lonsdale, 1988; Struik, 1992), and resulted in Eocene crustal extension and widespread magmatism (Andronicaos *et al.*, 2003). The conceptual thrust fault that marks the base of the CPC and its host rocks of Yukon-Tanana terrane is the Sumdum fault (Gehrels *et al.*, 1992). The transition to dextral transpression in the Paleocene resulted in the evolution of a broad regional shear zone, referred to as the Coast shear zone (CSZ; Crawford *et al.*, 2000; Klepeis *et al.*, 1998). The CSZ consists of 1) a km-scale northeast-dipping flattening and shear fabric with top to the west sense of transport, and 2) a km-scale vertical shear fabric with vertical stretching lineations and a west-side up sense of displacement which marks the western margin of the CSZ (Klepeis *et al.*, 1998). This fabric deforms plutons as young as 65 Ma, but not the Quattoon pluton, which is 58 Ma (Crawford *et al.*, 2000; Klepeis *et al.*, 1998). At the latitude of Juneau, the Sumdum thrust fault places Yukon-Tanana terrane and the Coast batholith over the rocks assigned to Wrangellia and the Taku terrane. The CSZ is a younger structure which locally truncates the Sumdum fault south of Berners Bay, and a 10-meter-thick shear zone marks the contact between Late Cretaceous foliated tonalite and the greenstone at Lion's Head above Kensington, which has been assigned to Wrangellia (Ford and Brew, 1993; Gehrels *et al.*, 1992).

Lion's Head

The break in slope below Lion's Head is underlain by the Kensington megashear (Redman *et al.*, 2003). The megashear is part of the CSZ and cuts across all rocks of Wrangellia, the Jualin diorite that intrudes Wrangellia, and the sedimentary rocks of the Gravina belt, and it does not form a primary or exclusive contact between any of these rock units. The Ivanhoe, Horrible, Kensington, Comet, and Jualin Au- quartz vein deposits are all located on splays or conjugates of the Kensington megashear (Redman *et al.*, 2003). Approximately three kilometers to the southwest, the Sweeney Creek-Slate Creek shear zone, an extension of the vertical Gastineau shear zone, also known as

the Coast Range megalineament (Brew and Ford, 1978), is parallel to the Kensington megashear, and cuts through Gravina belt sedimentary rocks with an unknown amount of offset. There is no mineralization identified in association with the Gastineau shear zone west of Berners Bay.

Berners Bay to the ferry dock in Auke Bay

Passing Berners Bay, cruising down through Favorite Channel, we are flanked by Douglas Island volcanics to the east, consisting of fairly homogenous augite porphyritic basalt flows. Benjamin and Sentinel Islands are made up of augite porphyritic basalt, and the mainland north of Eagle River is composed of pillow basalt that contains lenses of red chert. To the west, Shelter Island is underlain by phyllitic graywacke turbidites flanking massive polymictic conglomerate that forms the spine of the island. The conglomerate comprises the Shelter Formation and is inferred to underlie the basalt unit and correlate with polymictic conglomerate of the Seymour Canal Formation. The conglomerate is thick-bedded to massive, containing well-rounded, poorly sorted pebbles and cobbles of argillite, graywacke, limestone, marble, felsite, vein quartz, chert, greenstone, granite, and quartz diorite in a graywacke matrix. On Gravina Island, basal conglomerate contains Buchia of Kimmeridgian (Late Jurassic) age (Berg, 1973), and west of Berners Bay, conglomerate that unconformably overlies the Jualin diorite contains detrital zircons that have concordant U-Pb ages of ~105 Ma (Gehrels, 2000). Sedimentary rocks of the Gravina belt have detrital zircon age populations that indicate sources from Yukon-Tanana, Wrangellia, Taku, and Alexander terranes (Kapp and Gehrels, 1998). The shoreline of Auke Bay is underlain by alternating augite porphyritic mafic volcanic rocks and greywacke turbidites.

Gastineau Channel and Douglas Island

Sedimentary and volcanic rocks of the Gravina belt to the southwest of the Gastineau shear zone on Douglas Island host the mineralized Treadwell diorite. Dykes and sills the Treadwell diorite, which yielded a concordant U-Pb zircon crystallization age of 91 ± 2 Ma, intrude black phyllite, and thus provide a minimum age for the Treadwell slates and Douglas Island volcanic rocks (Gehrels, 2000). Late stage potassic alteration of the Treadwell sills is associated with pyrite and chalcopyrite with high Cu-Mo-Au contents, defining an early Late Cretaceous Au-mineralizing episode (Newberry *et al.*, 1995; Karl *et al.*, 2010). Later albite-carbonate-quartz-pyrite metamorphic alteration at Treadwell is associated with mineralized main stage Au-quartz veins that cut earlier fabrics and yielded sericite $^{40/39}$Ar ages of 55 to 56 Ma, 35 Ma younger than the gold-bearing intrusive host rocks (Karl *et al.*, 2010b; Miller *et al.*, 2000; Newberry *et al.*, 1995).

Rocks of the Gravina belt overlap rocks of Yukon-Tanana, Wrangellia, Taku, and Alexander terrane affinity, and were deposited in the oceanic basin between the Insular and Intermontane terranes that collapsed during accretion of the Insular terranes in the Late Jurassic to Late Cretaceous (McClelland and Mattinson, 2000). The Mesozoic and Paleocene contractional structures are shuffled by Eocene dextral strike-slip structures such as those that run up Gastineau Channel and juxtapose Gravina belt deposits of different age and metamorphic grade (Miller *et al.*, 1994; Miller *et al.*, 2000; Miller *et al.*, 1995).

DAY 2 – KENSINGTON MINE TOUR

Daily summary

4:15 am depart hotel for Coeur Alaska bus staging area on Engineers Cutoff Road. Transportation to the mine site consists of a 45 minute bus ride followed by a 45 minute ferry ride, and another 15 minute bus ride. We will arrive at the mine site 6:45 am. The tour will finish at 4:45 pm when we will begin the trip back to Juneau. We should arrive at the hotel at 6:30 pm. There is an optional hike to see the Glory Hole and host rocks of the historic Alaska-Juneau (AJ) gold mine after dinner. We will be staying at the Travelodge again tonight.

Daily schedule:

4:15 am – van departs hotel lobby

4:30-6:30 am – travel to Kensington mine

6:30-7:30 am – breakfast followed by safety briefing

7:30-8:30 am – geology overview talk/maps

9:00-10:30 am – surface tour Jualin vein

11:00-2:00 pm – underground tour of Kensington and Raven veins

2:30-4:00 pm – core viewing

4:00-4:45 pm – wrap up talk, discussion etc.

5:00-6:30 pm – travel from mine back to hotel

7:00-8:00 pm – dinner

8:00-10:00 pm – optional visit to Last Chance Museum and hike up the Perseverance trail

Introduction

The Kensington mine is located at the northern end of the Juneau gold belt, within the Berners Bay gold district, 75 km northwest of Juneau, Alaska (Fig. A-6). The belt hosts more than two hundred quartz-gold vein prospects and several major producers, such as Kensington, Jualin, AJ, Treadwell, and Sumdum Chief. Prior to 1945, the Juneau gold belt produced 6.7 million oz (190 t) of gold with 65,000 oz (1.84 t) from the Berners Bay gold district. Current gold production within the Juneau gold belt is restricted to the Kensington mine, which since 2010 has produced approximately 570,000 oz (16.2 t) Au (January 11, 2016 news release).

The Kensington property is located near the boundary of the Insular and Intermontane terranes with the local geology made up of greenschist facies mafic volcanic and sedimentary rocks intruded by the 105 ± 1 Ma Jualin diorite, both unconformably overlain by weakly metamorphosed siliciclastic sedimentary rocks of the Gravina belt (Fig. 2-1; Gehrels, 2000). The metamorphosed mafic volcanic rocks are assigned to

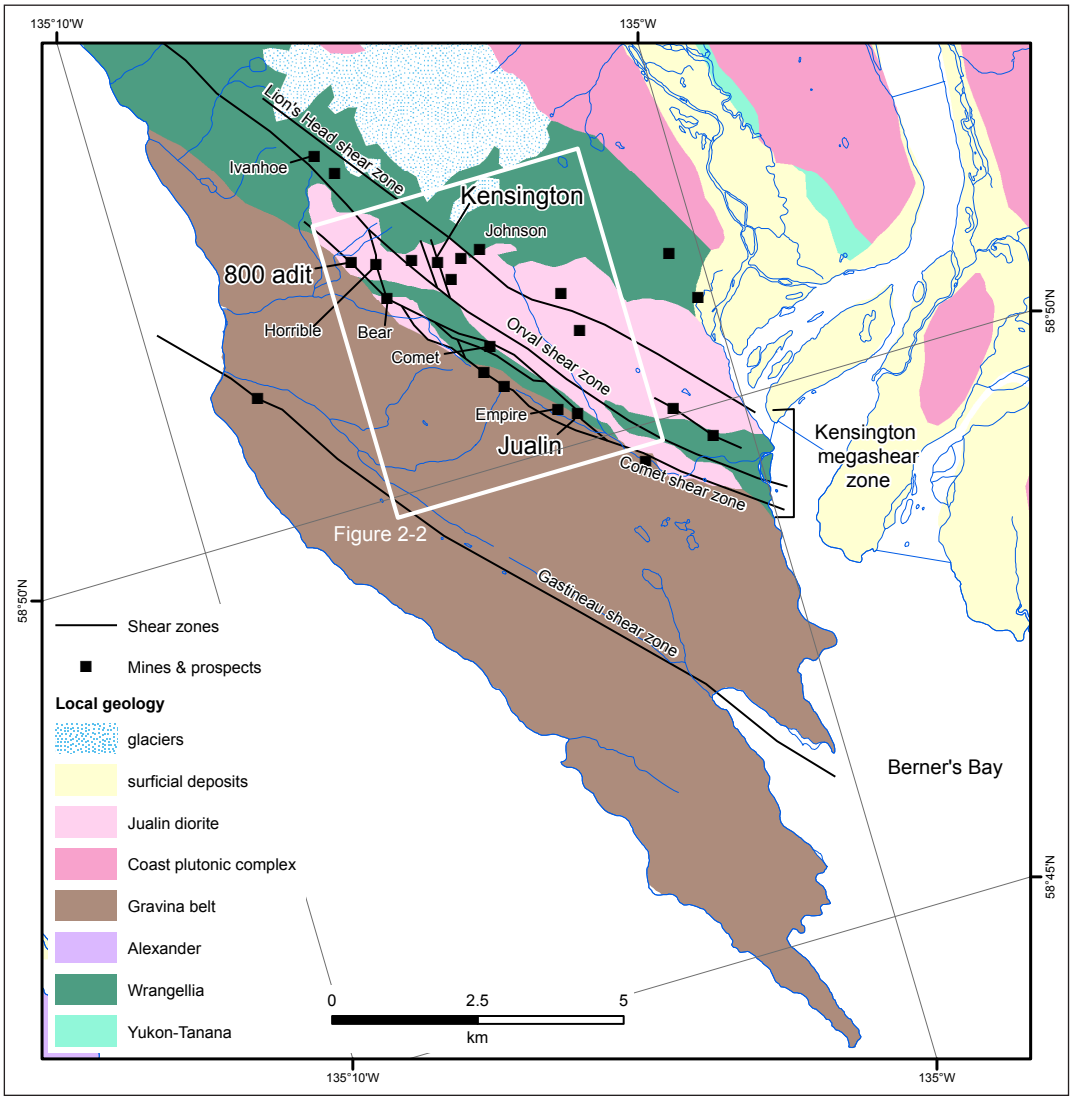

Figure 2-1. *Regional geology map of the Berners Bay area. Geology from Wilson et al. (2015), shear zones, mines and prospects from Redman (1988) and Redman et al. (2003).*

Wrangellia (Gehrels *et al.*, 1992) and are primarily porphyritic basalt with plagioclase phenocrysts up to 5 mm long. Remnant pillow textures are evident in outcrop and core. Locally, the sedimentary rocks of the Gravina belt are phyllite and slate, with minor conglomerate (Fig. 2-2; Gehrels, 2000). The Kensington deposits are dominantly hosted within the Jualin diorite, a medium-grained quartz monzodiorite to diorite that can be locally porphyritic with phenocrysts up to 1 cm. The pluton is mostly unaltered to weakly propylitically altered, and shows variable degrees of sericitic, potassic, and albitic alteration with proximity to the vein system. White mica $^{40/39}$Ar ages in the Juneau gold belt indicate orogenic gold mineralization occurred over a several m.y. period in the early Paleogene (Goldfarb *et al.*, 1991; Miller *et al.*, 1994). Current work on the Kensington property is focused on three main vein systems: Kensington, Jualin, and Raven (Fig. 2-2).

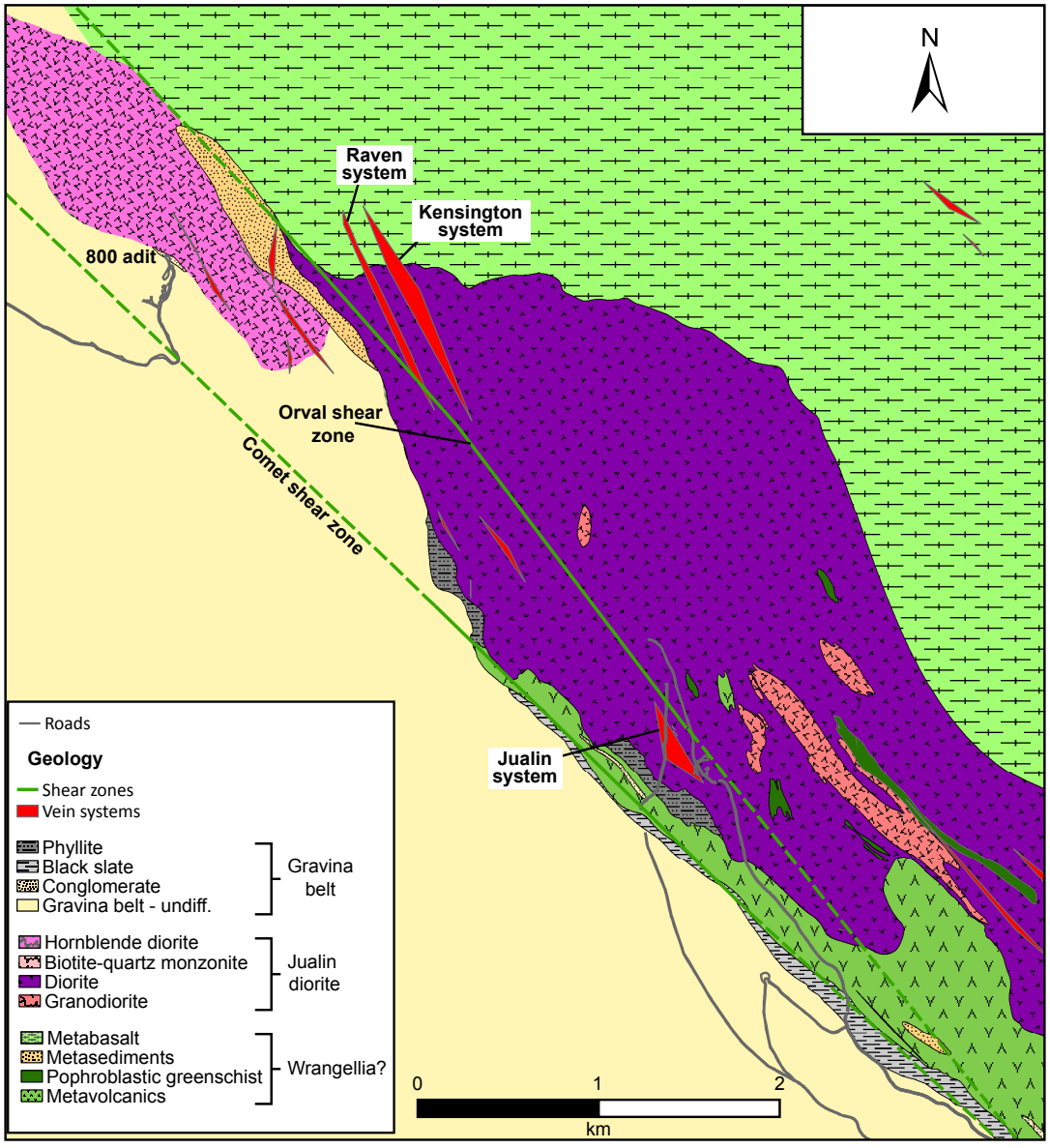

Figure 2-2. *Geology map of the Kensington mine area, prepared by Kensington Exploration Department, March 1, 2016, with contributions from Caddy and Redman (1988, unpublished mapping); Avalon (2005, unpublished mapping), and Coeur Mining (2012-present, unpublished mapping).*

Kensington system

The Kensington deposit is a gold vein system hosted within the Jualin diorite (Fig. 2-1). The mineralization is hosted in two types of veins: shear veins and extensional veins (Fig. 2-3 and 2-4). The shear veins are the controlling ore structures and they trend north-northwest, dip east, and have a shallow southern plunge. Extensional veins occur in high densities between the vertically stacked shear veins, often at conjugate angles. The combined vein packages have an average 350 azimuth and dip approximately 55° east. The vein packages have been separated into domains, or zones, for mining and resource purposes, but their combined thickness is 10 m with an estimated strike of 660 m. White mica $^{40/39}$Ar ages from shear veins in the Kensington system range from 54.0 to 56.4 Ma and tension veins range from 53.5 to 54.1 Ma, similar to ages elsewhere in the Juneau gold belt (Miller *et al.*, 1994).

Alteration is restricted to a small, less than 3 m halo around veins and is generally sericite with local zones of potassic alteration. The mineralization is hosted in pyrite-bearing quartz ± carbonate veins. The ore is generally associated with fine-grained pyrite and most commonly presents as calaverite ($AuTe_2$) with lesser amounts of native gold (Au) and petzite (Ag_3AuTe_2). Tellurium is the only reliable indicator element for gold in this system. Occasional occurrences of chalcopyrite and molybdenite can be seen.

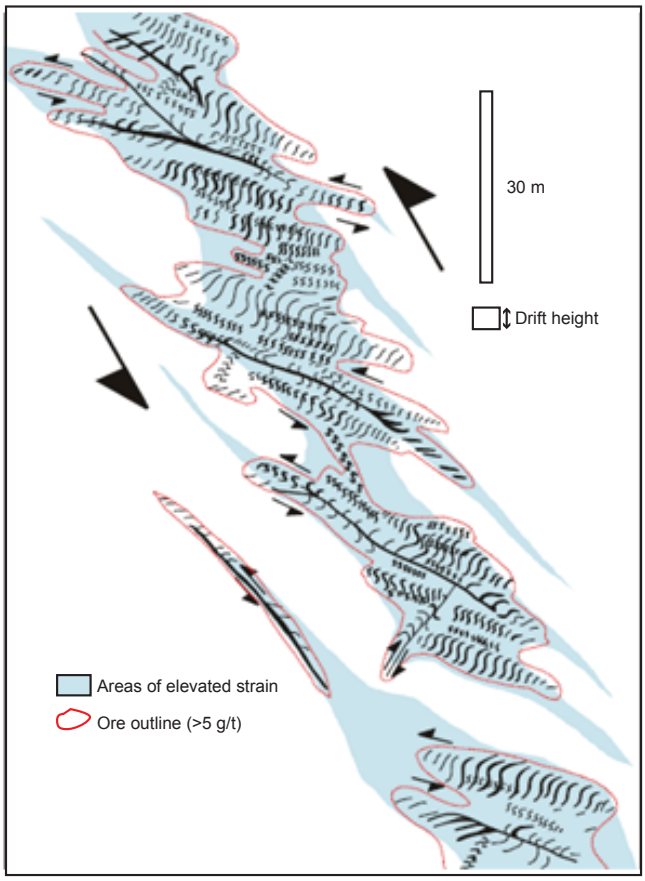

Figure 2-3. *Schematic cross-section of the relationship between shear veins and extensional veins in the Kensington system (Rhys, 2008).*

Figure 2-4. *Kensington fault-fill breccia vein, Juneau gold belt (Goldfarb et al., 2005).*

Raven system

The Raven deposit is also a quartz-gold vein system, located 600 m west of the Kensington vein system (Fig. 2-5). The veins are hosted in several lithologies, including the Jualin diorite, a hornblende monzonite, and a small sliver of the Gravina belt sedimentary rocks (Fig. 2-2). The system is comprised of two discrete mineralized vein sets. The mineralized veins strike northwest between 355 and 320, and dip to the east at approximately 55°, whereas unmineralized extensional veins are oblique and found within 30 cm to 60 cm of the mineralized veins. The average strike length of the veins is 480 m. The veins pinch and swell, but generally range between 1.5 m and 2.5 m in thickness.

The alteration associated with the veins is restricted to a 30 cm to 10 m halo dominated by sericite ± ankerite. The mineralization is hosted in pyrite-bearing quartz ± carbonate veins. The ore presents both as gold-tellurides (generally calaverite or petzite) associated with fine-grained pyrite and as free gold with less obvious relation to pyritic zones.

Correlations for the Raven system are more complex than those within the Kensington system, although the same strong correlation with tellurium is present. The Raven veins contain both galena and chalcopyrite, but correlation coefficients suggest an inverse relationship between Au and Pb and a moderate correlation between Au and Cu. Additional sampling is required within the Raven deposit to clarify these relationships.

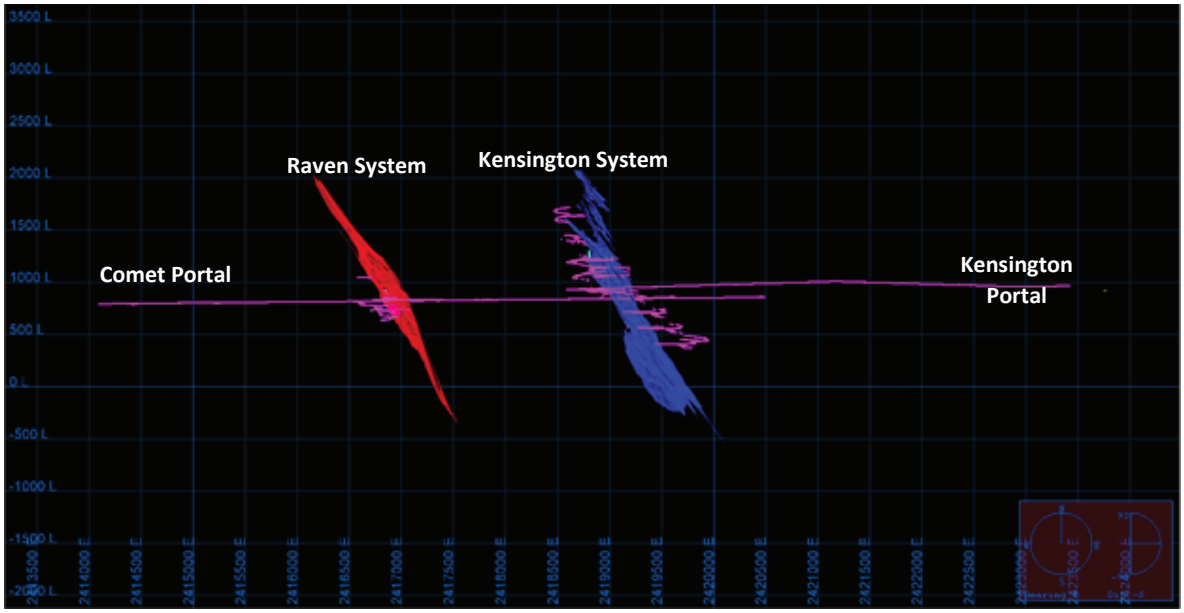

Figure 2-5. *Cross section of the Kensington mine workings, looking north, depicting the location of the Kensington and Raven deposits. Raven veins are merged to represent vein average azimuth. Elevation and grid coordinates are in feet.*

Jualin system

The Jualin deposit is also a quartz-gold vein system, located 360 m south of the Kensington deposit. The system is hosted within the Jualin diorite, which is overlain by Gravina belt sedimentary rocks toward the south (Fig. 2-2). The Jualin system consists of at least four stacked, en echelon, sheeted veins (Fig. 2-6). The first three veins (Veins 1, 2, and 3) nearest the surface were mined between 1880 and 1920. Veins 1, 2, and 3 produced approximately 45,000 oz (1.28 t) of gold. Vein 4 is currently being brought into production, development began on a decline in September of 2015 and is projected to reach the vein in August of 2016. A fifth vein, Vein 5, has been intercepted, but its extent has not been established.

The most recent exploration of the Jualin system focused on Vein 4. All the information provided below relates exclusively to this vein. Vein 4 ranges between 3 cm and 4 m in thickness, but is generally between 2 m and 2.5 m in thickness. The vein is typically a single, massive vein but it can separate into two or three veins within a mineralized zone. Vein 4 has a strike length of 284 m, and is open to the south and down dip.

Alteration is a narrow envelope extending between 30 cm and 3 m from the vein. Sericite ± ankerite are the most common alteration minerals proximal to the veining, but localized albitization has been identified based on ragged, secondary white feldspars. Potassic alteration is not as pronounced in the Jualin system as it is within the Kensington system.

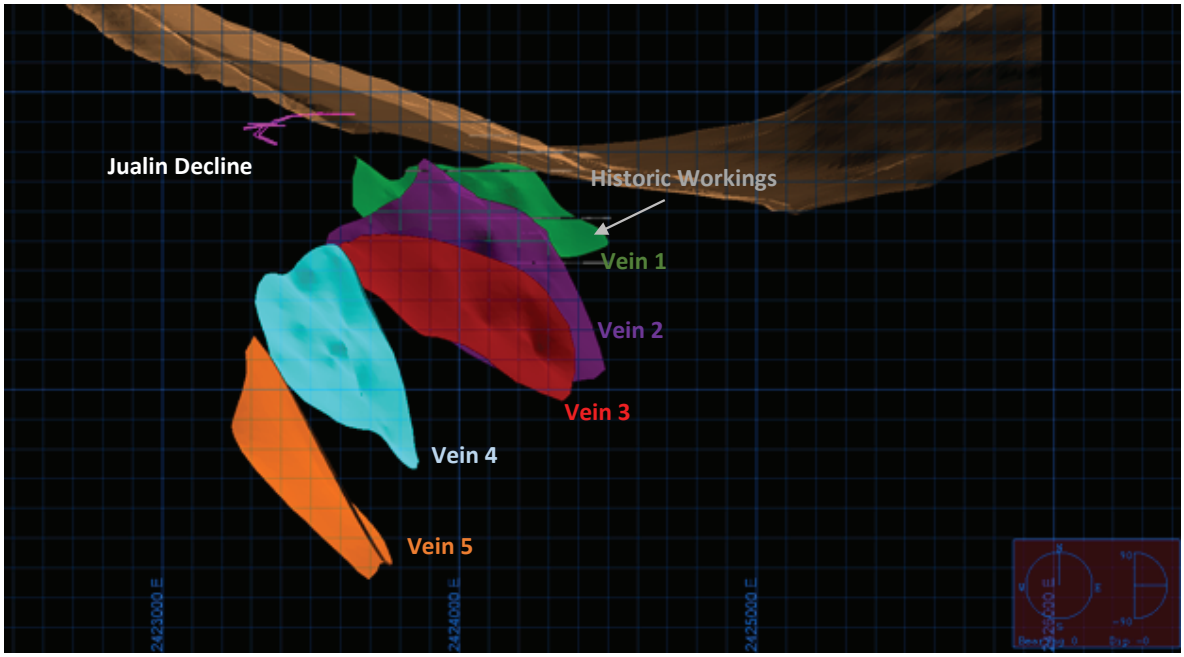

Figure 2-6. *Cross section of the Jualin deposit, looking north. Grid coordinates in feet.*

Gold is hosted within quartz ± carbonate veins primarily as native gold smaller than 100 μm. Average gold grades within the Jualin system generally exceed those found in Kensington and Raven. Gold grades greater than 15 g/t are common. The correlation with tellurium is less pronounced in the Jualin system and base metals play a larger role as gold indicators. Moderate correlations exist between Au, As, and Pb. The system has moderate Cu values, with Cu mainly in chalcopyrite, but the correlation coefficients suggest an inverse relationship. The Jualin veins have less pyrite than the Kensington or Raven and often contain tennantite, galena, sphalerite, and chalcopyrite.

Discussion

The Kensington area hosts three major quartz-gold vein deposits (Kensington, Raven, and Jualin) and several promising prospects. The systems share many characteristics and are likely related to each other, but unique characteristics exists within each. The deposits all trend north northwest, dip to the east, are dominantly hosted within the Jualin diorite, and all correlate strongly with tellurium.

The Kensington deposit does not contain significant base metals, with mineralization occurring almost exclusively as gold-tellurides in both massive shear veins and extensional veins. Gold shows trace element correlations with Te and Bi.

The Raven deposit is hosted in three different lithologies, has consistent Au-Cu correlation, contains no significant extensional veining, and mineralization occurs as gold-tellurides and as native gold.

The Jualin deposit is composed of vertically stacked veins with no significant extensional veining, has As-Au and Pb-Au correlations, and occurs primarily as native gold.

The Kensington deposits are generally interpreted to be of orogenic origin. However, variation in the geochemical signatures between the Raven and Jualin deposits suggests the possibility of intrusion-related mineralization or remobilization. The Kensington deposit shows no base metal to gold correlation and contains dominantly Au-Te mineralization and minimal base metal minerals. The Raven and Jualin deposits contain significantly more base metal sulphides and native gold. The correlation of base metals to gold suggests a decrease in the temperature of mineralizing fluid from northwest (Raven) to southeast (Jualin). Recent surface mapping and sampling efforts have identified a pluton, unrelated to the Jualin diorite, adjacent to and northwest of the Raven deposit. The age of the pluton has yet to be established, but lack of alteration suggests it is younger than the Cretaceous Jualin diorite. This intrusion may have played some role in the distribution of mineralization on the Kensington property, but additional study is required to determine the nature and extent of its influence.

Day 2 – Alaska Juneau deposit

Take a 15-minute drive up Gold Creek from downtown Juneau to the Last Chance Basin and park at the Last Chance Gold Mining Museum (Fig. 2-7).

The museum is located in the AJ mine's compressor building, and it is crammed with mining equipment, maps, photos, and rocks. The Perseverence trailhead also starts from the parking lot. We can hike up the Perseverence Trail as far as energy and time allow. From the museum to Ebner Falls is 800 m, with relatively fresh blasting along the trail to make it wider, so there are good exposures of the Perseverence Slate and the metalliferous quartz veins that it hosts. If we have time and energy, the Red Mill Trail takes off from the Perseverence Trail beyond Ebner Falls, for a view of the Glory Hole (Fig. 2-8). The total loop to the Glory Hole, starting and finishing at the parking lot is a total of 6.4 km. It will be approaching the solstice, so our limiting factor will not be available daylight, but our 4 am start the next morning.

History

Mining engineer and entrepreneur George Pilz learned from John Muir's notes that natives in the Auke Bay area were using gold-tipped bullets, and sent prospectors Joe Juneau and Richard Harris to look for gold. This dynamic duo traded their grubstake from Pilz for native hooch and returned empty-handed. Pilz remarkably had faith in them and sent them back. Auke Tlingit Chief Kaa wa.ee led the prospectors to Silverbow Basin, where they found placer gold and staked the first claims in 1880. This discovery initiated the Juneau gold rush, resulting in the two largest and lowest grade, lode gold mines in the world at that time: AJ and Treadwell.

The Perseverence Slate hosts the AJ and associated mines in the Silverbow basin (Fig. 2-7). The Perseverence Slate consists of dark gray, graphitic slate and phyllite that is well foliated and lineated, and contains sparse fine-grained quartzose layers, thin black, locally fossiliferous limestone layers, and meter-scale lenses of conglomerate. The slate alternates with thick sections of green phyllite. Fossils include Late Triassic ammonites and halobiid bivalves (Martin, 1926), but these collections have no species in common with the ammonites and halobiids on the Chilkat Peninsula (Plafker and Hudson, 1980). The slate unit overlies volcanic rocks of the Gastineau Group in the Juneau area, and locally overlies fossiliferous black limestone of Permian age in Holkham Bay. The Perseverence Slate extends from Juneau to Holkham Bay, essentially for the length of the Juneau gold belt and includes all of the important mineral deposits in the Juneau lode system (Twenhofel, 1952).

The Silverbow fault that crosses Silverbow basin and runs parallel to Gold Creek divides the north and south orebodies of the AJ mine: the north orebody is the Ebner mine and the south orebody is the Perseverence mine, and the location of the Glory Hole. The gold-bearing quartz veins are stringer vein networks hosted by ductile-brittle and brittle shear zones; in general the orebodies dip to the northeast parallel to the regional dip of the slate and metagabbro sills (Twenhofel, 1952). The veins are a few cm to a meter in width, and extend as much as a hundred meters along strike, cutting both the slate and the sills. The slate is nonreactive; the gabbro sills are intensely altered and barren of metal. The mineralized veins are more than 95% quartz and contain ankerite, pyrrhotite, arsenopyrite, galena, sphalerite, and minor pyrite typically near the vein contacts with wallrock. Gold was last to crystallize and also occupies fractures in the wallrock adjacent to the quartz veins (Twenhofel, 1952).

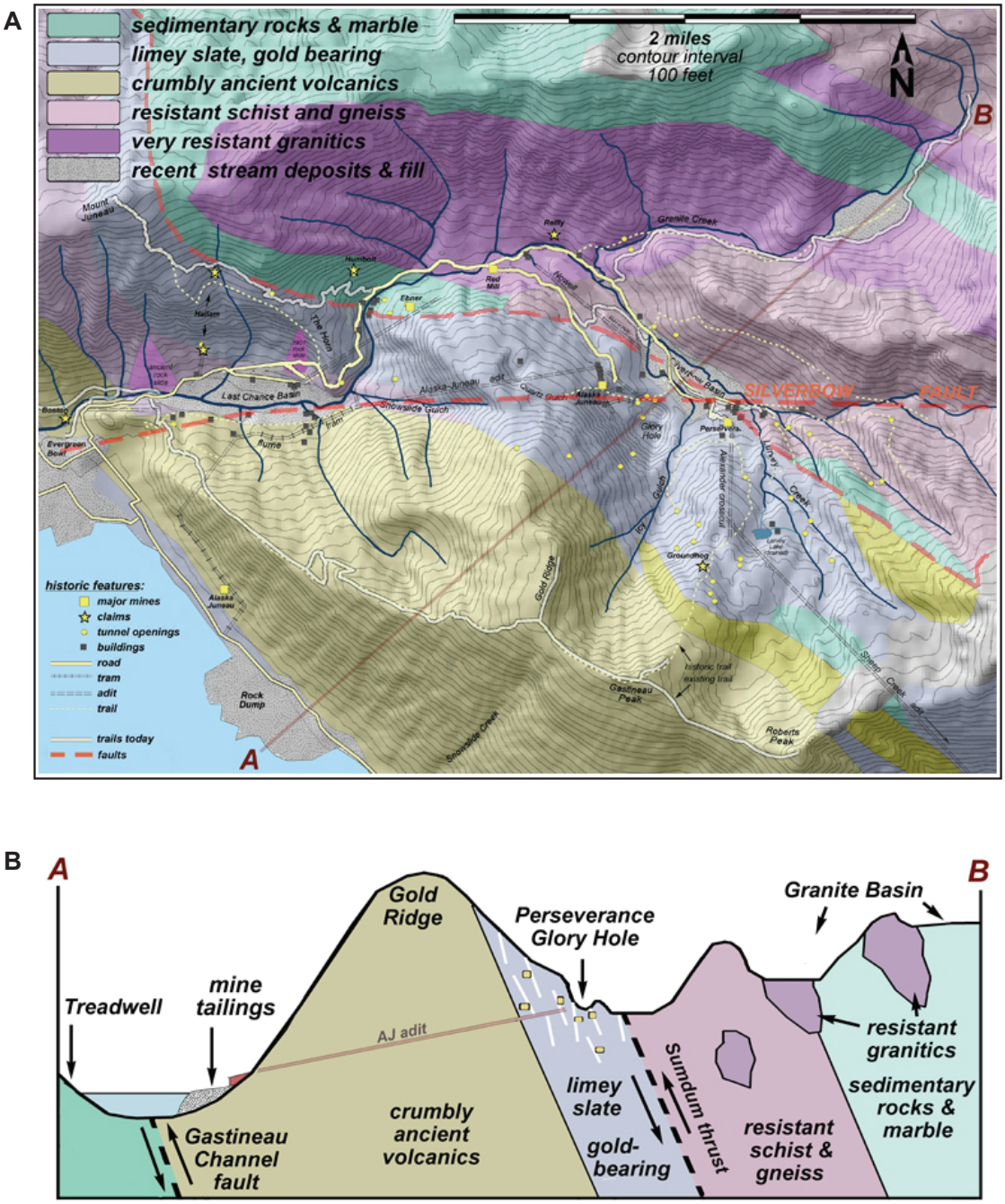

Figure 2-7. *A) Bedrock geology of Juneau area (from www.juneau.org/parkrec/trails/gold.php). B) Cross section looking NW, location shown on A. The AJ ore was delivered through the 2.5 mile (4 km) adit to the mill facilities on the shore of Gastineau Channel. After processing, the tailings were dumped in the channel, creating the rock dump visible today. Granite basin is one of the few places where the granitoids of the Coast plutonic complex can be seen on Juneau area trails; most of these rocks are found further northeast where they form the high peaks of the Juneau icefield. (From www.juneau.org/parkrec/trails/gold.php).*

The AJ Gold Mining Company was first organized as an agglomeration of 23 claims on May 6, 1897. Drilling started in 1911 to access ore in Silverbow Basin, and 108 miles (173 km) of tunnels were blasted out of hard rock to develop the Deep North ore body. A mill was built in Last Chance Basin above Gold Creek and a camp was established between the ore body and the mill. Mining operations continued until April 9, 1944, when the mine was closed due to the low price of gold and a shortage of men during WWII. Between 1880 and 1944, 2.9 Moz Au (82.2 t), 1.9 Moz (54 t) Ag and 1140 t Pb were recovered from the AJ deposit (Redman, 1986). In 1915, an additional mill, the Alaska Gastineau Mill was constructed on the southwest flank of Mount Roberts above Juneau. This mill received ore from a number of local mines. Horse-drawn ore carts arrived on rails and opened at the bottom to pour ore into a rotating pebble mill that crushed the rocks to sand size grains. This revolutionary mill introduced new technologies in ore processing and exceeded all expectations, processing 10,000 tons of ore per day. The mill closed in 1921 due to the price of gold, but during the time it operated it recovered 500,000 oz (14.2 t) of gold from 12 million tons of ore.

Figure 2-8. *Perseverance glory hole in centre of photo.*

DAY 3 – GREENS CREEK MINE TOUR

Daily summary

4:30 am depart hotel for Greens Creek ferry. Transportation to the mine site consists of a 45 minute ferry ride followed by a 45 minute bus ride. We will arrive at the mine site at 6:30 am. The tour will finish at 4:30 pm when we will begin the trip back to Juneau, we should arrive at the hotel at 6:30 pm. There is an optional walking tour to the historic Treadwell gold mine after dinner. This will be our final night at the Travelodge hotel.

Daily schedule

4:30 am – van departs hotel lobby

4:30-6:30 am – travel to Greens Creek mine

6:30-7:30 am – safety briefing

7:30-8:30 am – geology overview talk/maps

9:00-2:00 pm – underground tour

2:00-4:00 pm – core viewing

4:00-4:45 pm – wrap up talk, discussion etc.

5:00-6:30 pm – travel from mine back to hotel

7:00-8:00 pm – dinner

8:00-10:00 pm – optional hike on signed trail around the historic Treadwell mine and mill site

Introduction

The Late Triassic Greens Creek volcanogenic massive sulphide (VMS) deposit is located on northern Admiralty Island, south of Juneau in southeast Alaska. The Greens Creek mine is one of the top ten global silver producers and one of the most significant, though atypical massive sulphide deposits in the world. The host rocks are considered to be a part of the Late Triassic oceanic back-arc or intra-arc, rift-related sequence of the Alexander terrane, known as the Alexander Triassic metallogenic belt (ATMB; Taylor *et al.*, 2008). The most recent genetic model is a hybrid VMS-SEDEX (sedimentary exhalative) deposit driven by shallow mafic-ultramafic hypabyssal intrusions below a major seafloor detachment fault (Taylor *et al.*, 2010a; N. Duke, written comm., 2014). Intense, polyphase deformation, multiple rheologically contrasting ore and rock types, and low-grade metamorphism have resulted in very complex geology. The deposit has a combined resource of approximately 24.2 Mt grading 13.9% Zn, 5.1% Pb, 658 g/t Ag, and 5.1 g/t Au (Taylor and Johnson, 2010b).

Regional Geology

The ATMB is a globally significant Late Triassic VMS belt in southeast Alaska and northwest British Columbia that has a present day strike length of 750 km and includes, in addition to the Greens Creek deposit, the notable 300 Mt Windy Craggy deposit (Peter and Scott, 1999) and the Palmer (Glacier Creek) deposit (Steeves *et al.*, 2016). Basement to the ATMB is the Alexander terrane, one of the largest insular terranes in the northern Cordillera (Colpron *et al.*, 2006). The Alexander terrane has been subdivided into the Craig and Admiralty subterranes based on differences in pre-Permian stratigraphy and geologic history (Berg *et al.*, 1978; Gehrels and Saleeby, 1987) and is part of the larger Alexander-Wrangellia-Peninsular composite terrane that was assembled through the Permian (*e.g.*, Karl *et al.*, 2010a; Beranek *et al.*, 2014). The oldest rocks in the Greens Creek area are the Retreat Group which includes Ediacaran dioritic to tonalitic False Point Retreat intrusion that was emplaced within metasedimentary basement rocks of unknown age (Fig. 3-2; Karl *et al.*, 2006). The oldest rocks on the Greens Creek property are Early Silurian to Middle Devonian quartz-mica schists that contain rare intercalated conodont-bearing marbles (Fig. 3-2; Duke *et al.*, 2010; Oliver and Berg, 1981; Proffett, 2010). The quartz mica schists are overlain by the Late Devonian to Permian Cannery Formation. Above these rocks, and the stratigraphic footwall to mineralization, is an enigmatic succession of green chloritic phyllite (after mafic volcanic rocks) that is locally intercalated with black to grey phyllite (after graphitic shales) and marble (Fig. 3-1; Sack, 2009). These rocks are Carboniferous based on U-Pb ages of in-situ zircons (Sack, 2009). Primary layering is commonly overprinted by a pervasive foliation and original contacts not recognizable. The phyllites becomes increasingly hydrothermally altered towards the ore zones.

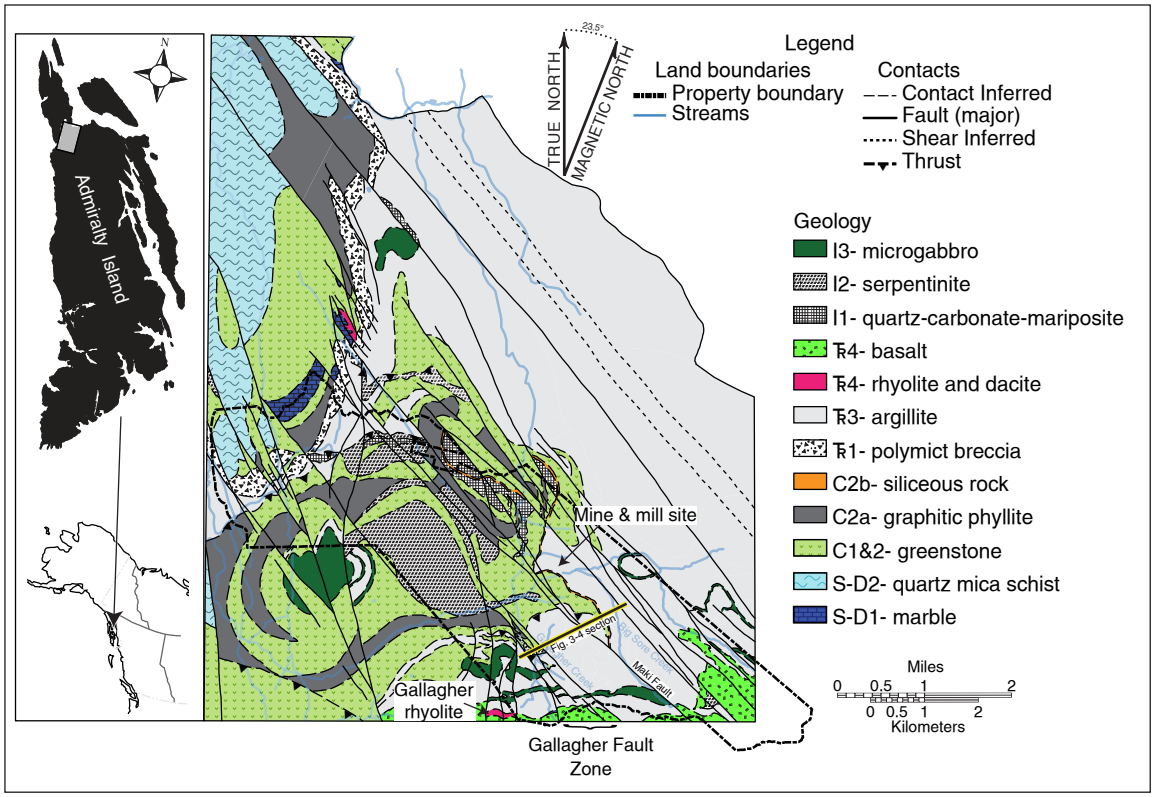

Figure 3-1. *Simplified geology of the Greens Creek property area (modified from Duke et al., 2010).*

The Late Devonian to Permian Cannery Formation is found stratigraphically above the Retreat Group regionally and consists of chert, greywacke-chert turbidites, and volcaniclastic sandstones (Karl *et al.*, 2010a). The Pybus formation typically occurs above the Cannery formation and consists of a light coloured fossiliferous dolomite with minor chert, ranging from not present to up to 300 m thick (Loney, 1964). The Cannery and Pybus formations are not recognized in the mine area, though Permian brachiopods have been recovered from graphitic slate near Eagle Peak 5 km to the east (Karl *et al.*, 2010a) confirming the presence of Cannery Formation nearby.

Late Triassic rocks in the mine area are part of the Hyd Group, which is characterized by a thin basal polymictic breccia interpreted to be a fault-scarp breccia, overlain by a thickly to thinly bedded dolomitic argillite succession of unknown thickness (possibly several hundred meters), in turn overlain by amygdaloidal basalt, and locally by dacite and rhyolite bodies (Fig. 3-1). Three mafic-ultramafic rock types intrude the pre-Triassic rocks, and are interpreted to have been emplaced during the Triassic (Premo *et al.*, 2010; Sack, 2009). A quartz-chlorite-mariposite-bearing rock and serpentinites intrude footwall rocks, and a microgabbro occurs in both footwall and hanging-wall rocks (Sack, 2009). Late Jurassic to Early Cretaceous rocks of the Seymour Canal formation overlie the Late Triassic rocks and occur east of the mine area (Proffett, 2010; Sack, 2009).

Greens Creek mine geology

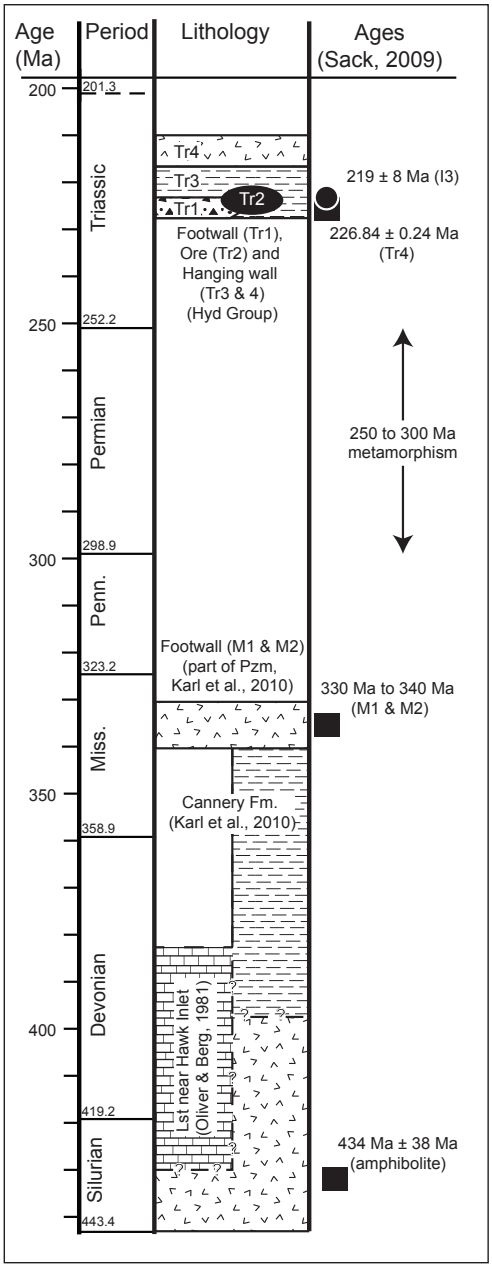

Figure 3-2. *Chronologic diagram showing stratigraphy with deformation and metamorphism events in the Greens Creek area. Timing of D2-D4 are relative. From Sack (2009).*

The Greens Creek deposit occurs at the unconformity between altered Carboniferous mafic metavolcanic rocks intruded by mafic-ultramafic rocks and Late Triassic conglomerate, dolostone, and graphitic argillite. The deposit is characterized by thin (<12 m) massive and semimassive sulphide lenses at the base of a thick (up to several hundred meters) section of Late Triassic (Norian) argillite and dolostone of the Hyd Group (Fig. 3-1; Premo *et al.*, 2010; Sack, 2009; Taylor and Johnson, 2010a). The descriptive term phyllite is used at the mine, adding the dominant mineral component as a prefix (*e.g.*, mariposite phyllite, sericite phyllite). The ore horizon at the contact between phyllite and argillite is the only marker horizon in the mine area.

The geology around Greens Creek is complicated by complex, polyphase deformation (Fig. 3-3). A pre-Triassic foliation present in footwall rocks does not affect the ores. An isoclinal folding event (F2), followed by two tight to open folding events (F3 and F4), affect all rocks and have overturned stratigraphy in the immediate mine area. An F2-related S2 foliation is pervasive throughout the mine area. Tension fractures throughout massive argillite beds and locally in ores are related to F2, and locally F3 folding (Proffett, 2010). At least two major shear zones that formed between D2 and D3 and three major dextral brittle fault zones that postdate D4 offset stratigraphy at the mine by 535 m (Fig. 3-1; Proffett, 2010). Metamorphism reached prehnite-pumpellyite to lower greenschist facies (Taylor and Johnson, 2010a) and is likely related to the mid-Cretaceous collision of the Alexander terrane to North America (Haeussler *et al.*, 1999; Karl *et al.*, 1998).

A <20 m thick, locally sourced polylithic breccia occurs discontinuously at the base of the Triassic section and is interpreted as a syngenetic fault-scarp breccia formed during incipient Late Triassic rifting (Figs. 3-1 and 3-3; Duke *et al.*, 2010). Massive sulphide occupies the same stratigraphic position, replacing and overlying the conglomerate and, in part, replacing and interbedded with massive dolostone and graphitic argillite beds at the base of the thick hangingwall argillite package. The lowermost and most abundant of the underlying Carboniferous phyllitic rocks is a light to dark green, fine-grained, plagioclase-phyric and chlorite-rich 'greenstone'. These rocks become increasingly foliated and altered by white mica towards the ore zone. Finely compositionally layered phyllites with variable

concentrations of chlorite, sericite, graphite, carbonate, mariposite and quartz dominate the footwall near the mine contact and are interpreted by Sack (2009) to have been volcaniclastic rocks altered by ore-forming hydrothermal fluids. Locally, the footwall rocks adjacent to VMS mineralization are very siliceous and brecciated by pyrite-rich cement, and likely represent a sulphide-stringer or feeder zone (Fig. 3-4).

No syngenetic volcanic rocks have been found near the ore horizon. Three Late Triassic volcanic units occur several hundred meters up stratigraphy, above the hangingwall argillite, and have been mapped as dacite northwest of the mine site, and rhyolite (Gallagher rhyolite) and basalt to the south of the mine site (Fig. 3-1; Sack, 2009). Voluminous, serpentinized mafic-ultramafic intrusive rocks throughout the footwall and structurally emplaced in the hangingwall may have been coeval with massive sulphide formation (Fig. 3-1; Duke *et al.*, 2010; Taylor and Johnson, 2010a).

Mineralization

Eight ore zones are outlined by mine geologists: East, West, 9A, Northwest West, Southwest, 200 South and Gallagher (Fig. 3-5). Each zone may also be divided into several "sub-zones", though the nomenclature is inconsistent. The boundaries are defined by faults, shear zones, or changes in thickness of ore. Ore lenses are typically thin (<10 m), though may be locally greatly thickened (up to 30+ m) by complex, polyphase deformation (Fig. 3-3).

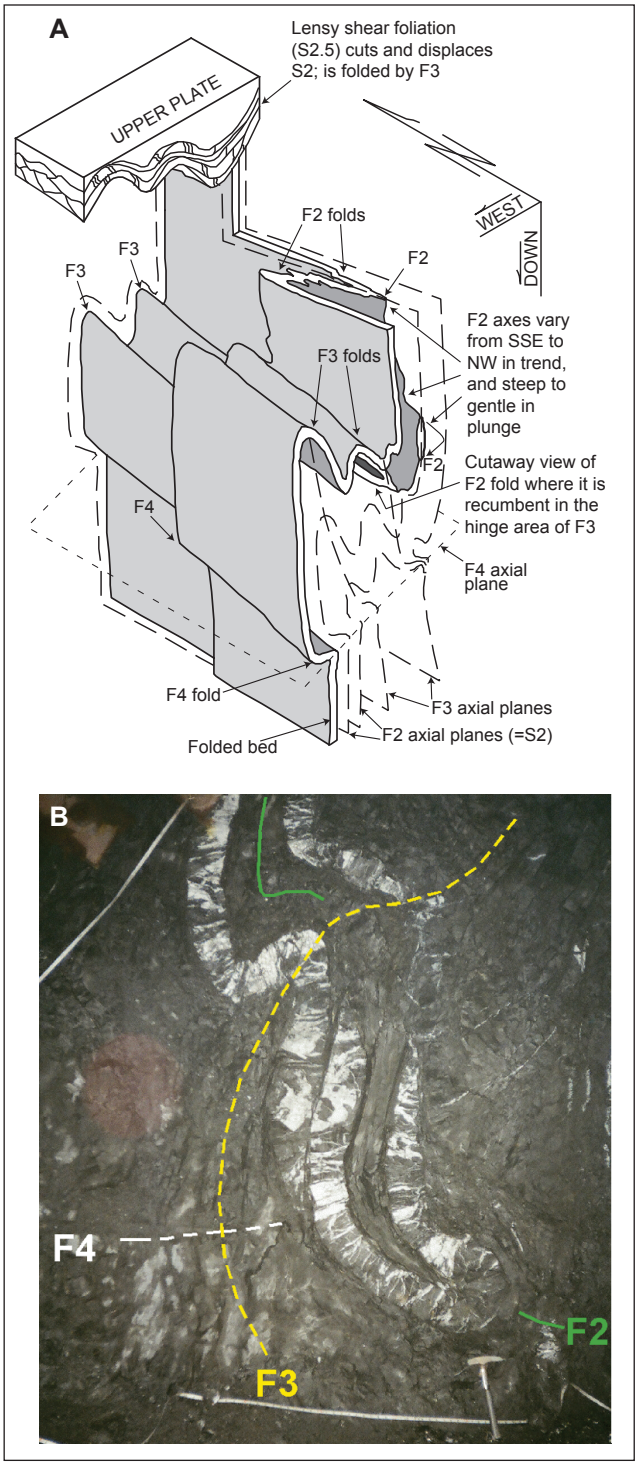

Figure 3-3. *A) Illustration of polyphase deformation at Greens Creek. B) Underground photo showing a single massive argillite bed affected by F2, F3, and F4. The bed is also offset by D2.5 shearing. From Proffett (2010).*

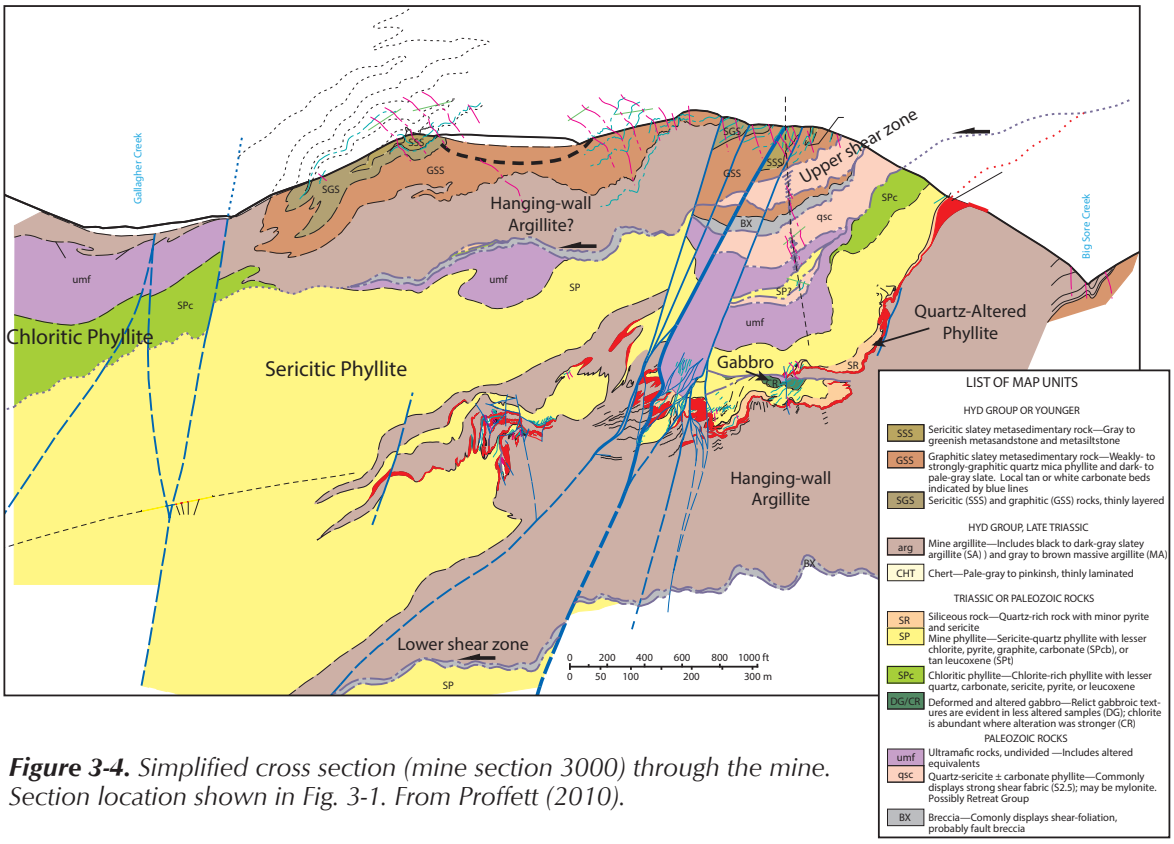

Figure 3-4. *Simplified cross section (mine section 3000) through the mine. Section location shown in Fig. 3-1. From Proffett (2010).*

Historically, five basic ore type end-members have been used for logging and mapping by mine geologists. A barite-rich ore (WBA), a carbonate-rich ore (WCA), and a quartz-rich ore (WSI) constitute the gangue-dominated (<50% sulphide) “white ores”. The massive sulphides (>50% sulphide) are divided into pyrite-rich ore (MFP) and base-metal sulphide-rich ore (MFB), and may have variable gangue mineralogy dominated by carbonate, quartz, or barite with subordinate mica and feldspar. The white ores are interpreted to have formed by low-temperature fluids and stratigraphically underlie the high-temperature massive sulphides, contradicting typical VMS-style deposit formation (cf. Lydon, 1984). However, this relationship is not consistent and intense deformation complicates stratigraphy (Fig. 3-6).

Common sulphide minerals at Greens Creek are pyrite, sphalerite, galena, and tetrahedrite, with subordinate chalcopyrite and local arsenopyrite, and colusite. Silver occurs dominantly within tetrahedrite, and subordinately as stromeyerite-mckinstryite and locally pyrargyrite-proustite. Gold commonly occurs as electrum. A wide array of sulphide microtextures is present throughout the Greens Creek deposit, ranging from well-preserved primary textures to microstructures indicative of metamorphism, deformation and remobilization. Pyrite, for example, in the baritic and base metal-rich ores (WBA and MFB) is significantly more recrystallized and euhedral than pyrite in

the pyrite-rich (MFP) or quartz- and carbonate-rich ores (WSI and WCA), which commonly have framboidal and colloform textures, owing likely to the high textural stability of pyrite and the shielding nature of abundant quartz and carbonate gangue (Gilligan and Marshall, 1987; McClay and Ellis, 1983). The quartz, carbonate-, and pyrite-rich ore types (WSI, WCA, MFP) behave more rheologically competent and contain pyrite deformed by cataclastic flow (*e.g.*, Gilligan and Marshall, 1987). In the more ductile ore types where pyrite is typically subhedral to euhedral, deformation was likely controlled by the more abundant ductile sulphides and masked by annealing (Gilligan and Marshall, 1987). The more ductile sulphides such as sphalerite, galena, tetrahedrite, and chalcopyrite are typically recrystallized in all ore types, though may locally exhibit colloform textures.

Exploration

Underground exploration remains a priority at Greens Creek. Mineralization occurs at or near the unconformable contact between footwall phyllite and hanging-wall argillite (Fig. 3-4). Detailed 3D interpretation of the geometry of this 'mine contact' and the distribution of ore zones along it has led to an outline of three major mineralization trends. Underground exploration is focused on testing the up and down plunge extensions of these trends as well as up and down dip for new trends. Up plunge and up dip projections intersect the upper shear zone and cub faults, of which the exact location and displacement are unknown. Understanding these structural boundaries is critical to exploration.

Regional exploration relies on ground and borehole TDEM geophysical surveys to identify conductive massive sulfide and barite accumulations. Feeder vein systems containing chalcopyrite and pyrrhotite in the footwall may be conductive. Challenges to using EM surveys at Greens Creek are the target depths and interference from conductive graphitic rocks. Gravity surveys have difficulty accounting for the steep topography and differentiating serpentinite from massive sulfide and barite accumulations.

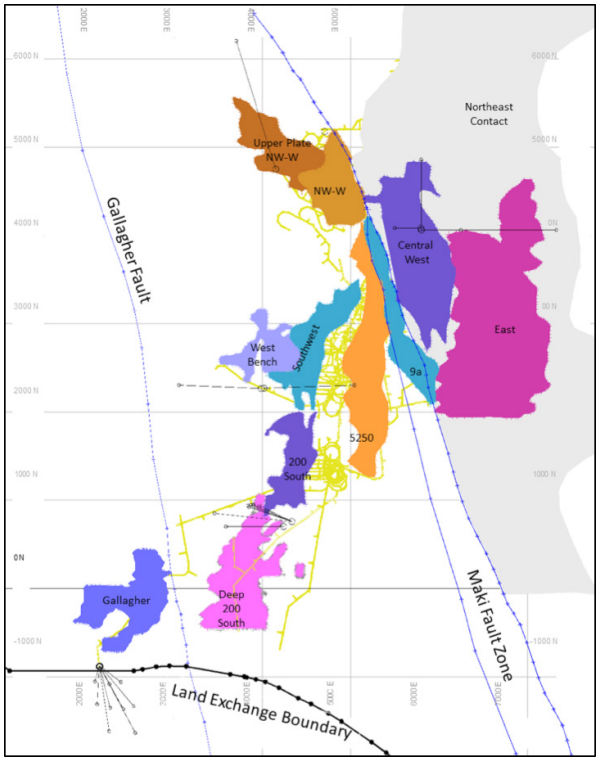

Figure 3-5. *Simplified plan view of the 9 general ore zones at Greens Creek mine. The NW-W and SW ore zones may be subdivided as shown into Upper Plate NW-W and West Bench.*

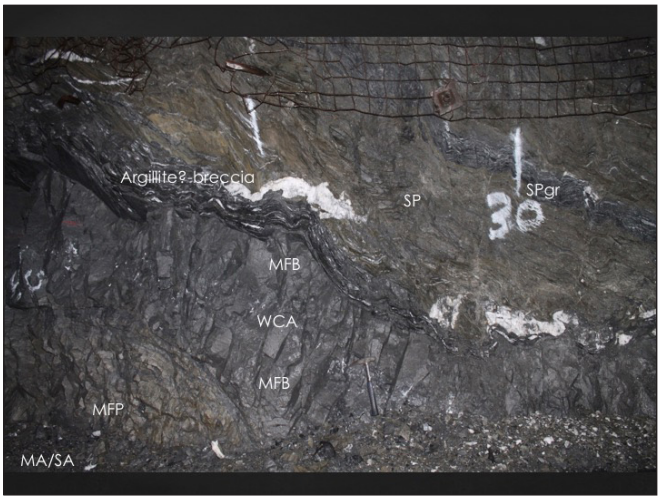

Figure 3-6. *Overturned mine contact with stratigrahic footwall lithologies in the upper right, ore lithologies in the lower left and stratigraphic hanging wall lithologies in the very bottom left corner. Hammer in bottom centre is 30 cm. SPgr = graphitic phyllite, SP = sericitic phyllite, MFB = base-metal sulphide-rich ore, WCA = carbonate-rich ore, MFP = pyrite-rich ore, MA = massive argillite, SA = slatey argillite.*

Discussion

The current genetic model for the Greens Creek deposit is a hybrid VMS-SEDEX with possible MVT-like features (Taylor *et al.*, 2010a; N. Duke, written comm., 2014). In the past it has been classified as a Besshi VMS deposit (Dressler and Dunbire, 1981), a VMS-sedimentary exhalative (SEDEX) hybrid deposit (Taylor *et al.*, 2010a; Taylor *et al.*, 1999), and a Kuroko VMS deposit (Nelson *et al.*, 2013; Nokleberg *et al.*, 2005). The mafic-ultramafic rocks are suggested as the likely heat source driving convection during the formation of the deposit, though they have not been directly dated. The deposit contains anomalously high Au and Ag grades and is not associated with volcanic rocks as is typical of VMS deposits (cf. Barrie and Hannington, 1999). The location of the deposit at a significant unconformity is also unusual for VMS deposits and may suggest formation along a major detachment. Furthermore, the proximity of submarine mineralization to a major unconformity suggests the massive sulphides were deposited soon after the footwall rocks were submerged. Metals and reduced sulphur may have been sourced in part from the overlying carbonaceous sediment, suggesting a SEDEX-like genesis below unconsolidated sediment, or sourced from the basement sedimentary rocks, however, no obvious source rocks have been identified.

Day 3 – Treadwell deposit

The Treadwell mine historic trail network is a walking tour well-signed with historic information and photographs. From the Sandy Beach parking lot south of Douglas, there is a 1 km trail to Cave-in Cove, and a slightly shorter trail to the Glory Hole Lakes (Fig. 3-7).

Gold deposits on Douglas Island are confined to carbonate-albite-altered monzodiorite sills and their contacts with Jura-Cretaceous carbonaceous phyllite. The rocks are tilted, so the sills are now nearly vertical "dykes" that have a collective strike width of nearly 2 km and a strike length of nearly 10 km (Newberry *et al.*, 1995). Individual sills range from 20 to 200 m in thickness, and are complexly anastomozing (Spencer and Wright, 1906). Trace element ratios indicate unaltered, unmineralized monzonite is moderately alkaline in composition, similar to the zoned Alaska-Urals ultramafic-gabbro complexes, one of which is exposed at the southeast end of the sill system on Douglas Island, where the Mineral Queen deposit is located in hornblende clinopyroxenite (Newberry *et al.*, 1995). A premetamorphic episode of propylitic alteration (albite-chlorite-actinolite-epidote-pyrite-calcite) and potassic alteration (K-feldspar-chlorite-pyrite-chalcopyrite) has associated concentrations of Cu-Au-Mo (Newberry *et al.*, 1995). The monzodiorite yielded a U-Pb zircon crystallization age of 91 ± 2 Ma, with an average upper intercept age of 270 Ma (Gehrels, 2000), and a $^{40/39}$Ar hornblende cooling age of 85 Ma (Goldfarb *et al.*, 1993), coincident with middle Cretaceous contraction and crustal thickening (Himmelberg *et al.*, 2004). Syn or post-metamorphic albite-quartz-carbonate-pyrite alteration with associated rutile, magnetite, hematite, scheelite, molybdenite, chalcopyrite, and tetrahedrite yielded a mica $^{40/39}$Ar age of 55 Ma (Goldfarb *et al.*, 1991), coincident with emplacement of large volumes of granitic magma in the CPC that may

have contributed a heat source. Molybdenite is common in veins that contain gold; Sb, Bi, and As are low and Co and Te are slightly anomalous (Newberry *et al.*, 1995). Gold is present in both quartz veins and altered dyke material, but major gold ore zones are only present in the vicinity of pre-metamorphic potassic alteration (Newberry *et al.*, 1995; Spencer and Wright, 1906). Anomalous concentrations of Mo, W, and Co in late alteration zones and quartz veins suggest a contribution from felsic igneous sources (Newberry *et al.*, 1995).

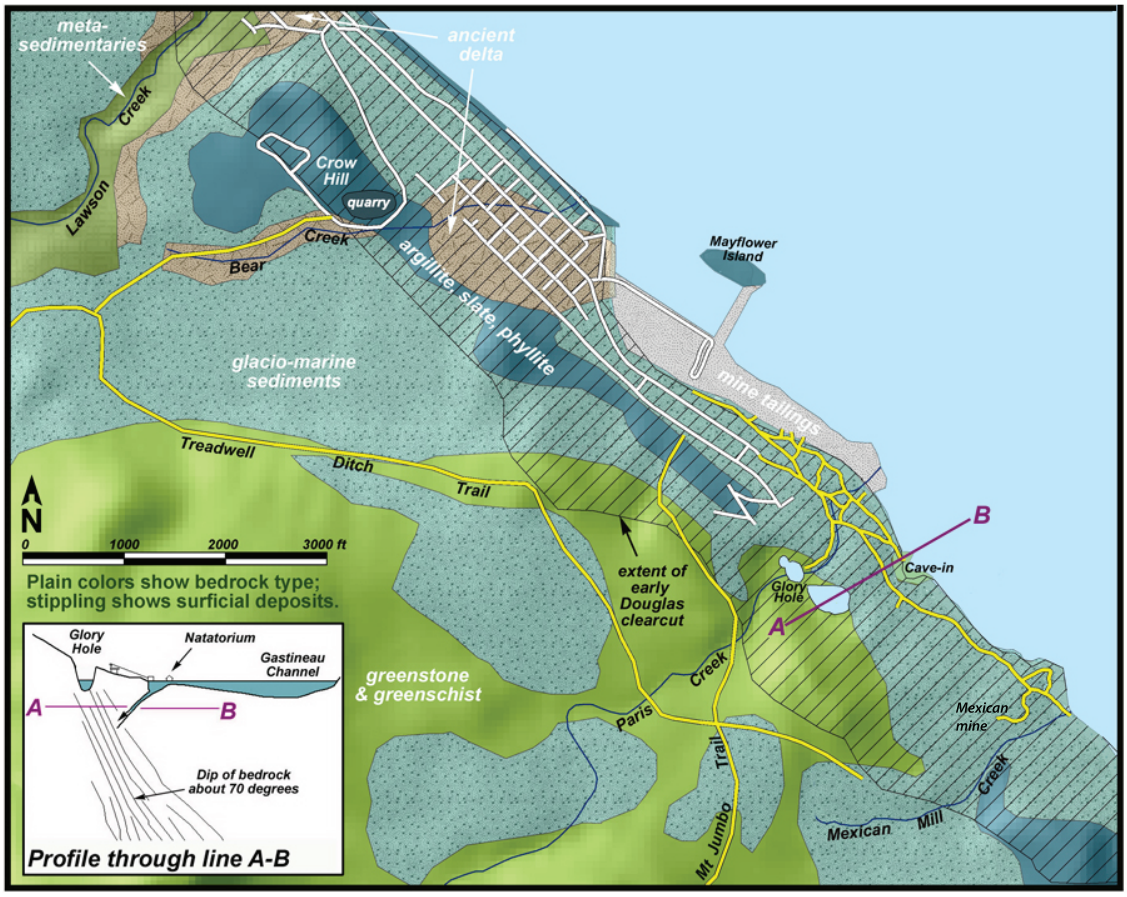

Figure 3-7. *A) Geology map of Treadwell area (from* www.juneau.org/parkrec/trails/paris.php*).*

History

Accompanied by Tlingit natives, Pierre Erussard, a French Canadian prospector, staked the Parris (later changed to Paris) claim on Douglas Island, on the site of what is now the Glory Hole, on May 1, 1881. He found only low grade ore and sold the claim to John Treadwell, a carpenter with a mining background from California, on Sept 13, 1881. Treadwell also bought adjacent claims from other prospectors. The first mill was constructed in 1882. Four initial mines, including the Paris, Bear's Nest, Treadwell, and Ready Bullion, were developed and consolidated with interconnected underground tunnels. A tunnel connection to the Mexican mine led to operations beginning there in 1886. Several other mines on southeastern Douglas Island were developed soon afterwards.

In 1899 in the small valley to the southwest of the Paris mine, the Alaska Treadwell Gold Mining Company constructed a 300 stamp mill containing the largest number of stamps ever installed under one roof in the world. Ore arrived from the mines in horse-drawn carts on rails and 1020-lb stamps crushed 6 tons of ore daily to a fineness that would pass through a wire screen with 40 holes per square inch. The crushed fines fell onto copper plates coated with mercury, free gold amalgamated with mercury, and was then heated and treated with chlorine gas to separate the gold from the mercury. Between 1881 and 1921, the Treadwell Complex produced 3.1 Moz (87.9 t) Au and 151,000 oz (4.3 t) Ag (Redman, 1986).

The mines operated 24 hours per day and 7 days a week, pausing only on Christmas day and July 4th. The five main mines had a working depth of 2800 feet but did not extend under Gastineau Channel. As of April 17, 1921, in excess of 10 million tons of ore had been removed from multiple mine levels. Removal of support structures in several levels coupled with an extremely high tide caused the ground to subside adjacent to Gastineau Channel and saltwater flooded into all but the Ready Bullion and Mexican mines. An estimated 3 million tons of seawater filled the mines in 3.5 hours. It took 1 hour and 40 minutes to evacuate the men after the alarm sounded, and water and rocks were pouring onto the cage when the hoist lifted the last men out. One man was reported missing, but it is uncertain whether he was in the mine. Twelve horses and a mule were lost. The Ready Bullion mine continued to operate until 1923.

DAY 4 - JUNEAU TO HAINES, PALMER DEPOSIT TOUR

Daily summary

4:45 am depart hotel for Alaska ferry terminal. Ferry departs 7 am and arrives in Haines at 11:30 am. We will drive straight from the ferry terminal in Haines to the Constantine camp where we will have lunch. We will tour the Palmer deposit between 1 and 6:30 pm. Accommodation for the night is at the Funny Farm, a heli-skiing lodge approximately 15 km from the Constantine camp. Dinner and tomorrow's breakfast are included with this night's accommodation.

Daily schedule:

4:45 am – van departs Travel Lodge lobby

5:00-7:00 am – ferry check in

7:00-11:30 am – ferry ride from Juneau to Haines

10:00-10:30 – Nathan Steeves' Palmer deposit talk

11:30-1:30 pm – drive Haines ferry terminal to Palmer camp

1:30-2:00 pm – site safety briefing/lunch

2:00-2:30 pm – site overview talk

2:30-4:30 pm – core viewing

4:30-6:30 pm – Palmer discussion and optional visit to Devonian fossil site

Stop 4-1 – Devonian limestone and Porcupine Slate

7:00-8:00 pm – dinner

8:00-10:00 pm – campfire and discussion

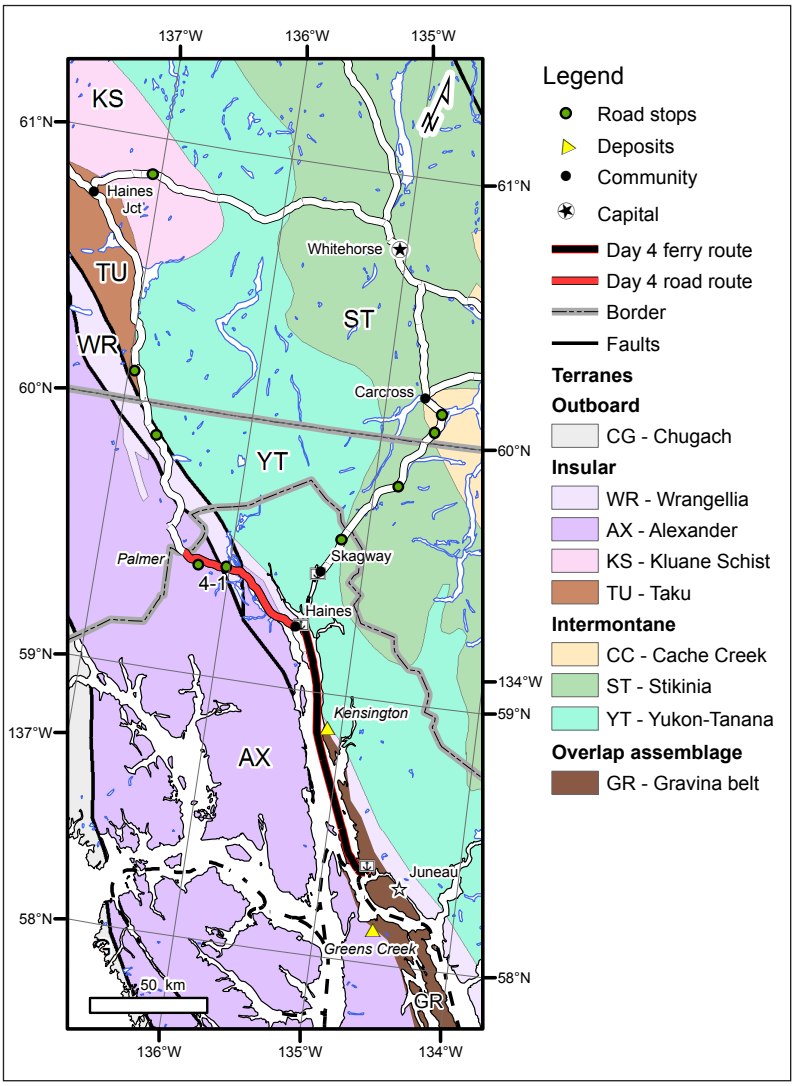

Figure 4-1. *Simplified terrane map with Day 4 route and field trip stops.*

Regional geology

The city of Haines is built on Quaternary outwash and alluvial deposits. South of town on the Chilkat Peninsula are coarse-grained biotite amphibolite with pegmatite dykes and pyroxenite that intrude the Triassic mafic metavolcanic rocks assigned to the Wrangellia terrane. A concordant U-Pb zircon age of 107.5 Ma from the pegmatite (Friedman, University of British Columbia, unpublished data), is similar to a K-Ar hornblende age of 111.7 Ma and a K-Ar biotite age of 110.7 Ma from the pyroxenite (recalculated with 1976 constants from MacKevett *et al.*, 1974). The Klukwan ultramafic body is located 35 km north of town and yielded hornblende K-Ar ages of 98.4 and 101.5 Ma from drill core that Lanphere (*in* Mackevett *et al.*, 1974) considered to be too young because of alteration. The ultramafic rocks are intruded by plagioclase porphyritic quartz diorite that contains magmatic epidote and garnet, and yielded a U-Pb zircon lower intercept (crystallization) age of 83.5 ± 2.5 Ma, an average upper intercept (inheritance) age of 1400 Ma, and a titanite age of 83 ± 2 Ma (Gehrels, 2000). These ages provide a minimum age for the ultramafic rocks. Magmatic fabrics in these plutons parallel host rock metamorphic fabrics and indicate syndeformational emplacement of the plutons and also indicate contractional deformation occurred before, during, and after regional emplacement of the belt of ~90 Ma plutons. Regional structural analysis indicates crustal thickening was accomplished by thrust burial. Replacement of andalusite by kyanite or sillimanite in pluton aureoles indicates thickening soon after emplacement (Cook and Crawford, 1994; Himmelberg *et al.*, 2004). Thermobarometric analyses indicate aureoles reached near-peak temperatures of 525 to 635° C at pressures of 570 to 630 MPa, consistent with emplacement depths greater than 20 km; the rate of thermal decay suggests rapid rates of burial at 5 to 8 mm/a (Himmelberg *et al.*, 2004). The presence of magmatic epidote is interpreted to indicate emplacement at high temperatures and pressures in the kyanite and/or sillimanite stability fields (Himmelberg *et al.*, 2004; Zen and

Hammarstrom, 1984). The ultramafic rocks and quartz diorites of this belt throughout southeast Alaska, including the Treadwell diorite, have whole-rock and mineral geochemistry supporting genesis in a volcanic arc (Himmelberg *et al.*, 2004; Himmelberg and Loney, 1995).

As we drive northwestward from Haines, on our right is a prominent ridge of the Triassic mafic metavolcanic rocks intruded by the Klukwan ultramafic rocks, part of the Alaska-Urals mafic-ultramafic belt in southeast Alaska, and the 83.5 Ma quartz diorite on the north side of Haines Harbor. The Chilkat River is underlain by the Denali fault.

History

The Chilkat River is famous for a large concentration of bald eagles in the late fall and winter. The eagles are attracted to the area by the availability of late-run salmon and open waters. A natural phenomenon of upwelling groundwater in deep river gravels keeps an 8 km stretch of the river from freezing. The Chilkat Bald Eagle Preserve, extending along mile 9 to 31 of the Haines Highway, was established by the State of Alaska in 1982 to protect and perpetuate the world's largest concentration of Bald Eagles in their critical habitat. The Preserve contains 48,000 acres that include the confluence of the Chilkat, Klehini, and Tsirku Rivers.

As we cross the Chilkat River and the Denali fault, we cross from Wrangellia into the Alexander terrane (Fig. 4-1). Some of the oldest rocks in the Alexander terrane are exposed on the north side of the Klehini River, and these include the Neoproterozoic to Ordovician Four Winds Complex. These rocks are metamorphosed to amphibolite facies, intruded by Silurian quartz diorite bodies, and structurally overlie Devonian to Triassic sedimentary and volcanic rocks. In contrast to the Triassic basalts of Wrangellia, these Triassic rocks have trace element signatures indicating arc and rifted arc affinities, and host a significant belt of VMS deposits (Taylor *et al.*, 2008), including the Palmer deposit that we are about to see (Steeves *et al.*, 2016).

After we cross the Klehini River, we will drive by tilted glacial outwash deposits and sheared fossiliferous Devonian and Mississippian limestones and shales that have kinematic indicators of recent dextral activity on a fault that the Klehini River follows. This road leads us to Porcupine, the location of a long-standing gold placer mine and the Constantine camp. If time permits, we can walk up a short road east of Porcupine Creek and find corals, brachiopods and gastropods in bedded limestone of Middle Devonian age (Stop 4-1; S.Karl and R. Blodgett, unpublished data). The Devonian limestone is gradationally overlain by black Mississippian limestone and chert, which is conformably overlain by the Porcupine Slate. The Porcupine Slate, upstream and west of the creek, contains brachiopods of Early Permian age (Eakin, 1919). The Porcupine Slate consists of black, limonite-stained slate and phyllite, commonly interlayerd with dark gray siltstone turbidites, and subordinate greywacke, chert, limestone, conglomerate, and mafic volcanic rocks. The Porcupine Slate is identical to the carbonaceous slate and phyllite of the Cannery Formation to the northeast of, and below the Hyd argillite on Admiralty Island east of the Greens Creek mine. There, the Cannery slates also contain Permian brachiopods (Karl *et al.*, 2010a; Lathram *et al.*, 1965), but are otherwise compositionally indistinguishable from the mine argillite that contains Late Triassic *Halobia*. The Porcupine Slate west and south of Porcupine Creek is gradational to black carbonaceous slate of Triassic age associated with the Palmer deposit.

Palmer Introduction

The Palmer deposit is a recent volcanogenic massive sulphide (VMS) discovery in southeast Alaska. It is located within the Alexander Triassic metallogenic belt (ATMB) and the same Triassic age marine sedimentary and volcanic rocks that also host the world-class Greens Creek Zn-Pb-Ag VMS deposit (180 km south), and the giant Windy Craggy Cu-Co VMS deposit in British Columbia (100 km north).

The property is located along the U.S.–B.C. border 60 km north of the town of Haines, AK, on the eastern margin of the St. Elias mountain range (Fig. 4-2). It is located adjacent to a paved Alaska state highway, with a short haul to year-round deep-sea port facilities in Haines, Alaska, which is favourable for shipping to Pacific Rim concentrate markets. The property is a district-scale land package that is host to multiple VMS prospects. The property totals approximately 108 000 acres, inclusive of the Palmer state and federal claims as well as the "Haines Block" leased from the Alaska Mental Health Trust Authority. Base metal sulphides and barite were initially discovered in the area by local prospector Merrill Palmer in 1969. Early exploration work was carried out by several operators, including Anaconda, Bear Creek, Newmont, Granges, Cominco and Kennecott. Exploration initially focused on the Upper, Lower, and Main Zone prospects, now known to be surface expressions of the Palmer deposit, and on locating the source of high-grade massive sulphide boulders in the area. Receding ice in the early 1990s exposed a massive sulphide outcrop at the Little Jarvis occurrence on the Palmer property; subsequent drilling by Rubicon Minerals in 1999 led to the discovery of the RW zone. No additional drilling occurred until Constantine Metal Resources acquired the property in 2006. In 2007, Constantine extended the RW zone and discovered three more lenses referred to as the "South Wall" zones. Presently, the Palmer deposit consists of four tabular massive sulphide lenses with a recently updated 43-101 compliant inferred resource estimate of 8.1 million tonnes grading 1.41% Cu, 5.25% Zn, 0.32 g/t Au and 31.7 g/t Ag (Gray and Cunningham-Dunlop, 2015). This resource update represents a 97% expansion relative to the January 2010 resource. Additionally, test work demonstrated that the deposit exhibits a very good response to conventional metallurgy, during which locked cycle flotation tests yielded smeltable copper and zinc concentrates, with high metal recoveries produced at moderate grind sizes (89.6% for Cu, 84.9% for Zn, 75% for Au and 89.7% for Ag).

Palmer property geology

Late Triassic rocks predominate on the Palmer property and consist of massive to pillowed basalt, fragmental basalt, and possible andesite, with intercalations of calcareous siltstone and tuff, and rare rhyolite flows and dikes. Folding and faulting likely repeats stratigraphy, and may, in part, be responsible for the broad distribution of exhalative mineralization and associated quartz-sericite-pyrite alteration across the property. Alteration is commonly several hundred meters in extent, and of such intensity that discrimination of the protolith is difficult without the use of immobile element geochemistry. Late Triassic rocks at Palmer have experienced lower to mid-greenschist

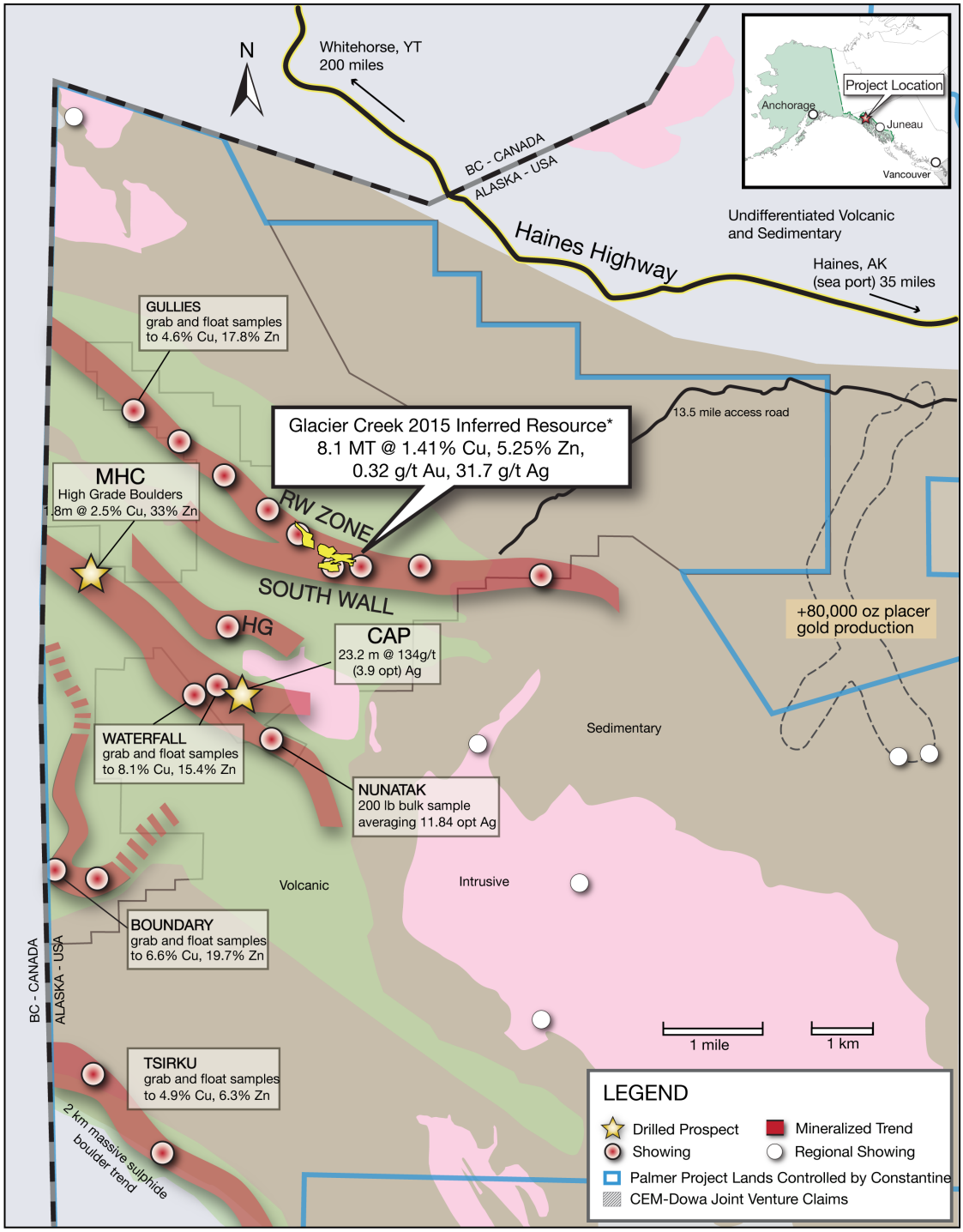

Figure 4-2. *Simplified geology of the Palmer property. From Constantine Metal Resources Ltd.*

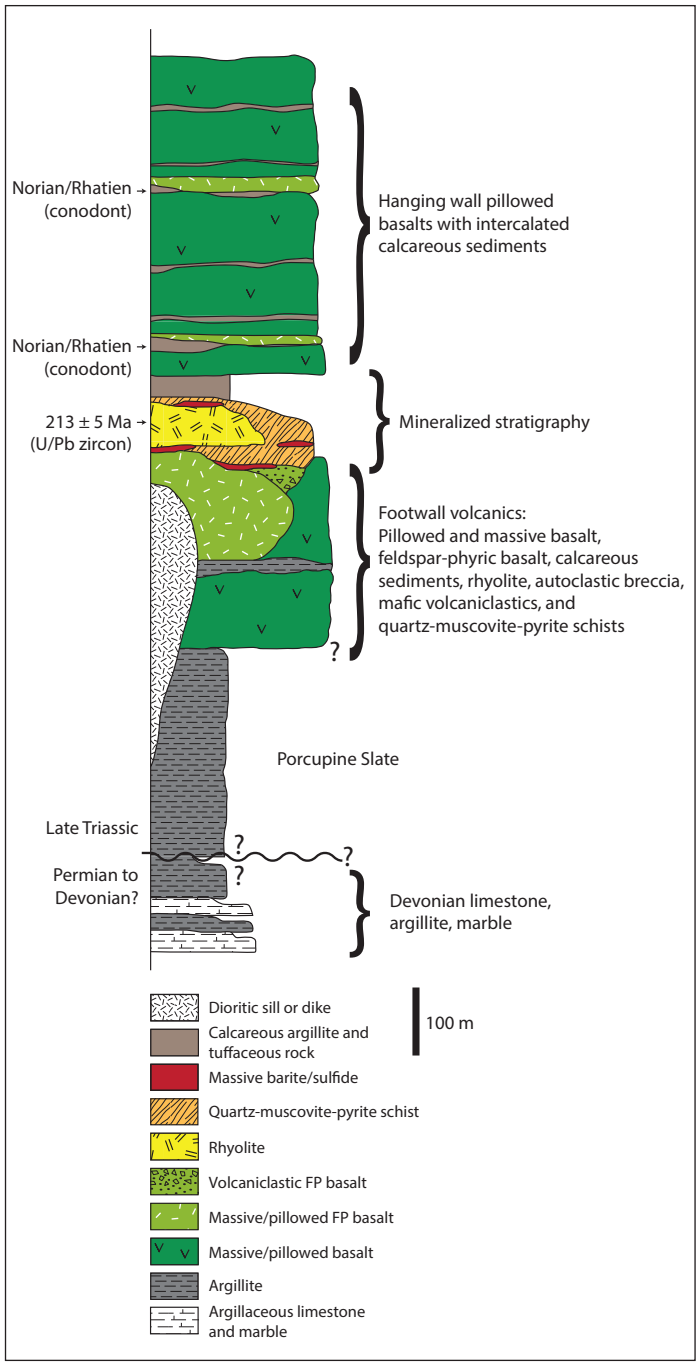

Figure 4-3. *Generalized stratigraphic column for the Palmer property. Most of the quartz-muscovite-pyrite schists are thought to be altered feldspar-phyric (FP) basalt. Scale is approximate. Age data are from Green (2001). From (Steeves et al., 2016).*

facies regional metamorphism (Green *et al.*, 2003) and record at least three different episodes of deformation.

The oldest rocks recognized in the area are thinly bedded limestone and massive marble, interpreted to be Carboniferous to Devonian in age based on crinoid fossils (MacIntyre and Schroeter, 1985). The contact relationship between these rocks and the overlying Late Triassic volcano-sedimentary package is uncertain (Fig. 4-3). The base of the Triassic section is a thick sequence of thinly bedded, fine-grained, basinal clastic rocks known as the Porcupine Slate. Overlying and interfingered with the Porcupine Slate is a dominantly mafic volcanic pile that is host to the known VMS deposits in the area. The volcanic pile comprises a thick package of pillowed, massive, and locally brecciated, aphyric to feldspar-phyric mafic flows and volcaniclastic rocks intercalated with thin units of tuffaceous limestone and argillite. The immediate host rocks of the massive sulphide deposits are a thick interval of quartz-sericite-pyrite schist overlain by massive to pillowed flows with interbedded calcareous, tuffaceous sediment. Minor rhyolite is present at the Palmer deposit and is also associated with several other VMS prospects in the area (Gray and Cunningham-Dunlop, 2015).

Four main deformation events affected the rocks in the Palmer area and relate to mid-Cretaceous accretion of the Alexander terrane to North America (Haeussler *et al.*, 1999; Karl *et al.*, 1998). D1 is characterized by south-verging folds and southerly directed movement along thrust faults (Lewis, 1998), as well as a pervasive strong to intense schistosity (S_1) in strongly altered rocks. D2 is represented by tight folds that plunge northwest. A weak, northeast-striking crenulation cleavage within schistose rocks is interpreted to be the result of D3 (Green, 2001; Lewis, 1998). Late southwest- and northwest-striking,

high-angle, conjugate brittle faults (D4) offset the stratigraphy, although the amount of displacement is poorly known. Peak regional metamorphism was lower to mid-greenschist facies (Green *et al.*, 2003) and was reached prior to 110 Ma (Forbes *et al.*, 1989).

Palmer deposit geology

The host rocks to the Palmer deposit are folded into a large, overturned, south-verging anticline with an axial surface that dips shallowly to the northeast (F1; Fig. 4-4 and Fig. 4-5). The volcanic stratigraphy is offset by up to 200 m along a deposit-scale thrust fault close to the axial surface of the anticline (D1; Green, 2001).

The stratigraphic footwall is dominated by 50 to 100 m of medium green, aphanitic, feldspar-phyric, weakly amygdaloidal basalt (Figs. 4-3, 4-4 and 4-5). Fresh samples contain up to 25% coarse, sub- to euhedral plagioclase phenocrysts up to 5 mm in size. Volcaniclastic equivalents of these rocks locally underlie the massive sulphide lenses. Thin volcaniclastic (tuffaceous) and rare sedimentary horizons are intercalated with the footwall basalts, but their primary nature is obscured by alteration. The stratigraphy below the feldspar-phyric basalt is poorly constrained. On the upright, north limb of the deposit-scale fold, massive sulphide mineralization occurs both above and below a 30-45 m-thick tabular body of aphyric rhyolite that pinches out towards the east. The rhyolite is locally fragmental along the upper margin and is pervasively altered to quartz, muscovite, and pyrite with rare chlorite.

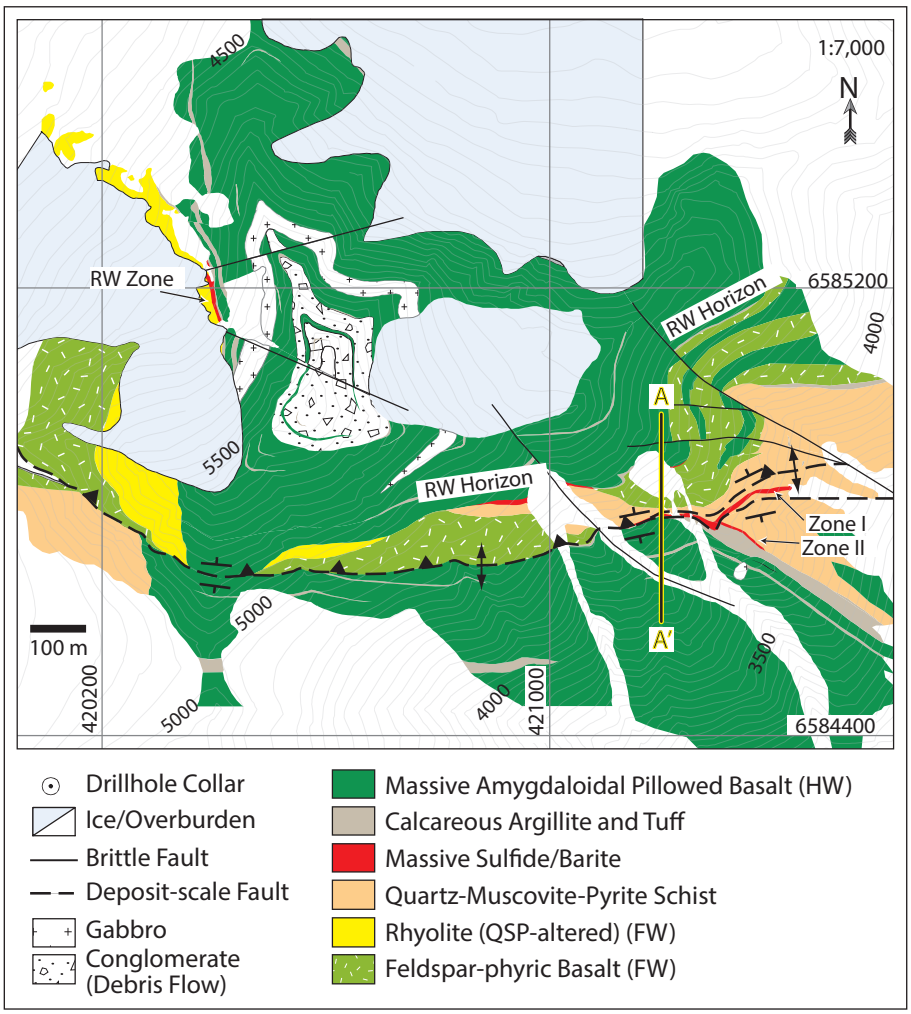

Figure 4-4. *Geologic map of the Palmer deposit (Mt. Morlan). A-A′ corresponds to the cross section. Contour interval = 50 ft. Based on Green (2001), from Steeves et al. (2016).*

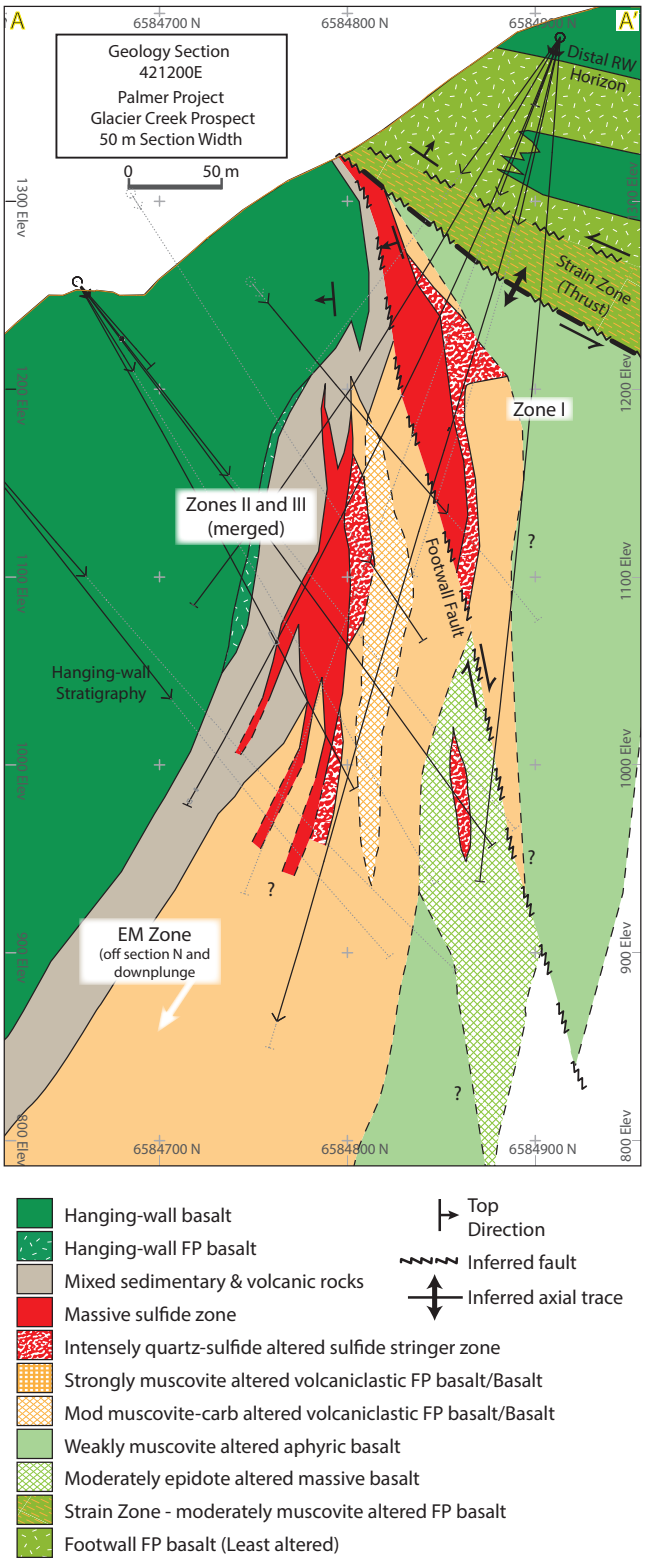

A thin unit of locally mineralized chert, argillite, and tuffaceous sediment (mixed sedimentary-volcanic unit) directly overlies the massive sulphides. The argillite is dark grey to black and composed primarily of carbonate (calcite) with 5-20 vol % quartz. These rocks continue along the mineralized horizon and are interpreted to be lateral equivalents of the massive sulphide mineralization.

A thick package of dark green pillowed and amygdaloidal basalt occurs stratigraphically above the mineralized horizon. The hanging-wall basalt is carbonate-altered to varying degrees, typically with pervasive calcite, particularly in amygdules and veins. Locally, the basalt is epidotized with epidote in veins and replacing feldspars.

Mafic dykes and sills are abundant throughout the stratigraphy and are especially common around massive sulphide mineralization. Some dykes may be feeders to local volcanic rocks based on their composition and field relationships (Green *et al.*, 2003). The intrusions range from less than 10 cm wide up to 10 m wide in drill core, are typically dark green and fine-grained with chlorite and carbonate alteration, and have well developed chilled margins.

Figure 4-5. *Cross section through the South Wall zone at 421200E (Fig. 4-3), showing Zones I, II, and III, surrounding lithologies, and dominant alteration types. Surface contacts are based on surface mapping; all other contacts are from drilling. The axial trace of the fold is interpreted to be along the thrust fault. FP = feldspar-phyric. From Steeves et al. (2016).*

Mineralization

Massive sulphide at Palmer is divided into several ore zones on either side of a slightly overturned, deposit-scale anticline. The South Wall zones (zones I, II, III, and the newly discovered EM zone) are located on the steep, south-facing limb of the anticline (Fig. 4-6). Zones II and III merge in some sections to form a single branching lens. The RW zone occurs on the upright, slightly north dipping limb of the anticline and is divided into RW east, west, and oxide zones. All of the ore zones at Palmer are interpreted to occur along the same stratigraphic ore horizon that has been structurally stacked and offset (Fig. 4-6).

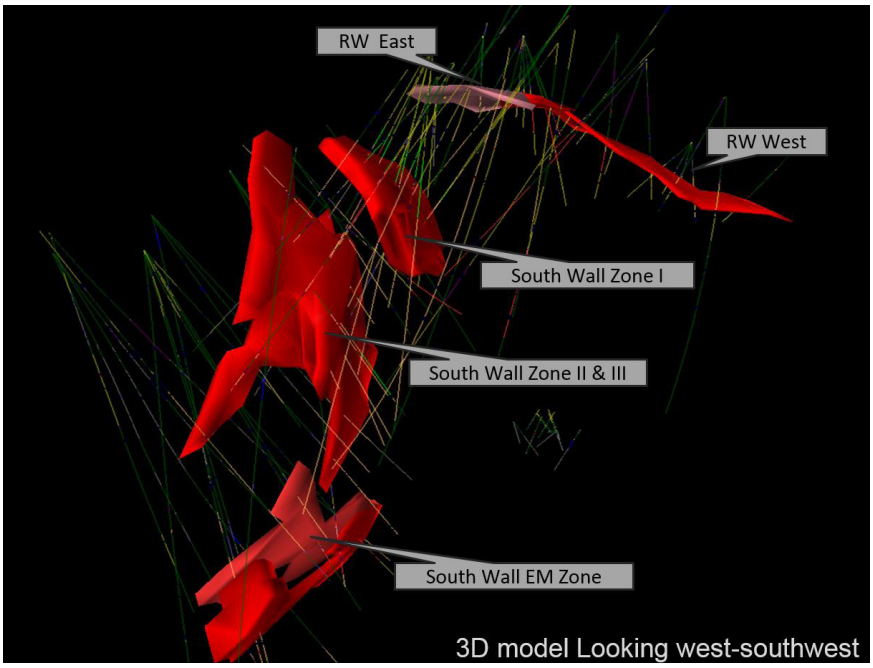

Figure 4-6. *3D model of the ore lenses at Palmer.*

Six main mineralization types are recognized at Palmer, dominated by massive barite-sphalerite-pyrite (barite-rich mineralization), which is replaced at the base and centre of the main lenses by massive and semi-massive chalcopyrite-pyrite-quartz (Fig. 4-5; pyrite-rich mineralization). The flanks and tops of the lenses are carbonate-rich and consist of interbedded carbonate, barite and sulphide, re-sedimented massive barite-sulphide, and mineralized massive carbonate rocks (Fig. 4-5; carbonate-barite, re-sedimented barite, and carbonate-rich mineralization). Tuffaceous hydrothermal sediment with a distinct positive Eu anomaly, overlies the massive sulphide. Pyrrhotite and chalcopyrite in stringers comprise the main "feeder zone". Stringer-style sphalerite-pyrite mineralization occurs above and below the lenses; Fe-poor sphalerite is dominant throughout the lenses, whereas Fe-rich sphalerite occurs at the stratigraphic top and bottom of the lenses in pyrrhotite-rich zones, which contrasts with typical VMS metal zonation (e.g., Franklin *et al.*, 2005). No large pipe-like stringer zone has been discovered at Palmer to date, although localized stringer mineralization has been intersected within coherent volcanic rocks stratigraphically below Zones I, II and the RW Zone.

Exploration

The project is currently being advanced by Constantine Metal Resources Ltd. in partnership with Dowa Metals & Mining Co., Ltd. who can earn 49% in the project by making aggregate expenditures of US$22 million over four years, of which they have currently spent in excess of $15M through year 3. Thus far, a total of 112 drill holes have been drilled on the property, totaling approximately 44,700m (~ 37000 m by Constantine since 2006). While the vast majority of drilling has been completed in the deposit area, there are at least 24 separate base metal and/or barite occurrences and prospects that define more than 15 km of favorable mineral trends, indicating the potential for discovery of multiple deposits. Many of these prospects have associated significant precious metal values and have had very little drilling, including the HG-Cap-Nunatak system (23.2 m grading 134 g/t (3.9 opt) Ag, and a 200 lb bulk sample averaging 336 g/t (11.84 opt) Ag; Fig. 4-2). Additionally, another drill-ready prospect is the Mount Henry Clay showing, which consists of large massive sulphide boulders (up to 1.8 m grading 2.5% Cu and 33% Zn) exposed at the base of a perched glacier.

Discussion

The current genetic model for Palmer is similar to the Kuroko VMS deposits of Japan. The Triassic belt shows similarities to modern intra-oceanic arc rifts such as the Lau Basin, which shows a transition from incipient or immature arc rifting with Kuroko like mineralization to a more mature, deep-water rift setting with distinctly higher temperature, Cu-rich mineralization. The Palmer deposit is located between the Greens Creek and Windy Craggy deposits, and geochemically the Palmer deposit is intermediate between the Zn-Pb-Ag-Au-rich Greens Creek and the Cu-Co-rich Windy Craggy deposits, suggesting it may represent a style of mineralization transitional between the two. Many of the occurrences on the Palmer property are also geochemically similar to either Greens Creek or Windy Craggy. Restoring approximately 180 km of dextral offset on the Chatham Strait fault (Karl et al., 2010a) indicates that the Palmer property deposits likely formed 30-50 km from the sediment-hosted Greens Creek deposit, though within a thick mafic-dominated bimodal volcanic sequence.

DAY 5 – HAINES – HAINES JUNCTION – WHITEHORSE REGIONAL GEOLOGY TRANSECT

Daily summary

We will load the van at 8:30 am, departing accommodation 9 am. Driving time from the Funny Farm to Whitehorse is 4.5 hrs, and we will make several regional geology road side stops along the way arriving in Whitehorse at 6 pm or earlier.

Daily schedule

8:30 am – load van

9:00-2:00* pm – drive Haines to Haines Junction (*Note – actual driving time is 4 hours, Yukon is 1 hour ahead of southeast Alaska; all times in local time)

Stop 5-1 – km 43.5 (mile 27.2), Mosquito Lake Road – Four Winds metamorphic complex

Stop 5-2 – km 129.2, Kwantini Creek – Denali-Duke River fault view point

Stop 5-3 – km 159.1, Million Dollar Falls – Dezadeash Formation

2:00-3:00 pm – lunch in Haines Junction

3:00-6:00 pm – drive Haines Junction to Whitehorse

Stop 5-4 – km 1547.5, Otter Falls – Kluane Schist

6:00 pm – drop off folks at hotels/airport

Introduction

Today's drive takes us from the Mosquito Lake Road, 27 miles northwest of Haines, Alaska to Haines Junction, Yukon before heading east to our final destination of Whitehorse, Yukon (Fig. 5-1). The geology between Haines and Haines Junction is complicated by a long history of contractional and translational faulting. To the northeast of Haines, the Coast plutonic complex records Late Cretaceous to Paleogene metamorphism and synkinematic emplacement of a continental margin arc. In the late Early Cretaceous, subduction of oceanic crust beneath the continental margin ceased as the various Insular terranes rafted into the subduction zone. The buoyant Insular terranes did not subduct but rather formed an orogenic welt. The Insular terranes, including the Wrangellia and Alexander terranes, consisted of an assortment of oceanic arcs overlying subduction complexes of their own, and as they amalgamated, a new arc formed on the western margin of the composite Insular terrane in the late Early Cretaceous. As the composite Insular terrane collided with Yukon-Tanana terrane at the margin of North America, significant crustal thickening along the collision zone formed a welt that was intruded by the eastward migrating arc magmatism on the composite Insular terrane. In the Early Tertiary the new arc on the Insular terrane migrated east of the collision zone, emplacing the Coast batholith into this pre-existing Mesozoic arc. In the Haines area, the Insular terrane that choked subduction beneath Yukon-Tanana terrane is Wrangellia. Very little of Wrangellia is preserved in this area because hundreds of km of dextral translation on the Denali fault, which underlies the Chilkat River, removed an unknown amount of Wrangellia and placed part of the Alexander terrane adjacent to the Chilkat basalts of Wrangellia. This part of the Alexander terrane, referred to as the Admiralty subterrane, consists of a long-lived oceanic arc, and can be tied

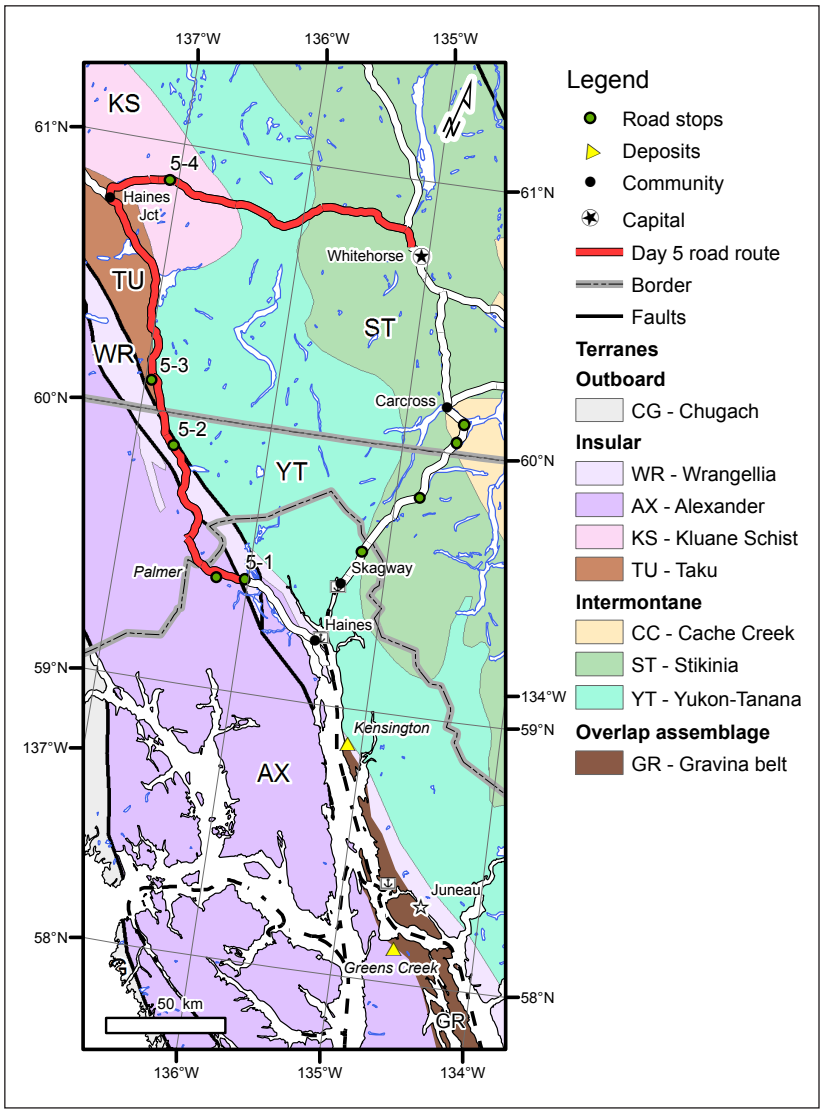

Figure 5-1. *Simplified terrane map with Day 5 route and field trip stops.*

stratigraphically to the rocks on Admiralty Island (Karl *et al.*, 2006; Karl *et al.*, 2010a; Lathram *et al.*, 1965). This correlation is also supported by the distinctive belt of VMS mineralization unique to the Alexander terrane and absent from Wrangellia.

The Admiralty subterrane and the belt of VMS deposits extends from Alaska into British Columbia, to the Windy Craggy area, where carbonate platform deposits of the Saint Elias sequence that underlies Wrangellia are thrust over the island arc deposits of the Admiralty subterrane (Plate 1, MacIntyre *et al.*, 1992). As we head north on the highway through British Columbia, rocks of the Saint Elias sequence overlie rocks of the Admiralty subterrane on a structure that is obscured by Cretaceous and Tertiary intrusive rocks. North of these plutons, rocks of the Saint Elias sequence are thrust over Permian and Triassic rocks of Wrangellia along the still-active Duke River fault. These rocks of Wrangellia likely restore south to some part of the Chilkat basalts on the opposite side of the Denali fault (Davis and Plafker, 1985; Lanphere, 1978). Crossing the Denali fault to the north, we encounter rocks of the Jura-Cretaceous Dezadeash Formation, part of the Gravina-Nutzotin belt of sedimentary rocks that overlaps Triassic basalt of Wrangellia. Continuing north, the Dezadeash overlap basin deposits are overthrust from the east by metamorphic rocks of Yukon-Tanana terrane and the older, latest Cretaceous, tonalites of the Coast plutonic complex. Farther to the north, we'll drive up a broad valley that separates the Dezadeash Formation from the Kluane Schist, which consists almost entirely of quartz mica schists that have sedimentary protoliths. New detrital zircon ages from the Kluane Schist indicate that it is entirely younger than the Dezadeash Formation, with youngest zircons providing a maximum depositional age of 94 Ma (Israel *et al.*, 2011). Metamorphic rims on the detrital zircons in the Kluane Schist yield U-Pb ages of 82 and 70 Ma (Israel *et al.*, 2011), which is correlative with the ages of crustal thickening in the Gravina belt in southeast Alaska (Himmelberg *et al.*, 2004). The Kluane Schist also contains high temperature metamorphic minerals, including garnet, staurolite, sillimanite, and cordierite, that are similar to the assemblages recorded in the metamorphosed Gravina belt in southeast Alaska. The Kluane Schist structurally underlies the Ruby Range batholith of the Coast plutonic complex and rocks of Yukon-Tanana terrane (Fig. 5-2). From Haines Junction to the east we cross through the Kluane Schist into the structurally overlying metamorphic rocks of Yukon-Tanana terrane, and both rock units are intruded by Paleocene granitic rocks of the CPC. As we approach Whitehorse, the CPC intrudes the contact between Yukon-Tanana and Stikine terranes, and we drive into metasedimentary and metavolcanic rocks of Stikinia on the east side of the CPC. We have come full circle from this same geologic boundary at Stop 1-3 south of Tutshi Lake.

Stop 5-1 – km 43.5 (mile 27.2), Mosquito Lake Road – Four Winds metamorphic complex

The Four Winds metamorphic complex is a tightly folded, multiply metamorphosed and deformed heterogeneous rock unit consisting of meter to 100-m scale alternations of biotite quartz schist, actinolite schist, biotite- hornblende semischist, graphitic schist, quartzite, felsic semischist, feldspathic quartz semischist, calc-schist, and marble.

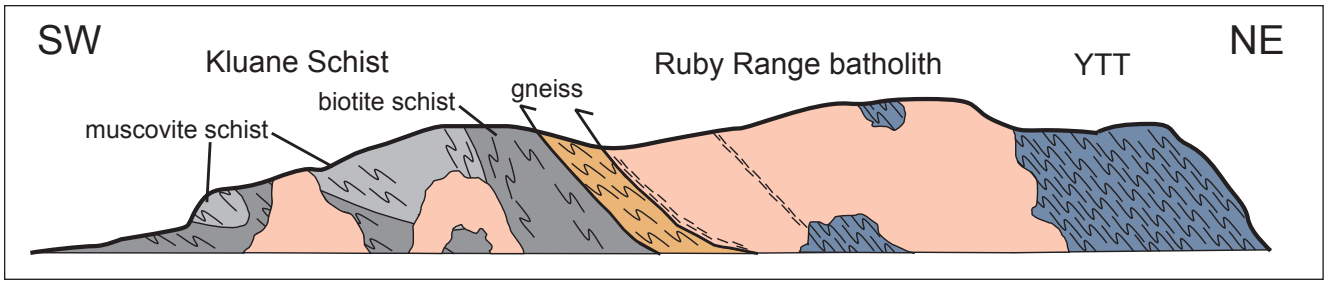

Figure 5-2. *Schematic cross section drawn from southwest to northeast, through the middle of the Coast Belt project area (Israel et al., 2011).*

These rocks contain synkinematic biotite, amphibole, and garnet. Protoliths are mainly sedimentary and volcanic rocks. It is intruded by felsic dikes that yielded a U-Pb zircon age of 455 Ma and contained a xenocrystic zircon with a concordant age of 544 Ma (Karl *et al.*, 2006) indicating that 1) the protoliths are Ordovician or older, and 2) basement to these rocks likely does not range older than Neoproterozoic. These rocks are correlated with rocks in the Retreat Group on northern Admiralty Island and in the Wales Group on southern Prince of Wales Island which have very similar compositions, crystallization ages, and limited Neoproterozoic inheritance ages (Karl *et al.*, 2006).

The Four Winds Complex was intruded by numerous quartz diorite, now orthogneiss, bodies that yielded U-Pb ages of 420 to 442 Ma, including a body by Mosquito Lake that we can visit, time permitting, which has a concordant U-Pb zircon age of 420.9 Ma (Karl *et al.*, 2006). The Silurian orthogneiss and host rocks of the Four Winds Complex are ubiquitously cut by steep cataclastic shear zones up to 20 m in width that may be associated with the nearby Denali fault system.

At the intersection of Mosquito Lake Road and the Haines Highway there is a large roadcut in amphibolite grade metamorphic rocks of the Four Winds Complex. The rocks are banded and folded chloritic semischists with subordinate marble that appear to retain primary compositional layering, suggesting a volcaniclastic protolith. The fabric is northwest-striking with a very steep northeast dip. Fold axes plunge steeply northwest. Mafic dikes, almost sills, cut the fabric in the metamorphic rocks at a low angle. Similar mafic dikes constitute up to 20% of outcrops in the Four Winds Complex and in the structurally underlying phyllite and marble along the highway from here to the border with British Columbia. The maroon color in the outcrop here is derived from biotite and pyrite that postdate emplacement of the dikes. The dikes are slightly boudinaged and the boudin necks are subhorizontal, indicating down-dip extension. A large horizontal quartz vein cuts across one dike, also indicating down dip extension and contractional deformation. Quartz veins are folded and faulted, indicating additional subsequent deformation (Fig. 5-3). The rocks are cut by a number of north-striking, east-dipping faults, some of which are filled with gouge up to 3 cm in thickness.

Biotite flakes on a foliation plane in marble at this outcrop yielded a $^{40/39}$Ar minimum age of 100 Ma, with severe argon loss and no plateau; diffusion modelling indicates a closure age of 115 Ma with 60% loss at 80 Ma (P.W. Layer, unpublished data, written interpretation, 2000). Approximately 1.5 km to the north of this outcrop, orthogneiss that contains biotite and white mica yielded a poorly constrained white mica $^{40/39}$Ar minimum age of 143 Ma, reset at 80 Ma (P.W. Layer, unpublished data, written interpretation, 2000). White mica from numerous locations in the structurally underlying, lower grade marble and phyllite along the highway yielded $^{40/39}$Ar plateau ages of 103 to 110 Ma (P.W. Layer, unpublished data, 2000). Similar marble and phyllite that we saw south of the Klehini River are less recrystallized and lack white mica. The white mica cooling ages for rocks north of the Klehini River are similar to the U-Pb zircon ages of 107.5 Ma for amphibolite and pegmatite at Haines and K-Ar ages of 111 Ma for hornblende and 110 Ma for biotite for a quartz diorite body just above the Haines Highway near the BC border (MacKevett *et al.*, 1974) that intruded the Four Winds Complex.

Figure 5-3. *Deformed quartz veins in the Four Winds Complex.*

The common syndeformational mafic sills and dikes you will see all along the Haines Highway intrude both the higher grade metamorphic rocks of the Four Winds Complex and the structurally underlying lower grade upper Paleozoic marble and phyllite, and are likely Middle Cretaceous in age, similar to the mica ages in the metamorphic rocks and to the plutons that intrude the Alexander terrane in this area. These dikes and plutons were emplaced at shallower depths than most of the regional Middle Cretaceous magmatic belt in the Alexander terrane, but were emplaced during the same contractional event documented by Himmelberg *et al.* (2004). In this area, the white mica cooling ages in the structurally lower rocks reflect exhumation following crustal thickening during the regional contractional event in the Middle Cretaceous.

Stop 5-2 – km 129.2, Kwantini Creek – Denali-Duke River fault view point

This stop is located close to the convergence of two very large, crustal-scale structures, the Denali and Duke River faults, both of which are still seismically active today. The Denali fault separates the inboard Intermontane terranes from the outboard Insular terranes and has an estimated 370 km of right-lateral offset that mainly occurred during

Figure 5-4. *Deformed rocks up Kwantini Creek.*

Figure 5-5. *Deformed gabbro.*

the Paleocene to the Oligocene (Lowey, 1998). At this locality the fault strikes northwest and is found to outcrop in Kwantini Creek (Fig. 5-4) near the mountain front and runs along the bench at the foot of the peaks to the east, separating rocks of the Jura-Cretaceous Deazadeash Formation in the east from rocks of Wrangellia.

The Duke River fault is a northwest verging thrust fault that places rocks of the Saint Elias sequence over rocks of Wrangellia. The fault has a protracted history beginning at least in the Middle Cretaceous and continuing until the present day (Cobbett, 2011). At this locality the Duke River fault is found in the valley just beyond the ridge to the west of the Haines Road. All the high peaks in the distance to the west are made up of rocks belonging to the Saint Elias sequence that underlies Wrangellia.

Rocks at this stop include strongly deformed gabbro of likely Triassic age (Fig. 5-5) intruding phyllitic mudstone, siltstone and sandstone of the Permian Hasen Creek Formation. Outcrops on the west side of the road are composed of pillow basalt of the Late Triassic (Norian) Nikolai Formation. These basalts unconformably overlie the Permian sedimentary rocks found on the east side of the road.

Stop 5-3 – km 159.1, Million Dollar Falls – Dezadeash Formation

At this locality the Takhanne River flows through a steep canyon into the Tatshenshini River below. The canyon is cut through Jura-Cretaceous basinal rocks of the Dezadeash Formation. These rocks are part of a series of large sedimentary basins found between the Intermontane terranes and Insular terranes from Alaska into southern British Columbia.

Rocks here are moderately metamorphosed siltstone, sandstone turbidites (Fig. 5-6). Primary sedimentary features are preserved even though the outcrop shows evidence for strong deformation, including folding and faulting. These rocks form the high peaks to the west of the Haines Road from this stop all the way to Haines Junction. The Dezadeash Formation regionally consists of a thick pile (up to 3000 m) of siltstone, sandstone turbidites with local conglomerate and tuffaceous horizons (Eisbacher 1976).

Figure 5-6. *Dezadeash Formation in outcrop at the Million Dollar Falls view point.*

History

Million Dollar Falls campground is located at a highway construction camp from 1949 during the building of the Haines Road. The Haines Road was built as an alternative to the White Pass Railway during World War II. The road closely follows the historic Dalton Trail established in 1894 by Jack Dalton connecting Haines, Alaska with Fort Selkirk on Yukon River. Dalton choose the route of his trail based on existing First Nation trails and during the Klondike Goldrush it was a popular route to the goldfields.

Stop 5-4 – km 1547.5, Otter Falls – Kluane Schist

Outcrops on the west side of the bridge in the canyon of the Aishihik River are monotonous brown-weathering, medium-grained, quartz-plagioclase, biotite schist assigned to the Kluane Schist. The Kluane Schist is a large package of metamorphic rocks that are likely Middle Jurassic to Late Cretaceous in age that originally formed as a forearc basin. Detrital zircon analyses from the schists indicate a maximum depositional age of ~95 Ma based on the youngest detrital age (Fig. 5-7; Israel *et al.* 2011). Source for the basinal rocks appears to be from Yukon-Tanana terrane and subsequent intrusions, including the mid-Cretaceous Dawson Range batholith. Overgrowths on detrital grains indicate burial and metamorphism occurred at approximately 82 Ma (Fig. 5-6) and likely represents the thrusting of Yukon-Tanana terrane, and the mid-Cretaceous arc built upon it, over the forearc sediments.

In this outcrop, discontinuous lenses of quartz are common and locally define tight to isoclinal intrafolial folds. A penetrative, steeply dipping, southeast-dipping foliation is well-developed. A quartz-rodding lineation along the foliation plane is parallel to the fold hinges.

Regionally, metamorphic mineral assemblages from the Kluane Schist record an early, syntectonic Late Cretaceous medium pressure event (ca. 7 kbar, 500°C) followed by a lower pressure event related to the emplacement of the Paleocene Ruby Range batholith (Mezger *et al.*, 2001).

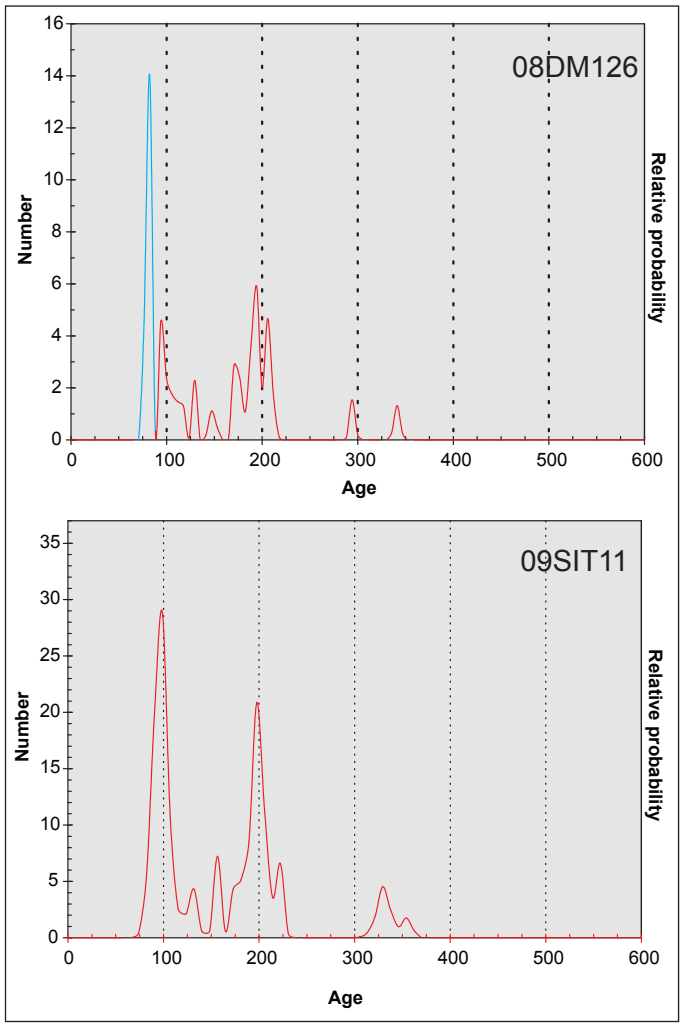

Figure 5-7. *Probability density plots of ages of detrital zircons from the Kluane Schist, showing only the Phanerozoic ages. Blue peak in sample 08DM126 is metamorphic overgrowth ages. The ~95 Ma peak in both samples is interpret as the maximum age of the onset of deposition of this part of the Kluane Schist (Israel et al., 2011).*

Mineralization in the Kluane Schist

Southwest Yukon geology east of the Denali fault is of similar age and affinity to that of southeastern Alaska and preserves the same structural juxtaposition (Fig. 5-8; Israel *et al.*, 2011). Most importantly, Yukon-Tanana terrane has been thrust to the southwest over rocks of the Kluane Schist (Taku terrane analogue) which has been thrust to the southwest over the Dezadeash Formation (Fig. 5-2; Israel *et al.*, 2011). The Ruby Range batholith is age-equivalent to the CPC, and occurs at the same structural level as the CPC, suggesting that it is a northwestward extension of the CPC (Israel *et al.*, 2011; Plate 1). Quartz-carbonate ± muscovite, arsenopyrite veins that host gold mineralization in the Kluane Schist have been described by Wengzynowski (1995) and Eaton (2003) as having characteristics typical of orogenic gold mineralization (Goldfarb *et al.*, 2005; Goldfarb *et al.*, 1988; Goldfarb *et al.*, 1993). The Kluane Schist is higher in metamorphic grade than the rocks that host gold mineralization in the Juneau gold belt, but the lower grade overprint identified by Mezger *et al.* (2001) would provide the necessary conditions for a syntectonic Paleocene mineralizing event, such as occurred in the Treadwell district.

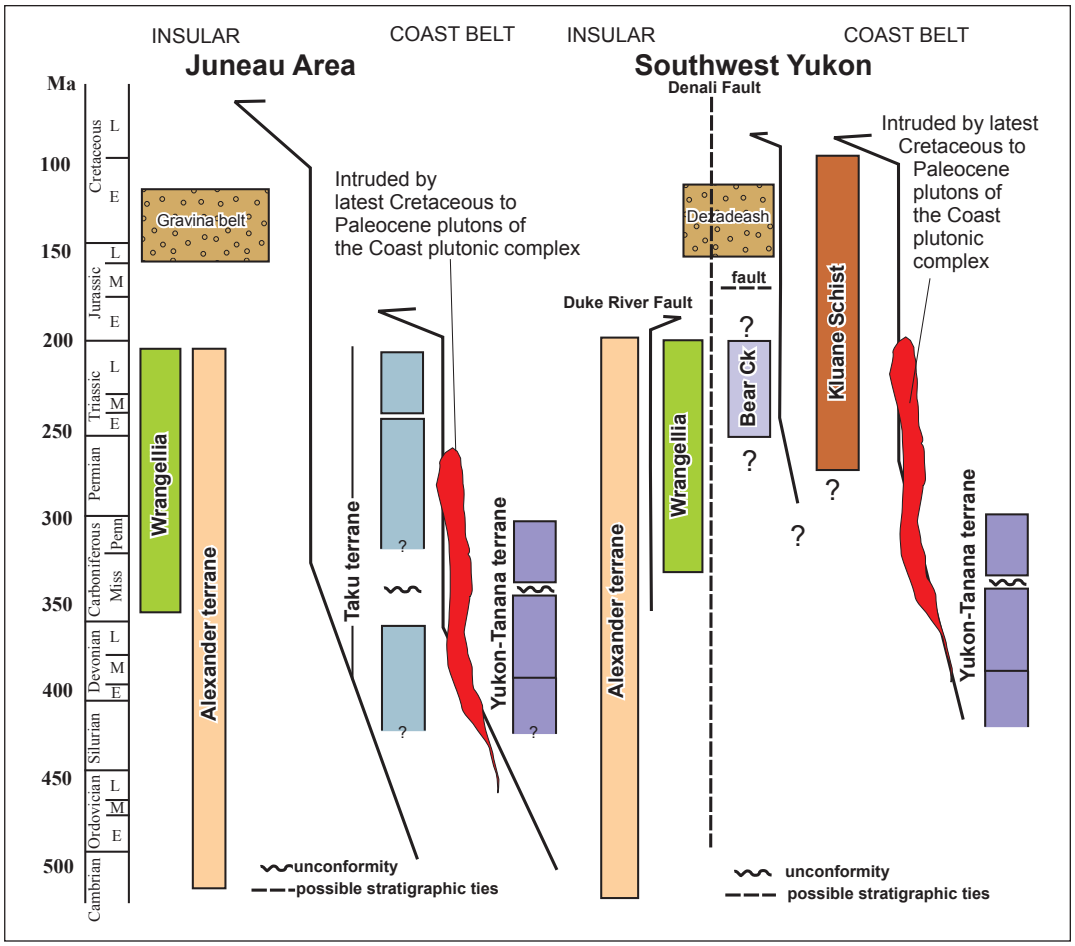

Figure 5-7. *Schematic stratigraphic sections from the Juneau area, southeast Alaska and the Coast Belt area, southwest Yukon (from Israel et al., 2011).*

History

In 1904, a wagon trail from Whitehorse was built to service placer gold operations in the Alsek River area. Sam McGee of Robert Service "Cremation of Sam McGee" infamy, and Gilbert Skelly constructed a substantial bridge over Canyon Creek at this location. In 1942, with Alaska Highway construction advancing at an incredible rate, the U.S. Army constructed a 'modern' bridge over Canyon Creek in 18 days. At the time, this new bridge was described as the most ambitious and important bridge built by the U.S. Army Corps of Engineers.

References

Aberhan, M., 1999. Terrane history of the Canadian Cordillera: Estimating amounts of latitudinal displacement and rotation of Wrangellia and Stikinia. Geological Magazine, vol. 136, p. 481-492.

Andronicos, C.L.C., Chardon, D.H., Hollister, L.S., Gehrels, G.E., and Woodsworth, G.J., 2003. Strain partitioning in an obliquely convergent orogeny, plutonism, and synorogenic collapse. Coast Mountains batholith, British Columbia, Canada: Tectonics, vol. 22, p. 10-12.

Andronicos, C.L., Hollister, L.S., Davidson, C., and Chardon, D., 1999. Kinematics and tectonic significance of transpressive structures within the Coast plutonic complex, British Columbia. Journal of Structural Geology, vol. 21, p. 229-243.

Ayuso, R.A., Karl, S.M., Slack, J.F., Haeussler, P.J., Bittenbender, P.E., Wandless, G.A., and Colvin, A.S., 2007. Oceanic Pb-isotopic sources of Proterozoic and Paleozoic volcanogenic massive sulfide deposits on Prince of Wales Island and vicinity, southeastern Alaska, in Studies by the U.S. Geological Survey in Alaska, 2005. U.S. Geological Survey Professional Paper 1732-C, 37 p.

Barker, F., Arth, J.G., and Stern, T.W., 1986. Evolution of the Coast Batholith along the Skagway traverse, Alaska and British Columbia. American Mineralogist, vol. 71, p. 632-643.

Barrie, C.T. and Hannington, M.D., 1999. Classification of volcanic-associated massive sulfide deposits based on host-rock composition. Reviews in Economic Geology, vol. 8, p. 1-11.

Bazard, D.R., Butler, R.F., Gehrels, G., and Soja, C.M., 1995. Early Devonian paleomagnetic data from the Lower Devonian Karheen Formation suggest Laurentia-Baltica connection for the Alexander terrane. Geology, vol. 23, p. 707-710.

Beranek, L.P., Van Staal, C.R., McClelland, B., Israel, S., and Mihalynuk, M.G., 2012. Baltican crustal provenance for Cambrian–Ordovician sandstones of the Alexander terrane, North American Cordillera: evidence from detrital zircon U–Pb geochronology and Hf isotope geochemistry. Journal of the Geological Society, London, vol. 170, p. 7-18.

Beranek, L.P., van Staal, C.R., McClelland, W.C., Joyce, N., and Israel, S., 2014. Late Paleozoic assembly of the Alexander-Wrangellia-Peninsular composite terrane, Canadian and Alaskan Cordillera. Geological Society of America Bulletin, vol. 126, p. 1531-1550.

Berg, H.C., 1973. Geology of Gravina Island, Alaska. U.S. Geological Survey Bulletin 1373, p. 41, 1 pl.

Berg, H.C., 1984. Regional geologic summary, metallogenisis, and mineral resources of southeastern Alaska: U.S. Geological Survey Open-File Report 84-572, 299 p.

Berg, H.C., Jones, D.L., and Coney, P.J., 1978. Map showing pre-Cenozoic tectonostratigraphic terranes of southeastern Alaska and adjacent areas. U.S. Geological Survey Open-File Report 78-1085, 2 sheets, scale 1:1,000,000.

Bradley, D.C., Dumoulin, J., Layer, P., Sunderlin, D., Roeske, S., McClelland, B., Harris, A.G., Abbott, G., Bundtzen, T., and Kusky, T., 2003. Late Paleozoic orogeny in Alaska's Farewell terrane. Tectonophysics, vol. 372, p. 23-40.

Brew, D.A. and Ford, A.B., 1978. Megalineament in southeastern Alaska marks southwest edge of Coast Range batholithic complex. Canadian Journal of Earth Sciences, vol. 15, p. 1763-1772.

Brew, D.A. and Ford, A.B., 1981, The Coast plutonic complex sill, southeastern Alaska, *In:* The United States Geological Survey in Alaska - Accomplishments during 1979, N.R.D. Albert and T.L. Hudson (eds.), U.S. Geological Survey Circular 823-B, p. 96-99.

Cobbett, R., 2011. Timing and kinematics of the Duke River fault; insights into the evolution of the Insular terrane, southwest Yukon. MSc thesis, University of British Columbia, 140 p.

Colpron, M., Mortensen, J.K., Gehrels, G.E., and Villeneuve, M., 2006. Basement complex, Carboniferous magmatism and Paleozoic deformation in Yukon-Tanana terrane of central Yukon: Field, geochemical and geochronological constraints from Glenlyon map area. *In:* Paleozoic Evolution and Metallogeny of Pericratonic Terranes at the Ancient Pacific Margin of North America, Canadian and Alaskan Cordillera, M. Colpron and J.L. Nelson (eds.), Geological Association of Canada, Special Paper 45, p. 131-151.

Colpron, M., and Nelson, J.L., 2011. A digital atlas of terranes for the Northern Cordillera: Yukon Geological Survey.

Cook, F.A., Clowes, R.M., Snyder, D.B., van der Velden, A.J., Hall, K.W., Erdmer, P., and Evenchick, C.A., 2004. Precambrian crust beneath the Mesozoic northern Canadian Cordillera discovered by Lithoprobe seismic reflection profiling. Tectonics, vol. 23, TC2010.

Cook, R. D., and Crawford, M. L., 1994. Exhumation and tiliting of the western metamorphic belt of the Coast Mountains orogeny in southern southeastern Alaska. Tectonics, vol. 13, p. 528-537.

Crawford, M.L., Crawford, W.A., and Gehrels, G.E., 2000. Terrane assembly and structural relationships in the eastern Prince Rupert Quadrangle, British Columbia. *In:* Tectonics of the Coast Mountains, southeastern Alaska and British Columbia, H.H. Stowell and W.C. McClelland (eds.), Geological Society of America, Special Paper 343, p. 1-21.

Davis, A.C. and Plafker, G., 1985, Comparative geochemistry and petrology of Triassic basaltic rocks from the Taku terrane on the Chilkat Peninsula and Wrangellia. Canadian Journal of Earth Sciences, vol. 22, p. 183-194.

Dawson, K.M., Panteleyev, A., Sutherland Brown, A., and Woodsworth, G.J., 1992. Regional metallogeny. *In:* Geology of the Cordilleran Orogen in Canada, H. Gabrielse and C.J. Yorath (eds.), Geological Survey of Canada, p. 707-768.

Dostal, J., Karl, S.M., Keppie, J.D., Kontak, D.J., and Shellnut, J.G., 2013. Bokan Mountain peralkaline granitic complex, Alexander terrane (southeastern Alaska): evidence for Early Jurassic rifting prior to accretion with North America. Canadian Journal of Earth Sciences, vol. 50, p. 678-691.

Dressler, J.S. and Dunbire, J.C., 1981. The Greens Creek ore deposit, Admiralty Island, Alaska. Canadian Institute of Mining, sixth annual meeting: Canada's gateway to Pacific markets, p. 57.

Duke, N.A., Lindberg, P.A., and West, A., 2010. Geology of the Greens Creek Mining District. *In:* Geology, geochemistry, and genesis of the Greens Creek massive sulfide deposit, Admiralty Island, southeastern Alaska, C.D. Taylor and C.A. Johnson (eds.), U.S. Geological Survey Professional Paper 1763, p. 89-106.

Eakin, H.M., 1919. The Porcupine gold placer district, Alaska. U.S. Geological Survey Bulletin 699, p. 29.

Eaton, W.D., 2003. Hand trenching, prospecting, and soil geochemistry at the Ruby Range Project. Yukon Territorial Assessment Report 094415, 102 p.

Elliott, J.L., Larsen, C.F., Freymueller, J.T., and Motyka, R.J., 2010. Tectonic block motion and glacial isostatic adjustment in southeast Alaska and adjacent Canada constrained by GPS measurements. Journal of Geophysical Research, vol. 115, 21 p.

Energy, Mines Ministers, 2006. Whitehorse, YT-Skagway, AK, Geological Fieldtrip Guidebook. Whitehorse, YT, Energy, Mines Ministers Conference, 6 p., 1 plate, unpublished field guide.

Engebretsen, D.C., Cox, A.V., and Gordon, R.G., 1985. Relative motions between oceanic and continental plates in the Pacific Basin. Geological Society of America Special Paper 206, 59 p.

Forbes, R.B., Gilbert, W.G., and Redman, E.C., 1989. Geologic setting and petrology of the metavolcanic rocks in the northwestern part of the Skagway B-4 Quadrangle, southeastern Alaska. Alaska Division of Geological & Geophysical Surveys, Public-Data File 89-14, 46 p.

Ford, A.B. and Brew, D.A., 1993. Geochemical character of Upper Paleozoic and Triassic greenstone and related metavolcanic rocks of the Wrangellia terrane in northern southeastern Alaska, *in* Dusel-Bacon, C., and Till, A. B., eds., Geologic Studies in Alaska by the U.S. Geological Survey in 1992: U.S. Geological Survey Bulletin 2068, p. 197-217.

Franklin, J.M., Gibson, H.L., Jonasson, I.R., and Galley, A.G., 2005. Volcanogenic massive sulfide deposits. *In:* J.W. Hedenquist, J.F.H. Thompson, R.J. Goldfarb, and J.P. Richards (eds.), Economic Geology, One Hundredth Anniversary Volume, 1905-2005: Littleton, Colorado, Society of Economic Geologists, p. 523-560.

Freeman, L.K., Athey, J.E., Lasley, P.S., and Van Oss, E.J., 2015. Alaska's mineral industry 2014. Alaska Division of Geological & Geophysical Surveys, Special Report 70, 60 p.

Gabrielse, H., Murphy, D.C., and Mortensen, J.K., 2006. Cretaceous and Cenozoic dextral orogen-parallel displacements, magmatism and paleogeography, north central Canadian Cordillera, *In:* Evidence for Major Lateral Displacements in the North American Cordillera, J.W. Haggart, J.W.H. Monger, and R.J. Enkin (eds.), Geological Association of Canada, Special Paper 46, p. 255-276.

Gardner, M.C., Bergman, S.C., Cushing, G.W., Mackevett, E.M., Plafker, G., Campbell, R.B., Dodds, C.J., McClelland, W.C., and Mueller, P.A., 1988. Pennsylvanian pluton stitching of Wrangellia and the Alexander terrane, Wrangell Mountains, Alaska. Geology, vol. 16, p. 967-971.

Gehrels, G.E., 2000. Reconnaissance geology and U-Pb geochronology of the western flank of the Coast Mountains between Juneau and Skagway, southeastern Alaska. *In:* Tectonics of the Coast Mountains, southeastern Alaska and British Columbia, H.H. Stowell, and W.C. McClelland (eds.), Geological Society of America, Special Paper 343, p. 213-234.

Gehrels, G.E., and Barker, F., 1993. Reconnaissance geochemistry of Permian and Triassic basalts of the Taku and Wrangellia terranes, southeastern Alaska. *In:* Geologic Studies in Alaska by the U.S.Geological Survey in 1992, C. Dusel-Bacon and A.B. Till (eds.), U.S.Geological Survey Bulletin 2068, p. 218-227.

Gehrels, G.E. and Berg, H.C., 1994. Geology of southeastern Alaska, *In:* The Geology of North America, G-1, Decade in North American Geology, G. Plafker and H.C. Berg (eds.), Boulder, Colorado, Geological Society of America, p. 451-467.

Gehrels, G.E., Berg, H.C., and Saleeby, J.B., 1983. Ordovician-Silurian volcanogenic massive sulfide deposits on Southern Prince of Wales Island and the Barrier Islands, southeastern Alaska. U.S. Geological Survey Open-File Report 83-318, p. 10.

Gehrels, G.E., Butler, R.R., and Bazard, D.R., 1996. Detrital zircon geochronolgy of the Alexander terrane, southeastern Alaska. Geological Society of America Bulletin, vol. 108, no. 6, p. 722-734.

Gehrels, G.E. and Kapp, P.A., 1998. Detrital zircon geochronology and regional correlation of metasedimentary rocks in the coast mountains, southeastern Alaska. Canadian Journal of Earth Sciences, vol. 35, p. 269-279.

Gehrels, G.E., McClelland, W.C., Samson, S.D., and Patchett, P.J., 1991a. U-Pb geochronology of detrital zircons from a continental margin assemblage in the northern Coast Mountains, southeastern Alaska. Canadian Journal of Earth Sciences, vol. 28, p. 1285-1300.

Gehrels, G.E., McClelland, W.C., Samson, S.D., Patchett, P.J., and Brew, D.A., 1991b. U-Pb geochronology of Late Cretaceous and early Tertiary plutons in the northern Coast Mountains Batholith. Canadian Journal of Earth Sciences, vol. 28, p. 899-911.

Gehrels, G.E., McClelland, W.C., Samson, S.D., Patchett, P.J., and Orchard, M.J., 1992. Geology of the Western Flank of the Coast Mountains between Cape Fanshaw and Taku Inlet, Southeastern Alaska. Tectonics, vol. 11, p. 567-585.

Gehrels, G.E., and Saleeby, J.B., 1987. Geology of southern Prince of Wales Island, southeastern Alaska. Geological Society of America Bulletin, vol.98, p.123-137.

Gilligan, L.B. and Marshall, B., 1987. Textural evidence for remobilization in metamorphic environments. Ore Geology Reviews, vol. 2, p. 205-229.

Godwin, C.I., 1975. Imbricate subduction zones and their relationship with Upper Cretaceous to Tertiary porphyry deposits in the Canadian Cordillera. Canadian Journal of Earth Sciences, vol. 12, p. 1362-1378.

Goldfarb, R.J., Baker, T., Dube, B., Groves, D.I., Hart, C.J.R., and Patrice, G., 2005. Distribution, character, and genesis of gold deposits in metamorphic terranes, *In:* One Hundredth Anniversary Volume, J.W. Hedenquist, J.F.H. Thompson, R.J. Goldfarb, and J.P. Richards (eds.), Society of Economic Geologists, Economic Geology, p. 407-450.

Goldfarb, R.J., Leach, D.L., Pickthorn, W.J., and Paterson, C.J., 1988. Origin of lode-gold deposits of the Juneau gold belt, southeastern Alaska. Geology, vol. 16, p. 440-443.

Goldfarb, R.J., Newberry, R.J., Pickthorn, W.J., and Gent, C.A., 1991. Oxygen, hydrogen, and sulfur isotope studies in the Juneau gold belt, southeastern Alaska; constraints on the origin of hydrothermal fluids: Economic Geology, vol. 86, p. 66-80.

Goldfarb, R.J., Snee, L.W., Miller, L.D., and Newberry, R.J., 1991. Rapid dewatering of the crust deduced from ages of mesothermal gold deposits. Nature, vol. 354, p. 296-298.

Goldfarb, R.J., Snee, L.W., and Pickthorn, W. J., 1993. Orogenesis, high-T thermal events, and gold vein formation within metamorphic rocks of the Alaskan Cordillera. Mineral Magazine, vol. 57.

Gray, J.N. and Cunningham-Dunlop, I.R., 2015. NI 43-101 Technical report and updated resource estimate for the Palmer exploration project Porcupine Mining District southeast Alaska, USA. Unpublished Report, Constantine Metal Resources Ltd., 169 p.

Green, D., 2001. Geology of the volcanogenic massive sulfide prospects of the Palmer property, Haines area, southeastern Alaska. Unpublished Masters thesis, Carleton University, 255 p.

Green, D., MacVeigh, J.G., Palmer, M., Watkinson, D.H., and Orchard, M.J., 2003. Stratigraphy and geochemistry of the RW Zone, a new discovery at the Glacier Creek VMS prospect, Palmer Property, Porcupine mining district, southeastern Alaska. *In:* Short Notes on Alaska Geology 2003, K.H. Clautice and P.K. Davis (eds.), Alaska Division of Geological and Geophysical Surveys, Professional Report 120, p. 35-51.

Haeussler, P.J., Bradley, D.C.G., Richard J., Snee, L.W., and Taylor, C., 1995. Link between ridge subduction and gold mineralization in southern Alaska. Geology, vol. 23, p. 995-998.

Haeussler, P.J., Karl, S.M., Mortensen, J.K., Layer, P.W., and Himmelberg, G.R., 1999. Permian and Mid-Cretaceous deformation of the Alexander Terrane on Admiralty and Kupreanof islands, Southeastern Alaska: Century of the Pacific Rim, "the past as prologue to the future". Geological Society of America, Cordilleran Section, 95th annual meeting; Centennial meeting 1899-1999; abstracts, vol. 31, p. 60.

Héon, D., 2004. The Whitehorse Copper Belt, Yukon. Yukon Geological Survey, 40 p.

Himmelberg, G.R., Brew, D.A., and Ford, A.B., 1991. Development of inverted metamorphic isograds in the western metamorphic belt, Juneau, Alaska. Journal of Metamorphic Geology, vol. 9, p. 165-180.

Himmelberg, G.R., Haeussler, P.J., and Brew, D.A., 2004. Emplacement, rapid burial, and exhumation of 90-Ma plutons in southeastern Alaska. Canadian Journal of Earth Sciences, vol. 41, p. 87-102.

Himmelberg, G.R., and Loney, R.A., 1995. Characteristics and petrogenesis of Alaskan-type ultramafic-mafic intrusions, southeastern Alaska. U.S. Geological Survey Professional Paper 1564, p. 47.

Hollister, L.S., 1982. Metamorphic evidence for rapid (2 mm/yr) uplift of a portion of the Central Gneiss Complex, Coast Mountains, B.C. The Canadian Mineralogist, vol. 20, p. 319-332.

Hulbert, L.J., 1997. Geology and metallogeny of the Kluane mafic-ultramafic belt, Yukon Territory, Canada: Eastern Wrangellia - a new Ni-Cu-PGE metallogenic terrane. Geological Survey of Canada, Bulletin 506, p. 265.

Hutchison, W.W., 1982. Geology of the Prince Rupert-Skeena map area. British Columbia, Geological Survey of Canada, Memoir 394, p. 116

Ingram, G.M. and Hutton, D.H.W., 1994. The Great Tonalite Sill: emplacement into a contractional shear zone and implications for Late Cretaceous to early Eocene tectonics in southeastern Alaska and British Columbia. Geological Society of America Bulletin, vol. 106, p. 715-728.

Israel, S., Beranek, L.P., Friedman, R.M., and Crowley, J.L., 2014. New ties between the Alexander terrane and Wrangellia and implications for North American Cordilleran evolution. Lithosphere, vol. 6, p. 270-276.

Israel, S., Murphy, D., Bennett, V., Mortensen, J.K., and Crowley, J., 2011. New insights into the geology and mineral potential of the Coast Belt in southwestern Yukon. *In:* Yukon Exploration and Geology 2010, K.E. MacFarlane, L.H. Weston, and C. Relf (eds.), Yukon Geological Survey, p. 101-123.

Johnston, S.T., Hart, C.J.R., Mihalynuk, M.G., Brew, D.A., and Ford, A.B., 1993. Field guide to the northern Intermontane Superterrane. 1993 Nuna Conference, Lakeview Marina, Marsh Lake, Yukon, 1993, p. 67.

Kapp, P.A. and Gehrels, G.E., 1998. Detrital constraints on the tectonic evolution of the Gravina belt, southeastern Alaska. Canadian Journal of Earth Sciences, vol. 35, p. 253-268.

Karl, S.M. and Brew, D.A., 1984. Migmatites of the coast plutonic-metamorphic complex, southeastern Alaska. *In:* The U.S. Geological Survey in Alaska: Accomplishments during 1982, K.M. Reed, and S. Bartsh-Winkler (eds.), U.S. Geological Survey Circular 939, p. 108-111.

Karl, S.M., Haeussler, P.J., Friedman, R.M., Mortensen, J.K., Himmelberg, G.R., and Zumsteg, C.L., 2006. Late Proterozoic ages for rocks on Mount Cheetdeekahyu and Admiralty Island, Alexander Terrane, southeast Alaska. Geological Society of America, Abstracts with Programs, vol. 38, p. 20.

Karl, S.M., Haeussler, P.J., Himmelberg, G.R., Zumsteg, C.L., Layer, P.W., Friedman, R.M., Roeske, S.M., and Snee, L.W., 2015. Geologic map of Baranof Island, southeastern Alaska. U.S. Geological Survey Scientific Investigations Map 3335, scale 1:200,000, pamphlet p. 82.

Karl, S.M., Haeussler, P.J., Layer, P., and Himmelberg, G.R., 1998. Two new events in the metamorphic and deformational history of the Alexander terrane on Admiralty Island, southeastern Alaska. Science and technology conference: Cutting edge in Alaska, 1998, p. 14.

Karl, S.M., Hammarstrom, J.M., Kunk, M., Himmelberg, G.R., Brew, D.A., Kimbrough, D., and Bradshaw, J.Y., 1996. Tracy Arm transect: Further constraints on the uplift history of the Coast plutonic complex in southeast Alaska. Geological Society of America Abstracts with Programs, vol. 28, p. A312.

Karl, S.M., Layer, P.W., Harris, A.G., Haeussler, P.J., and Murchey, B.L., 2010a. The Cannery Formation—Devonian to Early Permian arc-marginal deposits within the Alexander terrane, southeastern Alaska. *In:* Studies by the U.S. Geological Survey in Alaska, 2008–2009, J.A. Dumoulin and J.P. Galloway (eds.), U.S. Geological Survey Professional Paper 1776-B, p. 45.

Karl, S.M., Newberry, R.J., Maas, K.M., and Snee, L.W., 2010b. Mid-Cretaceous terrane accretion, syndeformational intrusions, and orogenic gold in southeastern Alaska. Alaska Miners Association Annual Meeting, Anchorage, Alaska, Program and Abstracts, p. 5-6.

Klepeis, K.A., Crawford, M.L., and Gehrels, G.E., 1998. Structural history of the crustal scale Coast shear zone near Portland Inlet, southeast Alaska and British Columbia. Journal of Structural Geology, vol. 20, p. 883-904.

Lanphere, M.A., 1978. Displacement history of the Denali fault system, Alaska and Canada. Canadian Journal of Earth Sciences, vol. 15, p. 817-822.

Lathram, E.H., Pomeroy, J.S., Berg, H.C., and Loney, R. A., 1965. Reconnaissance geology of Admiralty Island, Alaska. U.S. Geological Survey Bulletin 1181-R, p. 1-48, 2 plates.

Lewis, P., 1998. Palmer project preliminary field report: structural and stratigraphic setting of mineral occurrences, Glacier and Jarvis Creek area, Haines, Alaska. Unpublished Report, Rubicon Minerals Corporation, p. 11.

Logan, J.M. and Mihalynuk, M.G., 2014. Tectonic controls on early Mesozoic paired alkaline porphyry deposit belts (Cu-Au±Ag-Pt-Pd-Mo) within the Canadian Cordillera. Economic Geology, vol. 109, p. 827-858.

Loney, R.A., 1964. Stratigraphy and petrography of the Pybus-Gambier area, Admiralty Island, Alaska. U.S. Geological Survey Bulletin 1178, p. 102, pl. 2.

Lonsdale, P., 1988. Paleogene history of the Kula plate: Offshore evidence and onshore implications. Geological Society of America Bulletin, vol. 100, p. 733-754.

Lowey, G.W., 1998. A new estimate of the amount of displacement on the Denali fault system based on the occurrence of carbonate megaboulders in the Dezadeash Formation (Jura-Cretaceous), Yukon, and the Nutzotin Mountains Sequence (Jura-Cretaceous), Alaska. Bulletin of Canadian Petroleum Geology, vol. 46, p. 379-386.

Lydon, J.W., 1984. Volcanogenic massive sulphide deposits, Part I: A descriptive model. Geoscience Canada, vol. 11, p. 195-202.

MacIntyre, D.G., Mihalynuk, M.G., Smith, M.T., Schiarizza, P., Deschênes, M., and Timmerman, J., 1992. Tats Lake map area geology (114P/12): Northwest Tatshenshini River map area, northwestern British Columbia. B.C. Ministry of Energy, Mines, and Petroleum Resources, Open File 1993-13, sheet 3 of 6.

MacIntyre, D.G. and Schroeter, T.G., 1985. Mineral occurrences in the Mount Henry Clay area (114P/7, 8), Geological Fieldwork 1984. B.C. Ministry of Energy, Mines, and Petroleum Resources, Paper 1985-1, p. 365-379.

MacKevett, E.M., Jr., Cox, D.P., Potter, R.W., and Silberman, M.L., 1997. Kennecott-type deposits in the Wrangell Mountains: High-grade copper ores near a basalt-limestone contact. *In:* Mineral Deposits of Alaska, R.J. Goldfarb and L.D. Miller (eds). Economic Geology, Monograph 9, p. 66-89.

MacKevett, E.M., Jr., Robertson, E.C., and Winkler, G.R., 1974. Geology of the Skagway B-3 and B-4 Quadrangles, southeastern Alaska. U.S. Geological Survey Professional Paper 832, 33 p., scale 1:63,360.

Martin, G.C., 1926. The Mesozoic stratigraphy of Alaska. U.S. Geological Survey, Bulletin 776, 493 p.

Mazzotti, S., Leonard, L.J., Hyndman, R.D., and Cassidy, J.F., 2008. Tectonics, dynamics, and seismic hazard in the Canada-Alaska Cordillera, *In:* Active Tectonics and Seismic Potential of Alaska, J.T. Freymueller (ed.), Washington, D.C., American Geophysical Union, Geophysical Monograph Series 179, p. 297-319.

McClay, K.R. and Ellis, P.G., 1983. Deformation and recrystallization of pyrite. Mineralogy Magazine, vol. 47, p. 527-538.

McClelland, W.C., and Mattinson, J.M., 2000. Cretaceous-Tertiary evolution of the western Coast Mountains, central southeastern Alaska. *In:* Tectonics of the Coast Mountains, southeastern Alaska and British Columbia, H.H. Stowell and W.C. McClelland (eds.), Geological Society of America Special Paper 343, p. 159-182.

Mezger, J.E., Chacko, T., and Erdmer, P., 2001. Metamorphism at a late Mesozoic accretionary margin: a study from the Coast Belt of the North American Cordillera. Journal of Metamorphic Geology, vol. 19, p. 121-137.

Mihalynuk, M.G., Nelson, J., and Diakow, L.J., 1994. Cache Creek terrane entrapment: Oroclinal paradox within the Canadian Cordillera. Tectonics, vol. 13, p. 575-595.

Miller, L.D., Goldfarb, R.J., Gehrels, G.E., and Snee, L.W., 1994. Genetic links among fluid cycling, vein formation, regional deformation, and plutonism in the Juneau gold belt, southeastern Alaska. Geology, vol. 22, p. 203-206.

Miller, L. D., Stowell, H. H., and Gehrels, G. E., 2000. Progressive deformation associated with mid-Cretaceous to Tertiary contractional tectonism in the Juneau gold belt, Coast Mountains, southeastern Alaska. *In:* Tectonics of the Coast Mountains, southeastern Alaska and British Columbia, H.H. Stowell and W.C. McClelland (eds.), Geological Society of America, Special Paper 343, p. 193-212.

Miller, L.J., Goldfarb, R.J., Snee, L.W., Gent, C.A., and Kirkham, R.A., 1995. Structural geology, age, and mechanisms of gold vein formation at the Kensington and Jualin deposits, Berners Bay District, Southeast Alaska. Economic Geology, vol. 90, p. 343-368.

Monger, J.W.H., Price, R.A., and Tempelman-Kluit, D.J., 1982. Tectonic accretion and the origin of the two major metamorphic and plutonic welts in the Canadian Cordillera. Geology, vol. 10, p. 70-75.

Nelson, J.L., Colpron, M., and Israel, S., 2013. The Cordillera of British Columbia, Yukon, and Alaska: Tectonics and metallogeny. *In:* Tectonics, metallogeny and discovery: The North American Cordillera and similar accretionary setttings, M. Colpron, T. Bissig, B.G Rusk, and J.F.H. Thompson (eds.), Society of Economic Geologists Special Publication No. 17, p. 53-109.

Nelson, J.L., Colpron, M., Piercey, S.J., Dusel-Bacon, C., Murphy, D.C., and Roots, C.F., 2006. Paleozoic tectonic and metallogenic evolution of the pericratonic terranes in Yukon, northern British Columbia and eastern Alaska. *In:* Paleozoic Evolution and Metallogeny of Pericratonic Terranes at the Ancient Pacific Margin of North America, Canadian and Alaskan Cordillera, M. Colpron and J.L. Nelson (eds.), Geological Association of Canada, Special Paper 45, p. 323-360.

Newberry, R.J., Crafford, T.C., Newkirk, S.R. Young, L.E., Nelson, S.W., and Duke, N.A., 1997. Volcanogenic massive sulfide deposits of Alaska. *In:* Mineral Deposits of Alaska, R.J. Goldfarb and L.D. Miller (eds.), Economic Geology, Monograph 9, p. 120-150

Newberry, R.J., McCoy, D.T., and Brew, D.A., 1995. Plutonic-hosted gold ores in Alaska: igneous vs. metamorphic origins. Mining Geology Japan, Special Issue 28, p. 57-100.

Nokleberg, W.J., Bundtzen, T.K., Eremin, R.A., Ratkin, V.V., Dawson, K.M., Shpikerman, V.I., Goryachev, N.A., Byalobzhesky, S.G., Frolov, Y.F., Khanchuk, A.I., Koch, R.D., Monger, J.W.H., Pozdeev, A.I., Rozenblum, I.S., Rodionov, S.M., Parfenov, L.M., Scotese, C.R., and Sidorov, A.A., 2005. Metallogenesis and tectonics of the Russian Far East, Alaska, and the Canadian Cordillera. U.S. Geological Survey Professional Paper 1697, 429 p.

Oliver, J.W.A. and Berg, H.C., 1981. Report on referred fossils. U.S. Geological Survey, p. 1.

Oliver, J., Roberts, K., and Friedman, R., 2011. The Niblack Mine: A Neoproterozoic, precious metals enhanced, volcanic-hosted massive sulphide deposits, Prince of Wales Island, Alaska. Mineralized zones and mineral resources, structural style, stratigraphic and U-Pb geochronological relationships. Alaska Miners Association, development and mine operations, Annual Conference, Program and Abstracts, p. 60.

Peter, J.M., 1989. The Windy Craggy copper-cobalt-gold massive sulphide deposit, northwestern British Columbia (114P). British Columbia Geological Survey Geological fieldwork 1988, p. 455-466.

Peter, J.M. and Scott, S.D., 1999. Windy Craggy, northwestern British Columbia; the world's largest besshi-type deposit. *In:* Volcanic-associated massive sulfide deposits; processes and examples in modern and ancient settings, C.T. Barrie and M.D. Hannington (eds.), Reviews in Economic Geology vol. 8, p. 261-295.

Plafker, G., Blome, C.D., and Silberling, N.J., 1989. Reinterpretation of lower Mesozoic rocks on the Chilkat Peninsula, Alaska, as a displaced fragment of Wrangellia. Geology, vol. 17, p. 3-6.

Plafker, G. and Hudson, T., 1980. Regional implications of Upper Triassic metavolcanic and metasedimentary rocks on the Chilkat Peninsula, southeastern Alaska. Canadian Journal of Earth Sciences, vol. 17, p. 681-689.

Premo, W.R., Taylor, C.D., Snee, L.W., and Harris, A.G., 2010. Microfossil and radioisotopic geochronological studies of the Greens Creek host rocks. *In:* Geology, geochemistry, and genesis of the Greens Creek massive sulfide deposit, Admiralty Island, southeastern Alaska, C.D. Taylor and C.A. Johnson (eds.), U.S. Geological Survey Professional Paper 1763, p. 283-333.

Proffett, J., 2010, Geologic structure of the Greens Creek mine area, southeastern Alaska, *in* Taylor, C.D., and Johnson, C.A., eds., Geology, geochemistry, and genesis of the Greens Creek massive sulfide deposit, Admiralty Island, southeastern Alaska: U.S. Geological Survey Professional Paper 1763, p. 137-157.

Redman, E.C., 1986. History of the Juneau gold belt 1869-1985 development of the mines and prospects from Windham Bay to Berners Bay. U.S. Bureau of Mines, Open-File Report 91-86, p. 78, 1 sheet (scale 1:250,000).

Redman, E.C., 1988. Structure and mineralization at the Kensington Mine, Internal Report.

Redman, E.C., Caddey, S., Harvey, D., and Jaworski, M., 2003. Mineralization and structural controls in the Kensington mine and Berners Bay area, southeastern Alaska. *In:* Short Notes on Alaska Geology 2003, K.H. Clautice and P.K. Davis (eds.), Professional Report 120, Alaska Division of Geological & Geophysical Surveys, p. 63-69.

Rhys, D., 2008. Structural observations from a June 2007 reconnaissance visit to the Kensington deposit, southeastern Alaska. Internal Report.

Sack, P.J., 2009. Characterization of footwall lithologies to the Greens Creek volcanic-hosted massive sulfide (VHMS) deposit, Alaska, USA. University of Tasmania, PhD thesis, 442 p.

Schmidt, J.M. and Rogers, R.K., 2007. Metallogeny of the Nikolai large igneous province (LIP) in southern Alaska and its influence on the mineral potential of the Talkeetna Mountains. *In:* Tectonic growth of a collisional continental margin: Crustal evolution of south-central Alaska, K.D. Ridgeway, J.M. Trop, J.M.G. Glen, and J.M. O'Neill (eds.), Geological Society of America Special Paper 431, p. 623-648.

Sherlock, R.L., Childe, F., Barrett, T.J., Mortensen, J.K., Lewis, P.D., Chandler, T., McGuigan, P., Dawson, G.L., and Allen, R., 1994. Geological investigations of the Tulsequah Chief massive sulphide deposit, northwestern British Columbia (104K/12). Geological fieldwork 1993, British Columbia Geological Survey, p. 373-379.

Slack, J.F., Shanks, W.C.I., Karl, S.M., Gemery, P.A., Bittenbender, P.E., and Ridley, W.I., 2007. Geochemical and sulfur-isotopic signatures of volcanogenic massive sulfide deposits on Prince of Wales Island and vicinity, southeastern Alaska, Studies by the U.S. Geological Survey in Alaska, 2005. U.S. Geological Survey Professional Paper 1732-C, p. 37.

Smith, P.L., Tipper, H.W., and Ham, D.M., 2001. Lower Jurassic Amaltheidae (Ammotina) in North America: paleobiogeography and tectonic implications. Canadian Journal of Earth Sciences, vol. 38, p. 1439-1449.

Soja, C.M. and Antoshkina, A.I., 1997. Coeval development of Silurian stromatolite reefs in Alaska and the Ural Mountains: Implications for paleogeography of the Alexander terrane. Geology, vol. 25, p. 539-542.

Spencer, A.C. and Wright, C.W., 1906. The Juneau gold belt, Alaska; and a reconnaissance of Admiralty Island, Alaska. U.S. Geological Survey Bulletin 287, p. 161 p.

Steeves, N.J., Hannington, M.D., Gemmell, J.B., Green, D., and McVeigh, G., 2016. The Glacier Creek Cu-Zn VMS deposit, southeast Alaska: An addition to the Alexander Triassic metallogenic belt. Economic Geology, vol. 111, p. 151-178.

Struik, L.C., 1992. Intersecting intracontinental Tertiary transform fault systems in the North American Corillera: Canadian Journal of Earth Sciences, vol. 30, p. 1262-1274.

Taylor, C.D., 2003. Descriptions of mineral occurrences and interpretation of mineralized rock geochemical data in the Stikine geophysical survey area, southeastern Alaska. U.S. Geological Survey Open File Report 2003-154, 51 p.

Taylor, C.D. and Johnson, C.A., 2010a. Geology, geochemistry, and genesis of the Greens Creek massive sulfide deposit, Admiralty Island, southeastern Alaska. U.S. Geological Survey Professional Paper 1763, 429 p.

Taylor, C.D. and Johnson, C.A., 2010b. Introduction and overview of the U.S. Geological Survey–Kennecott Greens Creek Mining Company Cooperative Applied Research Project at the Greens Creek Mine. *In:* Geology, geochemistry, and genesis of the Greens Creek massive sulfide deposit, Admiralty Island, southeastern Alaska, U.S., C.D. Taylor and C.A. Johnson (eds.), Geological Survey Professional Paper 1763, p. 1-7.

Taylor, C.D., Lear, K.G., and Newkirk, S.R., 2010a. A genetic model for the Greens Creek polymetallic massive sulfide deposit, Admiralty Island, southeastern Alaska. *In:* Geology, geochemistry, and genesis of the Greens Creek massive sulfide deposit, Admiralty Island, southeastern Alaska, C.D. Taylor and C.A. Johnson (eds.), U.S. Geological Survey Professional Paper 1763, p. 417-429.

Taylor, C.D., Philpotts, J., Premo, W.R., Meier, A.L., and Taggart, J.E., 2010b. The Late Triassic metallogenic setting of the Greens Creek deposit in southeastern Alaska. *In:* Geology, geochemistry, and genesis of the Greens Creek massive sulfide deposit, Admiralty Island, southeastern Alaska, C.D. Taylor and C.A. Johnson (eds.), U.S. Geological Survey Professional Paper 1763, p. 9-59.

Taylor, C.D., Premo, W.R., Leventhal, J.S., Meier, A.L., Johnson, C.A., Newkirk, S.R., Hall, T.E., Lear, K.G., and Harris, A.G., 1999. The Greens Creek deposit, southeastern Alaska; a VMS-SEDEX hybrid. *In:* Proceedings of the Fifth biennial SGA meeting and the Tenth quadrennial IAGOD symposium; Mineral deposits; processes to processing, vol. 5, p. 597-600.

Taylor, C.D., Premo, W.R., Meier, A.L., and Taggart, J.E., 2008. The metallogeny of Late Triassic rifting of the Alexander terrane in southeastern Alaska and northwestern British Columbia. Economic Geology, vol. 103, p. 89-115.

Taylor, H.P., 1967. The zoned ultramafic complexes of southeastern Alaska. *In:* Ultramafic and related rocks, P.J. Wyllie (ed.), New York, John Wiley, p. 97-121.

Tenney, D., 1981. The Whitehorse copper belt: Mining, exploration and geology (1967-1980). Department of Indian and Northern Affairs, Bulletin 1, p. 36.

Trop, J.M., Ridgway, K.D., and Sweet, A.R., 2004. Stratigraphy, palynology, and provenance of the Colorado Creek basin, Alaska, USA: Oligocene transpressional tectonics along the central Denali fault system. Candian Journal of Earth Sciences, vol. 41, p. 457-480.

Twenhofel, W.S., 1952. Geology of the Alaska-Juneau lode system, Alaska, U.S. Geological Survey Open-File Report 52-160, p. 186, 2 sheets, scale 1:24,000.

Twenhofel, W.S. and Sainsbury, C.L., 1958. Fault patterns in southeastern Alaska. Geological Society of America Bulletin, vol. 69, p. 1431-1442.

Warner, L.A. and Goddard, E.N., 1961. Iron and copper deposits of Kasaan Peninsula, Prince of Wales Island, southeastern Alaska. U.S. Geological Survey Bulletin 1090, 136 p.

Wengzynowski, W., 1995. Prospecting, soil geochemistry, trenching, and geophysical surveys at the Ruby Range Project. Yukon Territorial Assessment Report, 060991, p. 90.

West, A., 2010. The history of Greens Creek exploration. *In:* Geology, geochemistry, and genesis of the Greens Creek massive sulfide deposit, Admiralty Island, southeastern Alaska, C.D. Taylor and C.A. Johnson (eds.), U.S. Geological Survey Professional Paper 1763, p. 61-88.

White, C., Gehrels, G.E., Pecha, M., Giesler, D., Yokelson, I., McClelland, W.C., and Butler, R.F., 2016. U-Pb and Hf isotope analysis of detrital zircons from Paleozoic strata of the southern Alexander terrane (southeast Alaska). Lithosphere, vol. 8, p. 83-96.

Wilson, F.H., Hults, C.P., Mull, C.G., and Karl, S.M., (comps.), 2015. Geologic map of Alaska. U.S. Geological Survey Scientific Investigations Map 3340, p. 196 p., 2 sheets, scale 1:1,584,000, doi:10.3133/sim3340.

Zen, E. and Hammarstrom, J.M., 1984. Magmatic epidote and its petrologic significance. Geology, vol. 12, p. 515-518.

Zumsteg, C.L., Himmelberg, G.R., Karl, S.M., and Haeussler, P.J., 2003, Metamorphism within the Chugach accretionary complex on southern Baranof Island, southeastern Alaska. *In:* Geology of a transpressional orogen developed during ridge-trench interaction along the north Pacific margin, V.B. Sisson, S.M. Roeske, and T.L. Pavlis (eds.), Geological Society of America Special Paper 371, p. 253-267.